SYNTHESIS AND CHARACTERIZATION OF FATTY ACID BASED HYPERBRANCHED POLYMERS FOR ANTI-CANCER DRUG DELIVERY

A THESIS SUBMITTED TO
THE GRADUATE SCHOOL OF NATURAL AND APPLIED SCIENCES
OF
MIDDLE EAST TECHNICAL UNIVERSITY

BY

ESRA GÜÇ

IN PARTIAL FULFILLMENT OF THE REQUIREMENTS
FOR
THE DEGREE OF MASTER OF SCIENCE
IN
BIOLOGY

JUNE 2008

Approval of the thesis:

SYNTHESIS AND CHARACTERIZATION OF FATTY ACID BASED HYPERBRANCHED POLYMERS FOR ANTI-CANCER DRUG DELIVERY

submitted by **ESRA GÜÇ** in partial fulfillment of the requirements for the degree of **Master of Science in Biology Department**, **Middle East Technical University** by,

Prof. Dr. Canan Özgen _____
Dean, Graduate School of **Natural and Applied Sciences**

Prof. Dr. Zeki Kaya _____
Head of Department, **Biology**

Prof. Dr. Ufuk Gündüz _____
Supervisor, **Biology Dept., METU**

Prof. Dr. Güngör Gündüz _____
Co-Supervisor, **Chemical Engineering Dept., METU**

Examining Committee Members:

Prof. Dr. Semra Kocabıyık _____
Biology Dept., METU

Prof. Dr. Ufuk Gündüz _____
Biology Dept., METU

Prof. Dr. Menemşe Gümüşderelioğlu _____
Chem. Eng. Dept., Hacettepe Univ.

Assist. Prof. Dr. Dilek Keskin _____
Eng. Science Dept., METU

Assist. Prof. Dr. Ayşen Tezcaner _____
Eng. Science Dept., METU

Date : 20/06/2008

I hereby declare that all information in this document has been obtained and presented in accordance with academic rules and ethical conduct. I also declare that, as required by these rules and conduct, I have fully cited and referenced all material and results that are not original to this work.

Name, Last Name : Esra Güç

Signature :

ABSTRACT

SYNTHESIS AND CHARACTERIZATION OF FATTY ACID BASED HYPERBRANCHED POLYMERS FOR ANTI-CANCER DRUG DELIVERY

Güç, Esra

MSc., Department of Biology

Supervisor: Prof. Dr. Ufuk Gündüz

Co-Supervisor: Prof. Dr. Güngör Gündüz

June 2008, 114 pages

Conventional methods of chemotherapy requires novel therapy systems due to serious side effects and inefficiency of drug administration. In recent years many studies are carried out to improve drug delivery systems. Polymers are one of the most important elements for drug delivery research due to their versatility. By the discovery of dendritic polymers, drug delivery studies gained a new vision. Highly branched monodisperse structure, multiple sites of attachment, well-defined size and controllable physical and chemical properties make them efficient drug delivery systems.

In this research hyperbranched dendritic polymers were sythesized and characterized for hydrophobic drug delivery. Dipentaerythritol which was used as core molecule, esterified with dimethylol propionic acid. Ricinoleic acid was esterified with the end groups of dimethylol propionic acid and hyperbranched resin (HBR) was formed. By considering the properties of HBR, hydrophobic tamoxifen and idarubicin were used for drug delivery study. The most efficient loading was determined as 73% for tamoxifen and 74% for idarubicin. Drug-HBR interactions and changes in properties of HBR were determined by FTIR, zeta potential and particle size measurements. FTIR results indicated that idarubicin chemically interacted with HBR

while tamoxifen physically loaded to HBR. Drug delivery profile of HBR was studied in the absence and presence of lipase from *Pseudomonas sp.* and sodium dodecyl sulfate (SDS). Results revelaed that lipase and SDS increased the release rate of tamoxifen while idarubicin release rate was not affected. The effect of lipase was also tested for the degradation of HBR and it was indicated that lipase sustain a faster degradation. Finally toxicity of HBR and drug loaded HBR on MCF-7 breast cancer cell line was determined with XTT proliferation assay. Empty HBR did not cause significant toxicity on MCF-7 cells while drug loaded HBR was more toxic than free drug. By this study the efficiency of novel synthesized hyperbranched polymer in drug delivery was shown.

Keywords: Controlled Drug Delivery, Hyperbranched Polymers, Idarubicin, Tamoxifen.

ÖZ

YAĞ ASİDİ KÖKENLİ AŞIRI DALLI POLİMER SENTEZİ, ÖZELLİKLERİNİN BELİRLENMESİ ve ANTİ-KANSER İLAÇ SALIMINDA KULLANILMASI

Güç, Esra

Yüksek Lisans, Biyoloji Bölümü

Tez Yöneticisi: Prof. Dr. Ufuk Gündüz

Ortak Tez Yöneticisi: Prof. Dr. Güngör Gündüz

Haziran 2008, 114 sayfa

Klasik kemoterapi yöntemleri ciddi yan etkilere neden olmakta ve ilacın tümör üzerindeki etkileri yetersiz kalmaktadır. Bu nedenle son yıllarda, yeni ilaç salım sistemleri geliştirilmiştir. Polimerler sahip olduğu özellikler sayesinde ilaç salım çalışmalarında kullanılan biyomalzemelerin başında gelmektedir. Dallanık polimerlerin üretilmesi ile birlikte ilaç salım çalışmaları yeni bir boyut kazanmıştır. Dallı yapıları, çoklu bağlanma grupları, fiziksel ve kimyasal özelliklerinin kontrol edilebilmesi bu polimerleri ilaç salım çalışmalarında etkin kılmaktadır.

Bu çalışmada aşırı dallı polimerlerin sentezi için, çekirdek molekül olarak dipentaeritritol kullanılmış ve dimetilol propiyonik asit ile esterleşmesi sağlanmıştır. Polimere hidrofobik özellik kazandırmak için uç gruplar risinoleik asit ile esterleştirilmiştir ve aşırı dallı reçinenin (ADR) oluşması sağlanmıştır. İlaç salımında karşılaşılan sorunlar en çok hidrofobik yapıdaki ilaçlardan kaynaklanmaktadır, bu nedenle bu çalışmada hidrofobik yapıdaki anti-kanser ilaçlardan tamoksifen ve idarubisin ADR'ye yüklenmiştir. İdarubisin en fazla %74 oranında, tamoksifen ise %73 oranında tutuklanmıştır. İlaç-ADR ilişkisi ve ADR yapısındaki değişiklikler FTIR, zeta potansiyel ve parçacık boyut analizleri ile belirlenmiştir. FTIR sonucunda

idarubisinin ADR'ye kimyasal olarak, tamoksifenin ise fiziksel olarak tutunduğu belirlenmiştir. İlaç salım çalışmaları için *Pseudomonas sp.* lipazı ve sodyum dodesil sülfat eklenmiş ve salım hızı üzerindeki etkileri incelenmiştir. Elde edilen sonuçlar ışığında tamoksifenin salım hızının arttığı, bununla birlikte idarubisinin salım hızında herhangi bir artma olmadığı belirlenmiştir. ADR'nin yıkım özellikleri için de lipazın etkileri çalışılmış ve yıkımın lipaz eklendiği zaman arttığı tespit edilmiştir. Çalışmanın son aşamasında boş ve ilaç yüklenmiş ADR'nin MCF-7 meme kanseri hücre hattı üzerindeki sitotksik etkileri XTT proliferasyon kiti kullanılarak belirlenmiştir. ADR'nin MCF-7 hücre hatlarında toksik etkiye neden olmadığı bununla birlikte ilaç yüklenmiş yapıların serbest ilaç uygulamasına oranla daha fazla toksik etki yarattığı belirlenmiştir. Tüm bu sonuçlar tasarlanan aşırı dallı polimerin ilaç salımında etkili şekilde kullanıldığını göstermiştir.

Anahtar Kelimeler: Kontrollü İlaç Salımı, Aşırı Dallı Polimerler, İdarubisin, Tamoksifen.

To My Family

ACKNOWLEDGEMENTS

I would like to express my sincere appreciation to my supervisor Prof. Dr. Ufuk Gündüz for her encouragement, valuable support and advises throughout my study. I would also thank to her for her humanity and kindly attitudes towards me.

I wish to express my sincere thanks to my co-supervisor Prof. Dr. Güngör Gündüz for his endless support, advice and deep experiences which is very precious for my future carrier. I would not succeed synthesis and characterization of polymer without his sincere guidance.

Special thanks go to my dear friends Sevilay Akköse, Mine Nuyan, Ömer Faruk Gerdan, Derya Özer, Yaprak Dönmez and Pelin Sevinç, for their unlimited friendship which is very precious for me.

I am grateful to Özlem İşeri, Meltem Kars, Gökhan Kars for sharing their experiences, advises and for their friendship throughout my study in Lab-206. I also wish to thank my lab friends Pelin Mutlu, Petek Şen, Gülşah Pekgöz, Demet Demetçi for their support, help and sincere friendship.

The greatest thank goes to my family for their endless support, love and care throughout my life. Everything would have been harder without them.

I would like to thank the staff of METU Central Laboratory R&D Center and Molecular Biology Biotechnology R&D Center for their kindly attitude, understanding and their sincere advises that was valuable for my study.

Fourier Infrared Spectroscopy, Nuclear Magnetic Resonance, Gel Permeation Chromatography analysis was carried on in METU Central Laboratory R&D Center. High Performance Liquid Chromatography analysis was done in METU Molecular Biology Biotechnology R&D Center, Ankara.

This project was supported by Middle East Technical University (2006-07-02-00-01) and Türkiye Bilimsel ve Teknolojik Araştırma Kurumu (TUBİTAK, 107T179).

TABLE OF CONTENTS

ABSTRACT……iv
ÖZ……vi
ACKNOWLEDGEMENTS……ix
TABLE OF CONTENTS……xi
LIST OF TABLES……xiv
LIST OF FIGURES……xv
ABBREVIATIONS……xviii
CHAPTER
1.INTRODUCTION……1
1.1 Biology of Cancer……1
1.1.1 Development of Cancer Cells……2
1.2 Cancer Chemotherapy……3
1.2.1 Types……4
1.2.2 Route of Delivery……5
1.3 Drug Delivery Systems……5
1.3.1 Controlled Drug Delivery Systems……7
1.3.2 Nano Drug Delivery Systems……10
1.4 Polymers……12
1.4.1 General Concepts……12
1.4.2 Polymers in Controlled Drug Delivery Systems……13
1.4.3 Controlled Release Mechanisms from Polymers……14
1.5 Dendritic Polymers……15
1.5.1 Synthesis of Dendrimers……17
1.5.2 Synthesis of Hyperbranched Polymers……18
1.5.3 Aliphatic Polyesters ……19
1.6 Dendritic Polymers in Drug Delivery Applications……20
1.7 Degradation of Aliphatic Polyesters by Lipases ……22
1.8 Role of Lipids in Drug Delivery……23
1.8.1 Fatty Acids in Drug Delivery Studies……23

1.8.2 Ricinoleic Acid.....24
1.9 Tamoxifen in Cancer Therapy.....25
1.10 Idarubicin in Cancer Therapy.....26
1.11Objectives of the Study.....27
2. MATERIALS AND METHODS.....29
2.1 Materials.....29
2.1.1 Materials for Hyperbranched Resin Synthesis.....29
2.1.2 Materials for Drug Loading, Release and Cell Culture Studies.....29
2.2 Dehydration of Raw Materials 30
2.3 Extraction of Fatty Acids.....30
2.4 Hyperbranched Resin Synthesis (HBR) 32
2.5 Purification of HBR 38
2.6 Loading of Tamoxifen and Idarubicin into HBR.....38
2.7 Degradation of HBR.....40
2.8 Drug Release Studies.....41
2.9 Chemical Characterization.....42
2.9.1 Fourier Transform Infrared (FTIR) Spectroscopy.....42
2.9.2 Gel Permeation Chromatography (GPC).....43
2.9.3 Nuclear Magnetic Resonance (NMR).....43
2.9.4 Particle Size Analysis and Zeta Potential Measurements.....43
2.9.5 High Performance Liquid Chromatography (HPLC) 43
2.10 Cell Culture 44
2.10.1 Cell Culture Medium Preparation and Passaging Cell Cultures.....44
2.10.2 Cell Proliferation Assay with XTT Reagent 45
2.10.3 Viable Cell Count 46
2.10.4 Statistical Analysis 46
3. RESULTS AND DISCUSSION.....47
3.1 Synthesis and Purification of Hyperbranched Resin.....47
3.1.1 Synthesis of Hyperbranched Resin.....47
3.1.2 Purification of Hyperbranched Resins.....48
3.2 Chemical Characterization.....49
3.2.1 Fourier Transform Infrared (FTIR) Spectroscopy….....49
3.2.2 Molecular Weight Determination.....51

3.2.3 Liquid ^{13}C NMR Analysis of HBR.....52
3.3 Use of HBR in Drug Delivery…….....55
3.3.1 *In vitro* Degradation of HBR.....55
3.3.2 Tamoxifen and Idarubicin Loading Studies.....58
3.3.2.1 Preliminary Experiments.....58
3.3.2.2 Loading Efficiency.....59
3.3.3 Chemical Characterization of Drug Loaded HBR.....62
3.3.3.1 FTIR Results.....62
3.3.3.1.1 Tamoxifen Loaded HBR.....62
3.3.3.1.2 Idarubicin Loaded HBR.....64
3.3.3.2 Particle Size Distribution and Zeta Potential.....65
3.3.4 Drug Release Study.....69
3.3.4.1 Tamoxifen Release.....69
3.3.4.2 Idarubicin Release.....71
3.3.5 Cytotoxicity.....73
3.3.5.1 Cytotoxicity of Empty and Drug Loaded HBR.....74
3.3.5.2 Cytotoxicity of Free Drugs and Drug Loaded HBR.....76
4. CONCLUSION.....82
4.1 Recommendations.....84
REFERENCES.....85
APPENDICES.....98
A. ACID NUMBER DETERMINATION.....98
B. PARTICLE SIZE DISTRIBUTION.....99
C. CELL PROLIFERATION GRAPHS AND LOGARITHMIC EQUATIONS.....105

LIST OF TABLES

TABLES

Table 1.1 The problems of the conventional drug therapies.....6
Table 3.1 Molecular weight and polydispersity of HBR.....52
Table 3.2 Particle Size (nm) and Zeta Potential (mV) results..... 68
Table 3.3 IC_{50} profiles HBR formulations 75
Table 3.4 IC_{50} concentrations of HBR formulations and free drugs.....78
Table B.1. Experimental conditions for particle size measurements.....99
Table B.2. Average particle size distribution data and average particle size values of HBR sample.....100
Table B.3. Average particle size distribution data and average particle size values of HBR-TAM (2.66μg/mg).....101
Table B.4. Average particle size distribution data and average particle size values of HBR-TAM (8μg/mg). 102
Table B.5. Average particle size distribution data and average particle size values of HBR-IDA (2.66μg/mg)..... 103
Table B.6. Average particle size distribution data and average particle size values of HBR-IDA (8 μg/mg).....104

LIST OF FIGURES

FIGURES

Figure 1.1 Conventional and desired drug release graph.....8
Figure 1.2 Illustration of enhanced permeation and retention effect.....9
Figure 1.3 Schematic representations of nanoparticles that are studied for cancer chemotherapy 11
Figure 1.4 Controlled release mechanisms of polymers.....15
Figure 1.5 Major macromolecular classes of polymer..... 16
Figure 1.6 Schematic representations of convergent and divergent dendrimers…...17
Figure 1.7 Representation of hyperbranch formation of AB_2 type of monomers.....18
Figure 1.8 Chemical structure of ricinoleic acid.....24
Figure 1.9 Chemical structure of tamoxifen.....25
Figure 1.10 Structure of idarubicin hydrochloride.....26
Figure 2.1 Saponification reaction of the castor oil.....31
Figure 2.2 Fatty acid production by using sulfric acid.....32
Figure 2.3 Experimental setup of the hyperbranched polyesters and HBR synthesis.....34
Figure 2.4 Theoretical representation of the synthesis of HBP-G_1.....35
Figure 2.5 Synthesis and theoretical representation of HBP-G_2.....36
Figure 2.6 Theoretical representation of hyperbranched resin.....37
Figure 2.7 Calibration curve of idarubicin by UV-vis.....39
Figure 2.8 Calibration Curve of tamoxifen.....40
Figure 2.9 Calibration curve of idarubicin determined by HPLC.....42
Figure 3.1 FTIR spectra of ricinoleic acid.....50
Figure 3.2 FTIR spectra of HBP-G_2 and HBR.....51
Figure 3.3 Functional carbon atoms in HBR structure.....54
Figure 3.4 ^{13}C NMR results of HBR structure.....54
Figure 3.5 Hydrolytic and enzymatic degradation of HBR 57
Figure 3.6 Loading efficiency of tamoxifen 59
Figure 3.7 Loading efficiency of idarubicin 60
Figure 3.8 The comparison of the loading efficiency of tamoxifen and idarubicin.....62

Figure 3.9 IR spectra of HBR and HBR-TAM.....64
Figure 3.10 The comparison of FTIR spectra of HBR and HBR-IDA.....65
Figure 3.11 Size distribution graph of the HBR-IDA and HBR-TAM.....67
Figure 3.12 Cumulative release of tamoxifen form HBR 70
Figure 3.13 Cumulative release of tamoxifen in the presence of SDS and lipase.....71
Figure 3.14 Cumulative release of idarubicin from HBR.....72
Figure 3.15 Cell Proliferation profiles after 96h incubation with HBR, HBR-IDA, HBR-TAM.....74
Figure 3.16 Cell Proliferation profiles after exposure to idarubicin and HBR-IDA ….77
Figure 3.17 Cell Proliferation profiles after exposure to tamoxifen and HBR-TAM....79
Figure C.1 Cell Proliferation after incubation with 96 h of empty HBR.....105
Figure C.2 Cell Proliferation after incubation with 96 h of HBR-TAM according to HBR concentration.....105
Figure C.3 Cell Proliferation after incubation with 96 h of HBR-TAM according to the tamoxifen concentration.....106
Figure C.4 Cell Proliferation after incubation with 72 h of HBR-TAM according to the HBR concentration.....106
Figure C.5 Cell Proliferation after incubation with 72 h of HBR-TAM according to the tamoxifen concentration.....107
Figure C.6 Cell Proliferation after incubation with 48 h of HBR-TAM according to the HBR concentration.....107
Figure C.7 Cell Proliferation after incubation with 48 h of HBR-TAM according to the tamoxifen concentration.....108
Figure C.8 Cell Proliferation after incubation with 96 h of HBR-IDA according to the HBR concentration.....108
Figure C.9 Cell Proliferation after incubation with 96 h of HBR-IDA. Logarithmic equation determinedaccording to the idarubicin concentration.....109
Figure C.10 Cell Proliferation of MCF-7 after incubation with 72 h of HBR-IDA according to the HBR concentration.....109
Figure C.11 Cell Proliferation after incubation with 72 h of HBR-IDA according to the idarubicin concentration.....110

Figure C.12 Cell Proliferation after incubation with 48 h of HBR-IDA according to the HBR concentration.....110
Figure C.13 Cell Proliferation after incubation with 48 h of HBR-IDA according to the idarubicin concentration.....111
Figure C.14 Cell Proliferation after incubation with 96 h of tamoxifen.....111
Figure C.15 Cell Proliferation after incubation with 72 h of tamoxifen.....112
Figure C.16 Cell Proliferation after incubation with 48 h of tamoxifen.....112
Figure C.17 Cell Proliferation after incubation with 96 h of idarubicin.....113
Figure C.18 Cell Proliferation after incubation with 72 h of idarubicin.....113
Figure C.19 Cell Proliferation after incubation with 48 h of idarubicin.....114

ABBREVIATIONS

DMF	Dimethylformamide
DMPA	Dimethylol propionic acid
DMSO	Dimethyl sulfoxide
Dipenta	Dipentaerythritol
FTIR	Fourier transform infrared spectroscopy
GPC	Gel permeation chromatography
HBP	Hyperbranched Polyester
HBR	Hyperbranched Resin
HBR-IDA	Hyperbranched Resin-Idarubicin
HBR-TAM	Hyperbranched Resin-Tamoxifen
HPLC	High performance liquid chromatography
IDA	Idarubicin
Mn	Number average molecular weight
Mw	Weight average molecular weight
NMR	Nuclear magnetic resonance
PBS	Phosphate buffered saline
PDI	Polydispersity index
p-TSA	Para-toluene sulfonic acid
RT	Room temperature
SEM	Standard error of the mean
SDS	Sodium dodecyl sulfate
TAM	Tamoxifen
XTT	XTT proliferation kit

CHAPTER 1

INTRODUCTION

1.1 Biology of Cancer

Cancer is formed by breaking down of the regulatory systems of normal cells. Cells grow and divide without responding appropriately to the signal that control normal cell behavior and start to invade to the normal tissues and finally spread whole body. There are also many differences from one type of the cancer to the other which make it impossible to identify the properties of the cancer in one type of definition (Cooper 2000, Karp 2002).

Cancer cells might be transformed into two types of tumors: benign or malignant. Benign tumors are similar to the tissue which they came from, they grow slowly and they do not invade to the other tissues. However, a malignant tumor invades to the other type of tissues and spread to body by circulatory lymphatic systems (metastases). Malignant cells often express the gene of telomerase which by this way the end of chromosome after DNA replication does not shorten (Purves *et al.* 2001, Cooper 2000).

Normal human cells are named according to the embryonic tissue origin, which is also be used for naming of tumor cells. If malignant tumors are derived from endoderm or ectoderm they classified as carcinomas and if they derived from mesoderm then they are named as sarcomas (Alberts et al. 2001).

1.1.1 Development of Cancer Cells

Development of cancer cell is a multi-step of process. The first step is the tumor initiation which could be the result of genetic alteration and abnormal cell proliferation of a single cell. By genetic alteration and deformation a typical cancer cell fail to respond apoptosis which make cells immortal that distinguishes many cancer cells from normal cells. Some tumor mutants continue to progress by additional mutations and have a success over other type of tumor populations which the ratio of the number of survival becomes higher than the rest. Selection makes them dominant within the tumor population (Cooper 2000, Lodish *et al.* 2000, Alberts *et al.* 2001). Even after they have become malignant, cancer cells continue to accumulate mutations and gain new properties which make them even more dangerous (Karp 2002).

Malignant tumors secrete chemical signals and growth factors that cause blood vessel growth, by this way oxygen and nutrients are supplied to the tumor. The process called angiogenesis. Angiogenesis can be summarized in a few steps: degradation of the basal lamina that surrounds a nearby capillary, migration of endothelial cells lining the capillary into the tumor, division of these endothelial cells, and formation of a new basement membrane around the newly elongated capillary (Purves et al. 2001, Lodish *et al.* 2000).

During the development of cancer some morphological changes occur in cytoplasm which involves organization of cytoskeleton and cell surface. Different from normal cells, cancer cells become less adhesive and motility activity continues with proliferation even contact with the neighboring cells. These changes provoke metastasis and cells break their contacts with other cells and other barriers. As a result, metastatic cells invade to circulation and they adjoin to other type of tissues (Karp 2002, Lodish *et al.* 2000.)

Carcinogens and epigenetic changes that cause an irreversible damage are called tumor initiators. In general the genetic error occurs by alteration of molecular structure of DNA or forming DNA adduct between chemical carcinogen and a

nucleotide in DNA. Solar ultraviolet radiation is the initiating agents that cause skin cancer. The carcinogens in tobacco smoke are also initiator agents that cause various types of cancers. Another type of carcinogen is the tumor promoters. They are non-mutagenic and are not carcinogenic alone. They induce tumor formation with a dose of initiator that is too low to be carcinogenic alone. Estrogen hormones could be example to the tumor promoters. They might cause endometrial cancer under the condition of excess stimulation (Cooper 2000, Kufe *et al.* 2003).

Generally transformation of cancer occurs by alteration in two kinds of genes: tumor suppressor genes and oncogenes. Tumor suppressor genes encode proteins that sustain cell growth and prevent cells being malignant. The absence and mutation of these genes are correlated with tumor growth. On the contrary, a gene that encodes proteins which promote loss of growth control and convert the cells into the malignant state is called oncogenes. Oncogenes are activated by mutation of proto-oncogenes which have various functions in normal cell activities (Karp 2002).

In addition to genetic modifications, the causes of many cancers are associated with chromosomal transformations and reorganizations involving deletion, duplication which causes the changes in the activity of the genes (Demetçi 2007).

1.2 Cancer Chemotherapy

To treat cancer, three major ways are commonly used: radiation therapy, surgery and chemotherapy. Due to limitations of other techniques, chemotherapy is the most efficient way to treat the metastatic cancers.

During last 50 years almost 500.000 of natural and synthetic compounds have been tested for anti-cancer activity but only about 25 of these drugs are used today which shows the difficulty of the success of the therapy (Denny 2005). Current chemotherapy drugs in general, work by blocking cell division or causing apoptosis mainly targeting fast dividing cells which make the drug as cytotoxic (Wikipedia 2008).

1.2.1 Types

Chemotherapy drugs are categorized as:

- **Alkylating agents:** These agents add alkyl groups to electronegative groups in the cells and permanently attach to the DNA, distorting its shape, prevent cell division process by cross-linking and breaking the DNA strands and cause abnormal base pairing. Cyclophosphamide, melphalan, procarbazine and bisulfan are some of the commonly used alkylating agents.

- **Antimetabolites:** These compounds behave as purines or pyrimidines and incorporate into bulding blocks of DNA or RNA to inhibit cell divisions of the dividing tumor cells. 6-mercaptopurine and 5-fluorouracil (5-FU) are two commonly used antimetabolites that could be used various types of cancer.

- **Anthracyclines:** These are working by forming free oxygen radicals that break DNA strands and inhibit DNA synthesis and function. Anthracyclines form complex with DNA and enzyme to inhibit topoisomerase enzyme. Topoisomerase causes supercoiling of DNA, allows DNA repair, transcription and replication. Doxorubicin, epirubicin, idarubicin are the examples of the commonly used anthracyclines.

- **Antitumor antibiotics:** Function these drugs are similar with anthracyclines. In general, this class of drug is used in combination chemotherapy. Bleomycin is the example of commonly used antitumor antibiotics.

- **Monoclonal antibodies:** This treatment was accepted in 1997 by Food and Drug Administration (FDA). They attach to the tumor cells and provoke immune system reaction; by this way tumor specific antigens are targeted. They also prevent the growth of cancer cells. Alemtuzumab (Campath), bevacizumab (Avastin), cetuximab (Erbitux) are the examples.

- **Platinum:** These agents work by cross-linking with DNA subunits and malfunctioning DNA synthesis transcription and function. Cisplatin is the most commonly used platinum-based metal derivative.

- **Plant Alkaloid:** They are plant derivatives and these types of drugs are classified into four categories: topoisomerase inhibitors (Type I and Type II inhibitors interfere with DNA transcription, replication and function to prevent DNA supercoiling, e.g. camptothecins), vinca alkaloids (inhibit tubulin assembly in the M phase of cell cycle, e.g. vincristine, vinblastine), taxanes (microtubules function is inhibited, e.g. paclitaxel, docetaxel) and epipodophyllotoxins (effective in G1 and S phase of cell cycle, e.g. etoptoside) (Mesothelomia 2008, Wikipedia 2008).

In addition to chemotherapy, hormonal therapy is also useful for some types of tumors. Although the mechanism does not clarify, steroid hormones disrupt the growth of hormone sensitive cancer types. As an example, tamoxifen which is a selective estrogen dependent modulator is used in breast cancer therapies (Oncolink 2001).

1.2.2 Route of Delivery

Most of the chemotherapeutic drugs are given by injection through the vein (intravenously). In some cases drug could also be injected through muscle, skin or directly to the tumor site. Besides there are numerous agents like melphalan or tamoxifen that could be given by orally. For skin cancers chemotherapy could be given topically by lotions or gels or could directly be applied onto the skin surface (Wikipedia 2008, Jelic 2005).

1.3 Drug Delivery Systems

In all types of drug delivery systems, the main principle is ability to target and kill cancer cells without damaging healthy cells. However, in conventional therapies drug is distributed to whole body and it leads to serious side effects. In addition, in order

to obtain satisfactory pharmacological reaction, high dose of drug has to be applied to the patient (Nori *et al*. 2004, Peppas *et al*. 2004). Table 1.1 summarizes the most common problems in conventional chemotherapy.

Table 1.1 The problems of the conventional drug therapies (Allen *et al*. 2004).

Problem	***Statement***
Poor biodistribution	Since there is no mechanism to inhibit the distribution of the drug to whole body, normal tissues are affected and dose limiting side effects are observed (like cardiotoxicity in doxorubicin therapies).
Unwanted pharmacokinetic properties	Toxic drugs are cleared so rapidly by the kidney. In order to obtain desired drug level, high doses should be given in continuous time periods.
Poor solubility	By conventional chemotherapy methods, poorly soluble drugs might precipitate in aqueous solutions.
Tissue damage on extravasation	Uncontrolled extravasation of cytotoxic drugs leads to tumor necrosis and tissue damage.

Table 1.1 The problems of the conventional drug therapies (Allen *et al*. 2004) (Continued).

Early and rapid breaking down	Because of the physiological differences drug might be broken down. As an example, camptothecins break down at physiological pH.
No targeting to selected tissues	Since no targeting elements are present, drug could distribute to the normal tissues which decreases the dose of the administered drug in cancer cells. Low concentration of the drug might lead to suboptimal therapeutic effects.

1.3.1 Controlled Drug Delivery Systems

Novel therapeutic technologies are based on rational design and highly targeted delivery of the chemotherapeutic drugs. More effort is required for drug designing, toxicological testing or finding appropriate drug vehicles instead of application of non-specific drug compositions (Razzacki *et al*. 2003).

The aim of many drug delivery systems is to maintain the desired dose of drug in blood in long period. In conventional therapies due to the problems that were mentioned before, it is impossible to sustain the dose in desired time periods (Figure 1.1). In controlled drug delivery systems it is designed by considering the key points; the agents should acted. For example by using both hydrophilic and hydrophobic carriers, solubility of poorly soluble drugs could be sustained in aqueous medium. Controlled release property could also inhibit accidental extravasations and tissue damages. In addition, carriers protect drug from early breakdown and pharmacokinetic behavior of the drugs are altered. By these systems since drug

does not spread to whole body, side effects are reduced and it did not reach to non-targeted tissues (Allen *et al.* 2004).

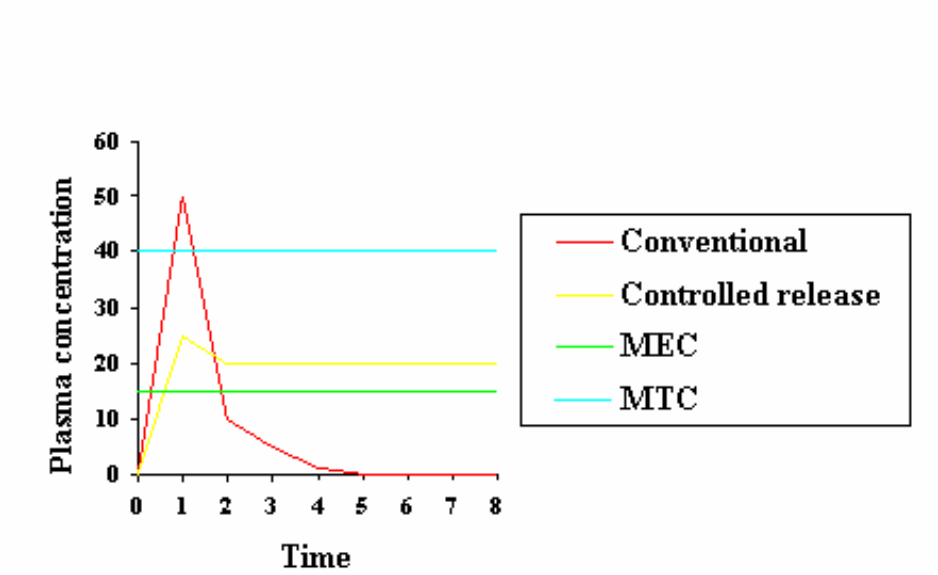

Figure 1.1 Conventional and desired drug release profiles. (MEC; Minimum efficient concentration, MTC; maximum tolerable concentration) (Drugdel.com 2005).

There are many structural and physical differences between cancer and normal cells which can be used for the designing of drug delivery systems. There are three destinations for targeting these systems; tumor cells, extracellular space and tumor vasculature. Tumor vasculature forms blood vessels and creates angiogenesis in order to sustain the growth of tumor. Since cancer tissues have the enhanced permeation and retention effect (EPR), nanoparticles and high molecular weight molecules accumulated to the tumor site with higher concentration than the normal tissues (Figure 1.2). To avoid extravasation of the particles into healthy tissues, the optimum size has to be determined. The endothelium of healthy blood vessels has a pore size 2nm and postcapillary venules have 6nm of pores. The vasculature pore size of tumor tissue is between 100 to 780nm. Therefore optimum size of the particles should be in range between 50-150nm sizes (Ulbrich *et al.* 2003, Marcucci *et al.* 2004).

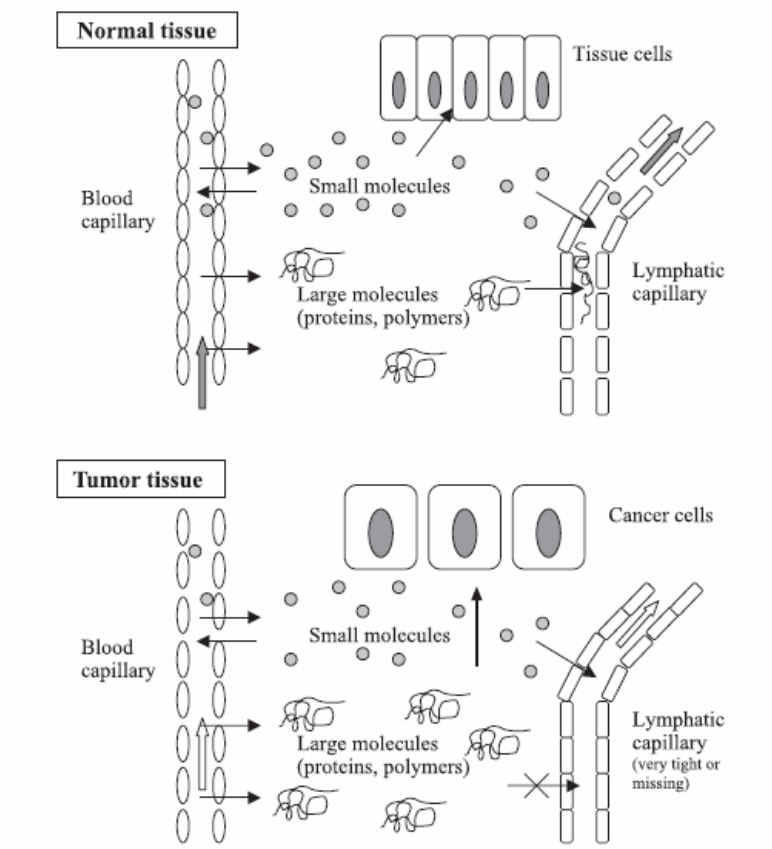

Figure 1.2 Illustration of enhanced permeation and retention effect (EPR) in tumor cells. (Ulbrich *et al.* 2003).

As a result of passive or active targeting through the cells, particles are internalized by endocytosis upon interaction of ligands with cell surface receptors. Internalized drug loaded particles then accumulated into the lysosomes. In lysosomes particles effected by enzyme and/or pH dependent disintegration makes the drug diffuse out from the system. Drug is released from these organelles and passes through the cytosol or nucleus in order to show its efficiency (Marcucci *et al.* 2004).

It has been known that tumor environment has more different conditions than normal healthy tissues like pH, presence of lipases, enzymes and oxidizing agents. In recent years the studies in certain type of tissues like breast cancer tissues have been

shown that tumor cells have higher enzymatic activity with post-translational modifications and up and down regulation mechanisms (Jessani *et al.* 2004). These type of differences results in rapid degradation of the particles in tumor microenvironment and in certain cases particles could not internalized into the cells but drug enter through passive diffusion or active transport (Marcucci *et al.* 2004).

1.3.2 Nano Drug Delivery Systems

The need of delivering drug to the targeted site with desired therapeutic efficiency encouraged researchers to develop new vehicles for drug delivery technology. A variety of drug carriers are FDA approved or in clinical research process including polymeric nano and micro particles, microcapsules, liposomes. Besides, there are also many new drug delivery systems that are in progress including implanted chemotherapy wafers, inhalation of polymeric materials to sustain gene or drug delivery to the lung, ultrasound mediated drug delivery, etc. (Orive *et al*. 2005, Singh 2006).

The terms “nanoparticle” and “microparticle” are referred to the particles in nanometer (<1μm) and micrometer (1-1000μm). Nanoparticles and microparticles are most commonly used vehicles for the drug delivery studies. Especially nanoparticles have numerous advantages due to the size advantage. They have smaller surface to volume ratio than microparticles, as a result greater proportion of the drug can access to the internal aqueous phase. In addition, water can penetrate into the particles more efficiently which increase the diffusion of the drug to the external medium. Second advantage is the fate of the particles after injection. Nanoparticles can easily circulate through the vasculature and does not cause any size dependent embolism as microparticles do. They can also cross through certain size dependent barriers like blood brain barrier and sustains the delivery (Kohane 2006).

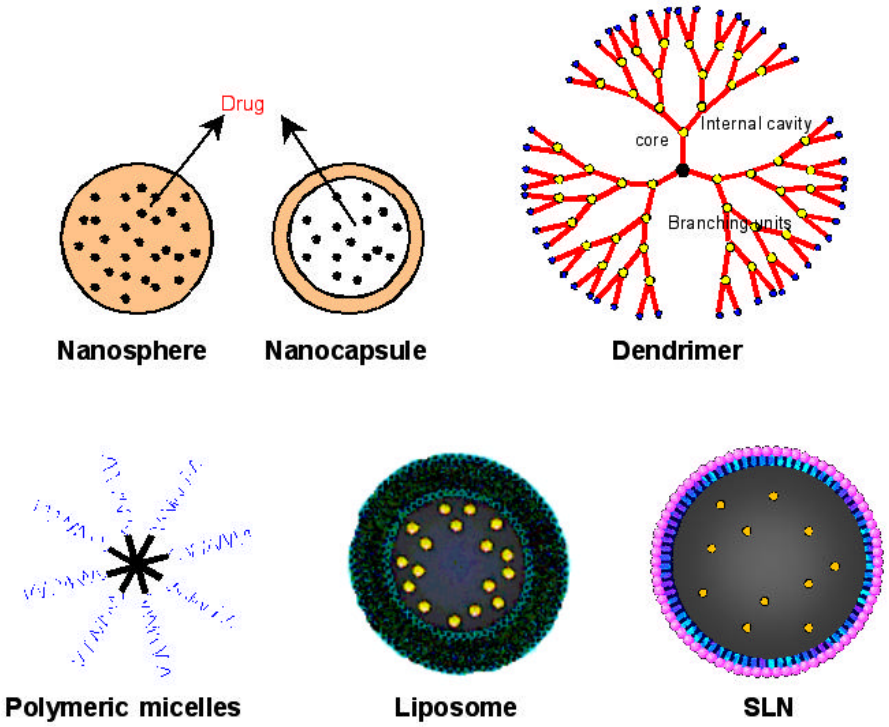

Figure 1.3 Schematic representations of nanoparticles that are studied for cancer chemotherapy (Orive *et al*. 2005).

Depending on the aim of the therapy numerous types of nanoparticles could be used. Recently used nanoparticles are shown in Figure 1.3. The main characteristics of these particles are listed below:

- **Nanocapsules:** They are vesicular systems, polymeric membrane surrounds and form capsules.
- **Nanospheres:** Polymeric matrix is dispersed uniformly and physically.
- **Micelles:** They are both hydrophilic and hydrophobic and can be safely associated in aqueous medium.
- **Liposomes:** They are formed from phospholipids and cholesterol which forms an artificial membrane spheres.
- **Ceramic Nanoparticles:** They are composed from inorganic materials like silica or titania.

- **Dendritic Polymers:** Macromolecules that are branched around inner core.
- **SLN particles:** Composed of solid lipid particles (Orive *et al*. 2005).

1.4 Polymers

1.4.1 General Concepts

Polymers are structures of high molecular weight macromolecules and they are composed from repetitive units called monomers. Polymers could be divided as biological polymers and non-biological polymers, in other words synthetic polymers. Some of the biological polymers are starch, cellulose and proteins. Science of synthetic polymer technology was begun in 1930s and today polymer industry is tremendously developed and could be used in various areas of science and industry (Bellmeyer 1984).

Polymer formation by repetition of monomers could be linear, branched, cross-linked or network structures depending on the interconnection of monomers. The most distinguishing property of polymers from other low molecular weight species is the distribution of chain length, means molecular weight distribution. Even different determination methods are used; experimental measurement of polymers always gives the average values which are an important parameter for characterization processes (Billmeyer 1984). By changing molecular weight, physical properties of the polymers could also be differed like toughness, viscosity, melting temperature, tensile strength, etc.

Polymerization were divided by Flory (1953) and Carothers 1940) into two groups; namely condensation and addition polymerization. In addition or chain reaction polymerization initiators could be an ion or free radical. Polymerization process occurs in a very short time with addition of monomers to the growing chain (Billmeyer 1984). In condensation polymerization technique, polymers are produced from carboxylic acids and their derivatives like esters and acid chlorides. By the end of polymerization some of the by products are formed such as water, ammonia, HCl, etc. Unlike addition type of polymerization in condensation polymers all monomers

are present in the polymers and synthesis of polymers occurs in slow reaction. By the end of the synthesis low molecular weight polymer is formed with active end groups that can be used for further reactions. There are various types of condensation polymers, the most common ones are polyamides, polyesters, polycarbonates, phenolic resins, urethanes (Billmeyer 1984, Reusch 1999).

Due to various advantages and facilities of polymers these macromolecules are also preferred in medical applications. They could be used in tissue engineering, artificial organs, dental fillings, bone replacement and repair, lenses, drug delivery studies, gene therapy studies, etc (Hule 2007).

1.4.2 Polymers in Controlled Drug Delivery Systems

Since the earliest drug delivery systems in 1970s, polymeric systems have been still the most preferred synthetic molecules in drug delivery technology. The studies show that these biomaterials are effective in drug targeting, have low systemic toxicity, improves absorption rates and they protect drug from an early degradation. In addition, polymers have unique characteristics which make hem special for drug delivery studies. Firstly, they have wide range of molecular weight distributions and have special properties related with phase transitions. They can interact and condense when heated and able to dissolute in various conditions. Besides, they have biodegradation property and by manipulating chemical, structural or physical properties of biodegradation could be controlled. Major factor that affect degradation are chemical structure, composition, presence of ionic groups, molecular weight distribution, physicochemical factors, processing conditions, etc (Vogelson 2008, Noble 2004, Peppas 1997).

The earliest polymer that has been worked by researchers was chosen because of their properties. For example poly(urethanes) were used for elasticity, poly(ethylenes) were preferred for its toughness and lack of swelling and poly(vinyl pyrrolidone) was used for suspension capabilities. Beside these polymers, in recent years other type of the polymers are mostly used, like poly(vinyl alcohol),

poly(ethylene glycol), polylactides, poly(lactide-co-glycolide), polyanhydrides (Peppas 1997).

1.4.3 Controlled Release Mechanisms from Polymers

There are three types of mechanisms that sustain the delivery of the drug; diffusion, degradation and swelling followed by diffusion (Figure 1.4). The three mechanisms could be achieved by increasing of the pore sizes of the polymer by changing the physiological condition of the external environment. By changing pH, ionic strength, chemical species, enzyme substrate, magnetic, thermal, electrical and ultrasound irradiation properties controlled release mechanisms are stimulated by increasing pore size, swelling or degradation of the polymers.

In diffusion process drug could pass through the pores or between polymer chains. In monolayer type of polymers drug is directly diffused out from the system to the external environment. Diffuse rate slows down by increasing the time of diffusion. For membrane controlled devices solid drug, highly dilute or highly concentrated drug are encapsulated into the core surround by polymeric membrane. Drug is released by rate controlling diffusion.

Drug encapsulated hydrophilic polymers that are dry or glassy could swell when placed in aqueous environment of body fluid or when changing physiological conditions. These types of systems are ideally used for oral delivery.

In most of the controlled delivery devices, biodegradable polymers are used. Polymers could be hydrolytically or enzymatically degraded or be broken down by metabolic processes. Poly(lactides co-glycolides), poly(glycolides) are the examples of biodegradable polymers (Noble 2001, Peppas 1997).

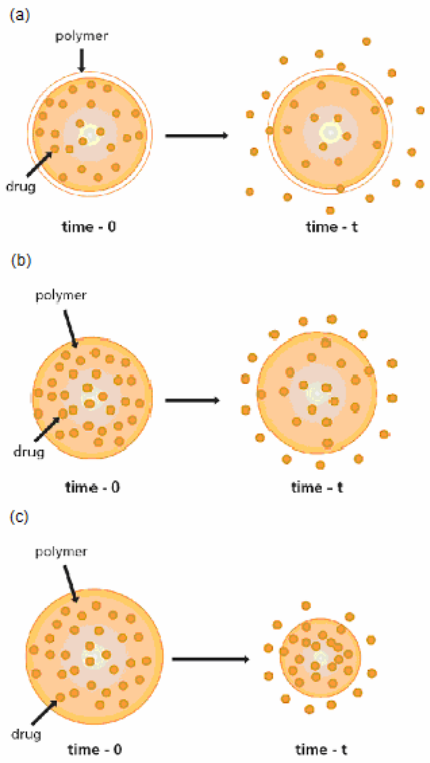

Figure 1.4 Controlled release mechanisms of polymers: diffusion (a), swelling (b), erosion/biodegradation (c) (Sigma-Aldrich 2008).

1.5 Dendritic Polymers

Dendritic polymers are the fourth major class of macromolecules after linear, crosslinked and branched polymers (Figure 1.5). These polymers are divided into four subgroups namely; hyperbranched polymers, dendrigraft polymers, dendrons and dendrimers (Tomalia *et al*. 2002). Dendritic polymers composed of core molecule with two or more functional groups which surround the core with branched repeated groups (AB_X type). Each surrounding of repetitive elements forms a generation.

The term dendrimer is orginated from Greek words “dendron” (tree) and “meios” (part) (Bat 2005). They are nanosized particles that are highly and uniformly branched structure. They are composed of central core branching units and terminal

groups and synthesis is obtained by multi-step process. Regularly branched well defined structures, low polydispersity index and multifunctional surface offers advantage in various areas.

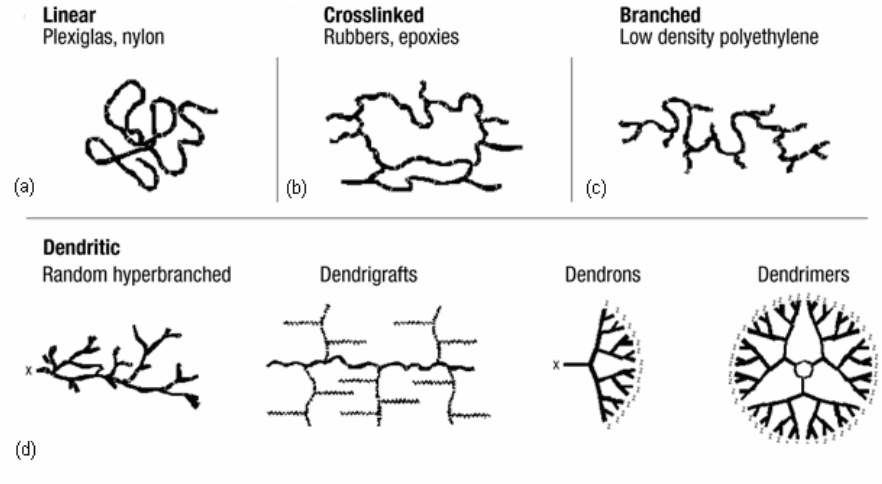

Figure 1.5 Major macromolecular classes; linear (a), crosslinked (b), branched (c), dendritic (d) (Tomalia *et al*. 2002).

Hyperbranched polymers have also branched structure with nanocavities but the difference from dendrimers is that they have nonsymmetrical polydispersed structures. In addition, syntheses of hyperbranched polymers are more convenient so they can be synthesized by less expensive methods with higher yields (Paleos *et al.* 2007).

Due to various uniform properties of dendritic polymers they have different application areas including drug delivery studies, imaging materials, diagnostics, optoelectronics, unimolecular nanoreactors (Fréchet *et al.* 2003).

1.5.1 Synthesis of Dendrimers

Dendrimers could be synthesized by two methods; divergent and convergent methods. Divergent synthesis which was firstly developed by Tomalia, occurs by polymerization of core molecules with the monomers by forming branching structure through outer region which forms generation. In this method, large quantities of polymer could be synthesized, however to sustain perfect generation excess monomers has to be used which lead to the chromatographic separation after each generation. As a result of divergent synthesis, some side reactions might also be observed and incomplete end branches might be synthesized. To eliminate these problems, another method was developed by Hawker and Fréchet which was named as convergent synthesis. By this method monomers are polymerized stepwise but starting from end groups to the inwards. As a result of convergent dendrimer formation, no excess purification steps are required and unwanted incomplete formations are minimized. Since polymerization is started from end groups, the formation of the generation is more limited than the divergently synthesized dendrimers (Swenson *et al* 2005, Klajnert *et al*. 2001). The illustration and properties of both divergent and convergent methods are given in Figure 1.6.

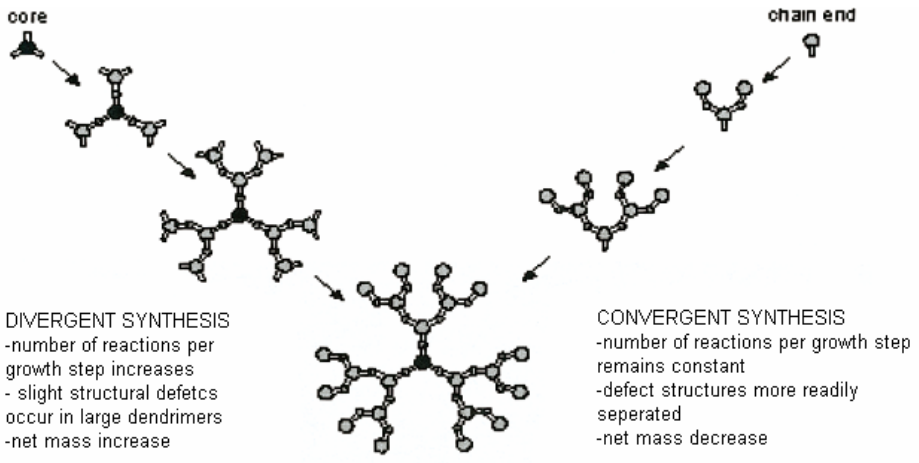

Figure 1.6 Schematic representation of convergent and divergent dendrimers (Tomalia *et al*. 2002).

1.5.2 Synthesis of Hyperbranched Polymers

As discussed previously, hyperbranched polymers and dendrimers have many common properties like several terminal groups, globular shape and large extent of end functional groups which cause higher solubility. In order to synthesize perfectly regular structure of dendrimers, convergent or divergent synthesis methods are used that requires time consuming purification. However for polymerization of hyperbranched polymers, one-step polymerization technique could be used such as by using AB_x type of monomers ($x \leq 2$), self-condensing vinyl polymerization and radical alternating copolymerization (Bharathi *et al.* 2000, Cheng 2003). The polymerization of AB_x type of monomers without controlling over the growth process was first discussed by Flory (Malmström 1995). The representation of polymerization of AB_x type monomers was illustrated in Figure 1.7.

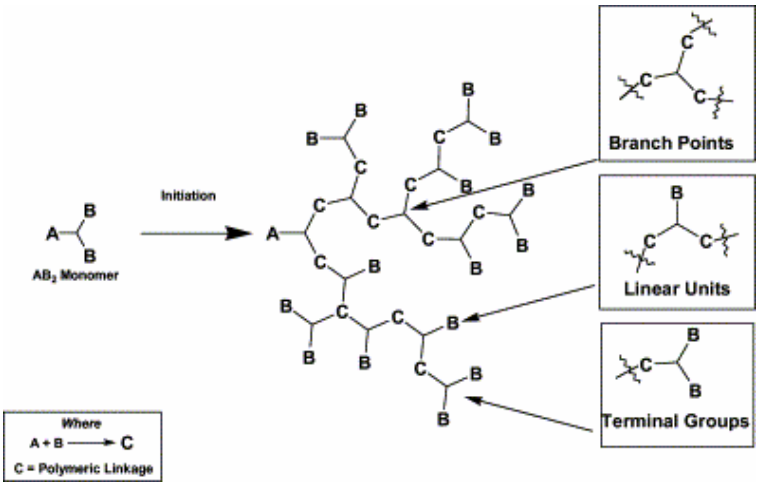

Figure 1.7 Representation of hyperbranch formation of AB_2 type of monomers (Yates *et al*. 2004).

The generation of hyperbranched polymers by one-step procedure provides larger yields, however controlling of molecular weight distribution is an important parameter, since molecular mass could be highly distributed. Molar mass and

polydispersity index of hyperbranched polymers depend on the polymerization of the monomers (Zagar *et al*. 2002).

Several studies have been achieved to lower the polydisperstiy of hyperbranched polymers. The theoretical studies of Frey *et al.* and Müller have shown the way of narrowing molecular weight distribution and controlling molecular weight which could be achieved by introduction of multifunctional core molecules. Bharati *et al.* and research of Fréchet *et al* was also studied on the same problem and they resulted that slow monomer addition to the core molecules in systematic conditions sustains lower polydispersity index with control over molecular weight (Bharathi *et al. 2000*). Malmström *et al.* (1994) was also studied aliphatic hyperbranched polymers by using 2,2-bis(hydroxymethyl)propionic acid (bis-MPA) as an AB_x monomer and 2-ethyl-2-(hydroxymethyl)-1,3-propanediol (TMP) as a core moiety. Narrowly distributed hyperbranched polymers were successed under acid catalyst and involved no purification steps.

1.5.3 Aliphatic Polyesters

There are many important hyperbranched polymer types that can be used in various areas. Some of the known hyperbranched polymers are include polyphenylenes, polyesters, aliphatic polyesters, aromatic polyesters, polyesters, polyamides, vinyl polymers, etc.

Aliphatic polyesters are member of large family that are originated either naturally (β-hydroxy acid) or synthetically (polycondensation of hydroxyl acids, and diacids, dialcohols or condensation of lactone-type heterocycles) (Vert 2005). For example 2,2 bis methylol propionic acid (dimethylolpropionic acid [DMPA]) is one of the monomer that is used for the synthesis. For the aliphatic hyperbranched polyester the only commercially available ones are found Perstorp, Sweden and named as Boltorn™.

Aliphatic polyesters are also preferred for the drug delivery studies. In the study of Padilla de Jesus and co-workers (2001) they prepared hydrophilic polymeric

scaffolds by using DMPA. Then they covalently attached doxorubicin molecules to the hydrazone group of the high molecular weight 3-arm (polyethylene oxide) dendrimer hybrid. By this conjugation, serum half life of doxorubicin increased and drug release was sustained as a response to pH. Another study was carried on by Zou *et al*. (2005) which they used sustained a novel controlled release system based on polyesters. The used Boltorn™ (H20) with succinic hydride and succinic anhydride and then glycidyl methacrylate, and nanoparticles are formed in aqueous solution. They studied the delivery of daidzein, a hydrophobic Chinese medicine, and showed the encapsulation and release behaviour of the system.

1.6 Dendritic Polymers in Drug Delivery Applications

Dendritic polymers have several advantages over linear polymers in drug delivery applications. Branched structure forms nanocavities between repeated groups and terminal groups of multibranched structure serves as a more than one functional group. By these properties dendritic molecules can be used for attaching more than one type of drug, targeting group or solubilizing agent (Gillies *et al.* 2005, Patri *et al*. 2002).

There are several of examples of dendritic polymers that are commonly used in drug delivery studies. Polyamidoamine dendrimers (PAMAM) are the first dendrimers that are commonly used in drug delivery and gene delivery studies. Since amine end groups and polycationic surface charges of PAMAM dendrimers could create toxicity, these dendrimers could be modified by hydrophilic polymers such as poly (ethylene oxide) and poly (ethylene glycol) (Papagiannaros *et al*. 2005, Gillies *et al. 2005*).

In recent years dendritic aliphatic polymers based on polyesters gain considerable attention due to biocompatible hydrophilic and nontoxic behavior without making any further modification. Commercially available Boltorn™ hyperbranched aliphatic polyester and dendritic polyester that was synthesized by using dimethylol propionic acid (DMPA) are the examples that are preferred for the recent drug delivery studies (Ihre *et al.* 2002, Zou *et al.* 2005).

Dendritic polymer could interact with drug in two ways. By using dendritic polymers as dendtiric boxes, a non-covalent interaction could be obtained with drug. In certain cases where branches of the polymer do not enough to keep drug in the branches, drug could be released so rapidly. To inhibit uncontrolled release long chain polymers or biological products could be used. In the review of Gillies *et al*. (2005), a study that was done by using poly (ethylene oxide) was given as an example.

Dendritic polymers could also covalently attach to the drugs. As an example, in the study of Duncan and co-workers (1996) PAMAM dendrimers was covalently attached to the cisplatin drugs which this conjugation decreased the systemic toxicity and increased the solubility of the drug.

More than 40% of drugs that are discovered by pharmaceutical companies are hydrophobic so solubilizing drug in aqueous medium appears to be one of the major problems. Dendritic polymers with hydrophobic cores and hydrophilic outer groups behave as a micellar behavior which makes them one of the ideal candidates to sustain solubility of hydrophobic drugs (Gupta *et al*. 2006).

Najlah *et al*. (2006) discussed the crossing cellular barriers by dendrimer nanotechnologies. Cationic surface charged polymers may interact electrostatically with negatively charged epithelial cells and could enter via fluid phase pinocytosis. In addition Najlah *et al*. discussed another study which shows the mechanism of internalization by using gold-dendrimer nanocomposites. Nanocomposites that applied to Caco-2 cells shows endocytosis mediated internalization of cells. By this property dendrimers and hyperbranched polymer could also be used for gene delivery studies as an ideal candidate for non-viral delivery.

1.7 Degradation of Aliphatic Polyesters by Lipases

Lipases are water soluble enzymes that effects on water insoluble substrates and they are activated when they adsorbed onto the oil-water interface. It was reported that lipases could enzymatically degrade polyesters from their ester bonds and produces lower mass oligomers that become water soluble (Rizarelli *et al 2004*, Mueller *et al. 2006*).

First studies about enzymatic degradation were carried on by Tokiwa and Suzuki and detailed degradation studies with lipases were worked by Marten *et al.* (Herzog *et al 2006*). In these studies the most common way to determine the enzymatic degradation is measuring weight loss of the polyester or determines the molecular weight changes.

The rate of enzymatic degradation could be affected by several parameters including molar mass, chemical structure, copolymer composition, stereochemistry and chain mobility. Hydrophobicity, hydrophilicity, type of ester bond and type of the enzymes are the other factors that affect the degradation rate of the polyesters (Marten *et al 2005*, Rizarelli *et al 2004*).

When the degradation of polyester types is compared, studies indicate that polyesters that are composed of aliphatic polyesters are more degradable than aromatic polyesters. Aromatic polyesters are generally characterized by biologically inert and it was detected that enzymatic degradation is slowed down by increasing aromatic groups to the copolyesters (Mueller *et al. 2006*).

In vitro degradation studies of aliphatic polyesters are generally worked by lipases of microorganisms. *R. delemer* lipase, *Rhizopus arrhizus* lipase, *Pseudomonas cepacia* lipase, *Pseudomonas sp.* lipase are the examples that are commonly used for the enzymatic degradation studies (Miao *et al.* 2005).

1.8 Role of Lipids in Drug Delivery

Lipids are natural organic molecules that are insoluble in water whereas soluble in non-polar organic solvents. Lipids could be listed as fatty acids, soap detergents, fats, oils, waxes, phospholipids, eicosonoids, terpenes, steroids, lipid soluble vitamins or molecules that are found in biosynthetic pathways (Reusch 1999).

Lipid based drug delivery systems in the form of liposomes, triglycerides, fatty acids or micellar systems have been worked for many years. They have properties that are favored for delivery systems. Most of the lipid based systems are used for the delivery of toxic hydrophobic drugs and prevent the fragile ones from early degradation. By lipids passive targeting is also more effective than other hydrophilic systems and has long-circulating property which prevents an early break down. There are many clinically approved lipid based delivery agents which preferred for the therapies like AmBisome®, Visudyne® DOXIL®, Myocet® (Nothern Lipids Inc. 2008).

1.8.1 Fatty Acids in Drug Delivery Studies

Fatty acids are found in oils or fats. By hydrolyzing of triesters, oils or fats become fatty acids, glycerol or fatty alcohols and it could be modified to other forms (Papkov *et al* 2008).

Fatty acids and lipids are commonly preferred in drug delivery systems. These types of drug delivery agents could enhance bioavailability of lipophilic drugs. In addition, lipid and fatty acid based carriers are easily captured by lymphatic cells which makes them good candidate for lymphatic targeting (Suresh *et al.* 2007).

Fatty acid based polymeric formulations have several advantages including flexibility, low viscosity, low melting point which makes the injection or implantation more easily. Due to hydrophobic character it could entrap lipophilic drugs longer time thus sustain controlled drug release property. Besides, manufacturing are easy at a reasonable cost (Papkov *et al.* 2008).

1.8.2 Ricinoleic Acid

Ricinoleic acid is dominantly found in castor oils (85-90%). Double bond is present in 9^{th} position and has hydroxyl group on 12^{th} carbon (cis-12-hydroxyoctadeca-9-enoic acid). The chemical structure of ricinoleic acid is shown in Figure 1.8. Due to this property it is one of the few commercially available hydroxyl fatty acids that have two functional groups (Prakash *et al.* 2006). In addition ricinoleic acid could be easily extracted from castor oil by enzymatic degradation or saponification and additional processes (Teomim *et al.* 1998)

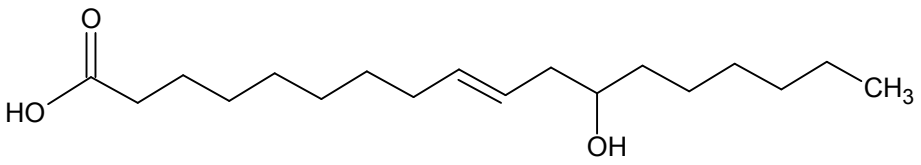

Figure 1.8 Chemical structure of ricinoleic acid.

Ricinoleic acid is used in cosmetic products like bath oils and tablets, colognes and toilet waters (TCI 2007). It is now been used in drug delivery studies. Shikanov *et al*. (2004) worked on the poly (sebacic acid-co-ricinoleic acid) polymers for the delivery of paclitaxel, an anti-cancer drug. The group sustained long term delivery of the drug and biodegradation of the system. Besides they showed that empty polymers did not cause any toxicity while drug loaded ones have effect on tumors of the mice. Another study was done by Slivniak *et al*. (2006). They synthesized ricinoleic acid-lactic acid copolyesters which were used for drug delivery study. They also sustained long term delivery of the drug and showed *in vitro* hydrolytic degradation of the system. The number of researches that has been made by ricinoleic acid based polymers, increase and hold promise.

1.9 Tamoxifen in Cancer Therapy

Tamoxifen, (triphenylethylene derivative) is a highly hydrophobic drug (water solubility 0.04 *μ*g/ml at 37◦C) and is a selective estrogen receptor modulator (SERM) that can function for both estrogenic and anti-estrogenic type of cancer tissues depending on the targeted side (Figure 1.9) (Ring *et al. 2004,* Kufe *et al.* 2003, Fontana *et al* 2005). It is the only drug that is used for the healthy women to prevent the risk of breast cancer (Hu *et al.* 2006). Tamoxifen was first used as anti-neoplastic agent in 1971 and now it has been used for the treatment of the hormone dependent breast cancer (Singh *et al*. 2006).

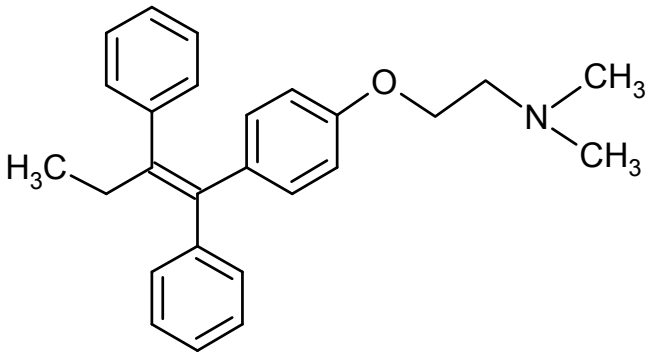

Figure 1.9 Chemical structure of tamoxifen.

Estrogen receptor (ER) which tamoxifen binds is a member of nuclear receptor family of ligand activated transcription factors. When estrogen binds to the ER (ERα or ERβ) it is released from heat shock proteins and goes to conformational changes (phosphorylation and dimerization) then it interacts with the estrogen response elements (ERE) which leads to the regulation of transcription of estrogen dependent genes (Chawla *et al.* 2002, Ring *et al*. 2004).

Tamoxifen has a pro-estrogenic activity and leads to some advantages over post-menopausal women. It could restore bone mineral balance or reduce the bone fractions and also it was found that tamoxifen has the cholesterol lowering effect.

Although it could lead several advantages clinical studies showed that tamoxifen therapy increase the risk of endometrial cancer between 2-7 folds. As a result of the threat, IARC (International Agency for Research on Cancer) named tamoxifen as carcinogen agents (Singh *et al.* 2006). In addition, cancer cells develop resistance against tamoxifen treatment which might result to further tumor formation (Chawla *et al*. 2002). Besides, conventional administration of tamoxifen could cause many side effects like blood clots in lung or legs, stroke, nausea, vomiting, weight loss, pain or reddening on the tumor site (Medline 2007). In order to prevent all these side effects, tamoxifen is one of the mostly preferred chemotherapy drug which is used for targeted and controlled drug delivery therapies.

1.10 Idarubicin in Cancer Therapy

Idarubicin (4-demethoxydaunorubicin) is a lipophilic antracycline agent (Zara *et al* 2001). It has an inhibitory effect on nucleic acid synthesis and inhibits the functioning of topoisomerase II. This anti-cancer drug also generates free radicals and G2 cell cycle arrest. Idarubicin is more lipophilic than the other anthracyclins like daunorubicin and doxorubicin which increases its rate of the cellular uptake (Pfizer 2008, Zara *et al*. 2001, Santos *et al.* 2005). The chemical configuration of idarubicin is shown in Figure 1.10.

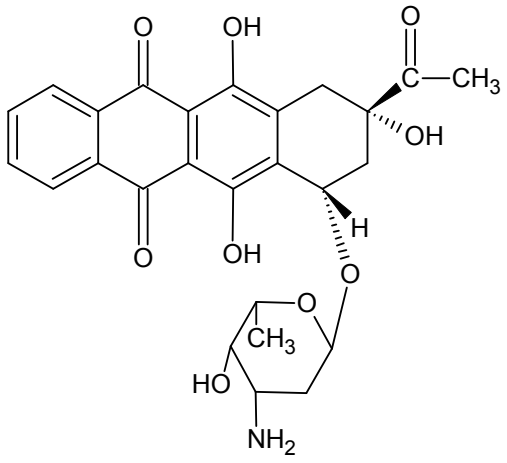

Figure 1.10 Structure of idarubicin hydrochloride

Idarubicin is effective in various cancer types including breast cancer, non-Hodgkin's lymphoma, plasmacytomas, myelodysplastic syndromes, acute myelogenous leukemia (Zara *et al. 2001*).

Although idarubicin has less cardiotoxic effect than other anthracyclins, it still might cause myocardial toxicity due to its strong hydrophobic effect. Additionally, bone marrow suppression and mutagenic and carcinogenic properties might be detected in certain cases (Demetçi 2007, Pfizer 2008).

Since idarubicin has serious side effects, it is also a candidate for the drug delivery studies. Furthermore highly lipophilic structure is suitable for the lipid based drug delivery systems.

1.11 Objectives of the Study

Major problems of conventional chemotherapies still exist therefore it is important to develop sustained drug delivery system. This study focuses on the problems of the delivery of hydrophobic anti-cancer drugs which are insoluble and create toxicity over healthy tissues. To deliver these drugs, hyperbranched polymers are preferred in order to benefit the physical and chemical properties of these types of polymers. In addition, to obtain hydrophobicity, ricinoleic acids are added to the system. To be successful in controlled drug delivery studies it is also important to determine the chemical properties of polymers and analyze the degradation behavior of them in *in vitro* conditions.

For the cancer therapy researches to show the efficiency of the polymeric system the first way is applying these formulations to the cells. Therefore in this study the toxicity effect of the drug loaded and an empty polymer over breast cancer cell lines has been tested. The aim of the study is summarized as follows:

- To synthesize hyperbranched aliphatic polyesters and make esterification with the end groups of polyesters and ricinoleic acid in order to form hyperbranched resins.

- To characterize and determine the molecular and chemical properties of synthesized hyperbranched resin (HBR).

- To load hydrophobic anti-cancer drugs (idarubicin and tamoxifen) to the HBR and determine the loading efficiency profiles.

- To be able to sustain the controlled release of tamoxifen and idarubicin from the system *in vitro* conditions.

- To characterize the molecular and physical changes after drug loading to the system.

- To show the molecular degradation property in *vitro* conditions and with the presence of enzyme.

- To show the non-toxic property of the HBR and show the efficiency of drug loaded HBR to kill the breast cancer cells comparing with free drug application.

CHAPTER 2

MATERIALS AND METHODS

2.1 Materials

2.1.1 Materials for Hyperbranched Resin Synthesis

- Castor oil was obtained from Akzo Nobel Kemipol.
- Sodium hydroxide (NaOH), para-toluene sulfonic acid (p-TSA), potassium hydrogen phthalate (KHP), ethyl alcohol were purchased from Merck A.G. (Germany).
- Sulfuric acid (95-98 %), (H_2SO_4) was obtained from Sigma-Aldrich (USA).
- Dimethylol propionic acid and dipentaerythritol was obtained from Perstorp AB (Sweden).
- Toluene was from Best Kimya (Turkey), isopropyl alcohol was from Volkan Boya (Turkey), nitrogen gas was obtained from Oksan (Turkey).
- Sodium chloride (NaCl), magnesium sulfate hepta hydrate ($MgSO_4.7H_2O$) were purchased from Applichem (Germany).

2.1.2 Materials for Drug Loading, Release and Cell Culture Studies

- Tamoxifen (minimum 99% pure), phosphate buffered saline tablets, N,N dimethylformamide, Type XIII lipase from *Pseudomonas sp*. species, were purchased from Sigma-Aldrich (USA).
- Trypsin-EDTA solution (0.25% Trypsin&EDTA), gentamycin sulphate (50mg/ml as base), tryphan blue solution (0.5%), cell proliferation kit (XTT based colorimetric assay) were obtained from Biological Industries, Kibbutz Beit Haemek (Israel).

- RPMI 1640 medium [(1x), 2.0g/l $NaHCO_3$ stable glutamine], fetal bovine serum (tested for mycoplasma) were obtained form Biochrom Ag. (Germany).
- Methanol (gradient grade for liquid chromatography), acetonitrile and ortho-phosphoric acid, triethylene amine were from Merck (Germany).
- Dialysis membranes (MwCo 3500, Diameter 26mm) were obtained from Serva (Germany).
- Dimethylsulfoxide (cell culture grade), sodium dodecyl sulfate (molecular biology grade) were obtained from Applichem (Germany).
- MCF-7 monolayer type human epithelial breast adenocarcinoma cell line was provided from Food and Mouth Disesase Institue (Şap) (Ankara). Idarubicin.HCl (Pharmacia, Italy) was kindly donated by Prof Dr. Ali Uğur Ural, Gülhane Military Medical School Hospital, Department of Hematology (Ankara).

2.2 Dehydration of Raw Materials

Magnesium sulfate heptahydrate was first ground and then dried in an oven at 120°C for 2-4 hours. Para-toluene sulfonic acid was dried at 85°C for 1-2 hours.

2.3 Extraction of Fatty Acids

Extraction of fatty acids from castor oil first began with saponification procedure. For this purpose stoichiometric amount of sodium hydroxide was dissolved in 1:1 ethanol:distilled water mixture. The volume of the mixture was prepared as at least equal volume of the oil and the amount of the sodium hydroxide was determined considering the saponification value. Saponification process was commenced by mixing castor oil, NaOH and ethanol:distilled water in a necked flask by using mechanical stirrer. Mixture was reacted under a reflux at 80°C until a homogenous mixture was obtained (1-1.5h). At the end of the process reacted mixture was gently mixed with saturated NaCl solution. By this way soap (organic phase) rested on the top, while glycerol and inorganic solution rested at the bottom phase. Soap was

eluted from glycerol by using filter paper and vaccum. Filtered soap was then dissolved in distilled water and the solution was transferred to seperatory funnel. In order to differentiate fatty acids, 15-20% (v/v) sulfuric acid was added to the dissolved soap. When fatty acid phase was clarified on the top layer, the rest of the solution was removed by using separatory funnel. Seperated fatty acids were washed with distilled water for several times in order to remove remained glycerol and other inorganic solutions. By centrifugation at 4,000 rpm for 10 min (Hettich, Universal 16R, Germany) fatty acids were separated from water. Remained water phase was excluded by using $MgSO_4.7H_2O$.

At the end of the process ricinoleic acid (85-95%), oleic acid (2-6%), linoleic acid (1-5%) linolenic acid, stearic acid and palmitic acid (0.5-1%) was extracted from castor oil. By using melting point differences of fatty acids, a second centrifugation was applied at 4,000rpm at 8-10°C for 15 minutes. Solid state stearic acid, palmitic acid and oleic acid were removed from the other fatty acids. At the end of the extraction, mainly ricinoleic acid and linoleic and linolenic acid were obtained. Saponification and fatty acid extraction reactions are showed in the Figure 2.1 and Figure 2.2.

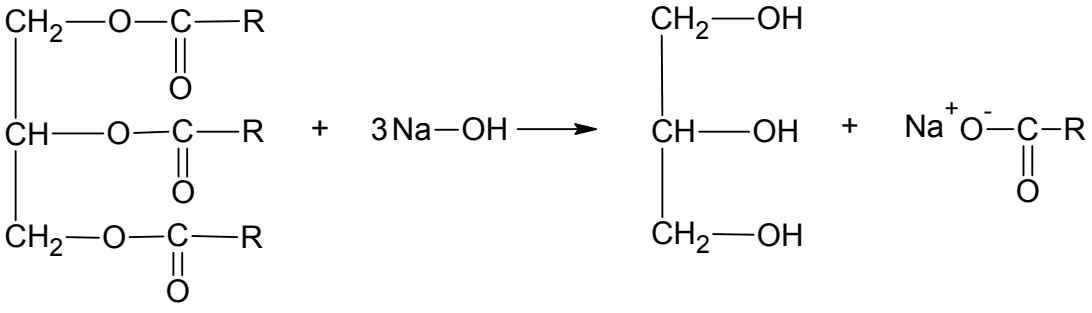

Figure 2.1 Saponification reaction of the castor oil

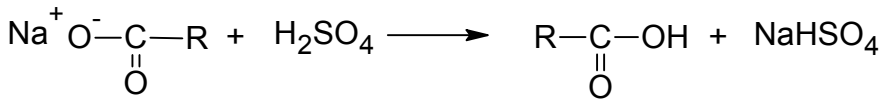

Figure 2.2 Fatty acid production by using sulfuric acid

2.4 Hyperbranched Resin Synthesis (HBR)

Hyperbranched resin was synthesized in two step reaction. In the first part, hyperbranched polyester synthesis was obtained by esterification of dipentaerythritol and dimethylolpropionic acid (DMPA). Then castor oil fatty acids which are mainly composed of ricinoleic acid were esterified by hydroxyl end groups of polyester and hyperbranched resins were synthesized.

In the study, in order to sustain the reaction of hyperbranched polyesters and hyperbranched resins an experimental setup was formed. All reactions were done in five-necked glass. System was placed in an oil bath and reactions were started in a reflux system with the aid of mechanical stirrer under nitrogen atmosphere. The temperature of the reaction was set differently for hyperbranched polyester synthesis and hyperbranched resin formation. In order to obtain a successful synthesis it was important to maintain the reaction temperature stable, so during the reaction temperature had to be controlled regularly. Before terminating the system, water product of the condensation reactions was removed by using azeotrophic distillation with toluene. It was important to remove water product completely in order to prevent unwanted hydrogen bondings or cross-linking formations between polymers. The schematic representation of the experimental setup is shown in Figure 2.3 (Bat 2005).

In the first part of the synthesis, hyperbranched polyesters were synthesized. The principle of hyperbranched polyesters formation was based on one-step polymerization reactions. One-step polymerization of hyperbranched polymers which was explained in the literature is mainly based on esterification of AB_x type of

monomer with core moiety. Esterification performed in the bulk using an acid catalyst and involves no purification steps. By this method molecular weight distributions could be controlled and could be narrowed down (Malmström *et al*. 1995, Zagar *et al.* 2002). The main principle of the hyperbranched polyester synthesis was explained in *1.4.2 Synthesis of Hyperbranched Polymers.*

In the study, hyperbranched polyesters were synthesized by using dipentaerythritol as core molecule of the structure and dimethylolpropionic acid (DMPA) as branching unit. To esterify six hydroxyl end groups of dipentaerythitol, six moles of DMPA were added in order to obtain perfect one generation. Para-toluene sulfonic acid (p-TSA) was added as catalyst (0.4% w/w of DMPA). All requirements were introduced into five-necked glass and placed into experimental setup which was explained previously. The reaction was done at 140°C for 3-4 hours. When water product was completely removed the reaction was stopped and first generation of hyperbranched polyesters were obtained (HBP-G_1). Illustration of first generation of hyperbranched resins are shown in Figure 2.4.

For second generation of hyperbranched polyester (HBP-G_2) synthesis, stochiometric amount of DMPA and p-TSA catalyst was added to the HBP-G_1 and synthesis was begun in the same experimental setup. HBP-G_2 synthesis was done at 140°C for 3-4 hours. The reaction of second generation of hyperbranched polyesters are shown in Figure 2.5.

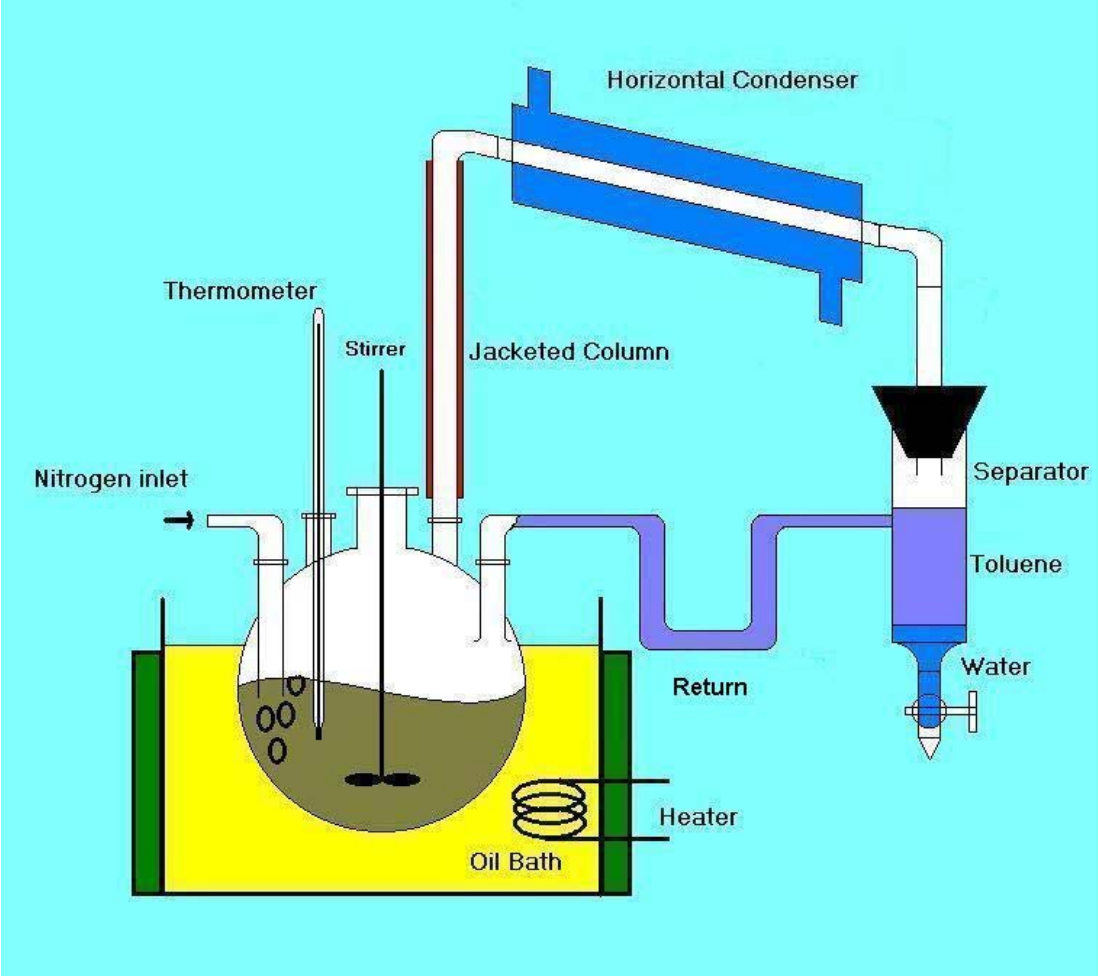

Figure 2.3 Experimental setup of the hyperbranched polyesters and HBR synthesis (Bat 2005).

In the second part of the reaction, in order to esterify the ricinoleic acids (castor oil fatty acids mainly composed of ricinoleic acid, rarely linoleic and linolenic acid which might be neglectable) with hyperbranched polyesters, stochiometric ratio of fatty acids were added to the system and esterification was started in same experimental conditions but at 220°C. In certain periods of the reaction, a sample of synthesized hyperbranched resin (HBR) was removed from the system to make an acid value determination (Appendix A). Acid value shows the mg of KOH required to neutralize free fatty acids that are found in 1 gram of sample. In order to prevent complete fatty

acid esterification, reaction was terminated when acid number was dropped below 40mgKOH/mg HBR. Theoretical representation of HBR polymer is shown in Figure 2.6.

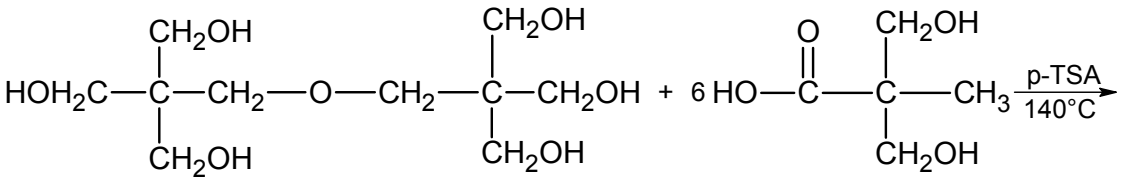

Dipentaerythritol DMPA

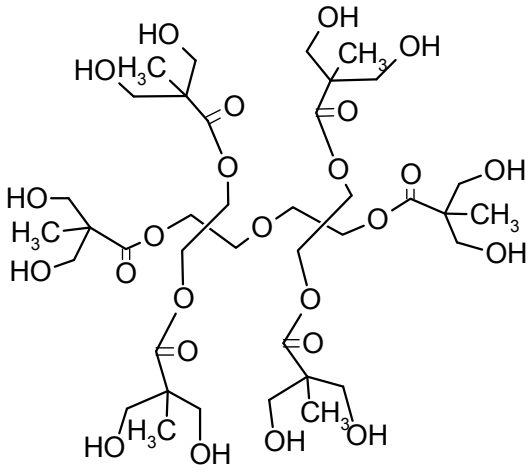

HBP-G_1

Figure 2.4 Theoretical representation of the synthesis of first generation hyperbranched polyesters (HBP-G_1).

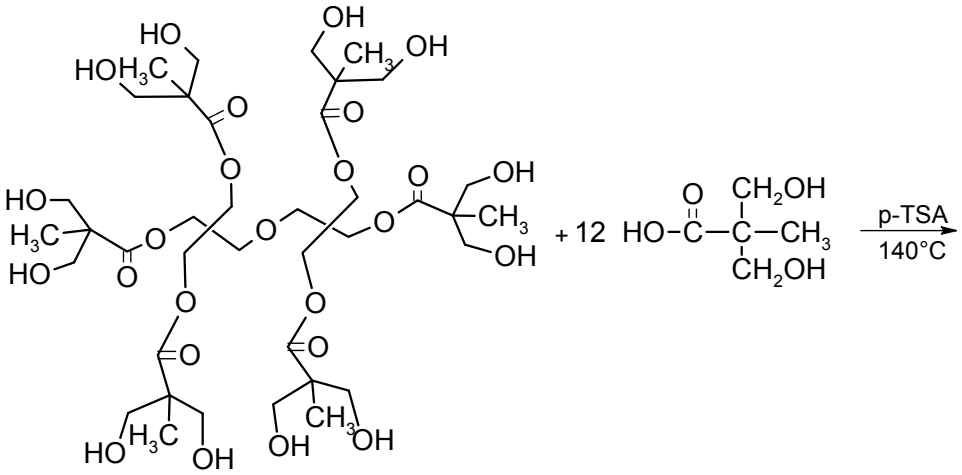

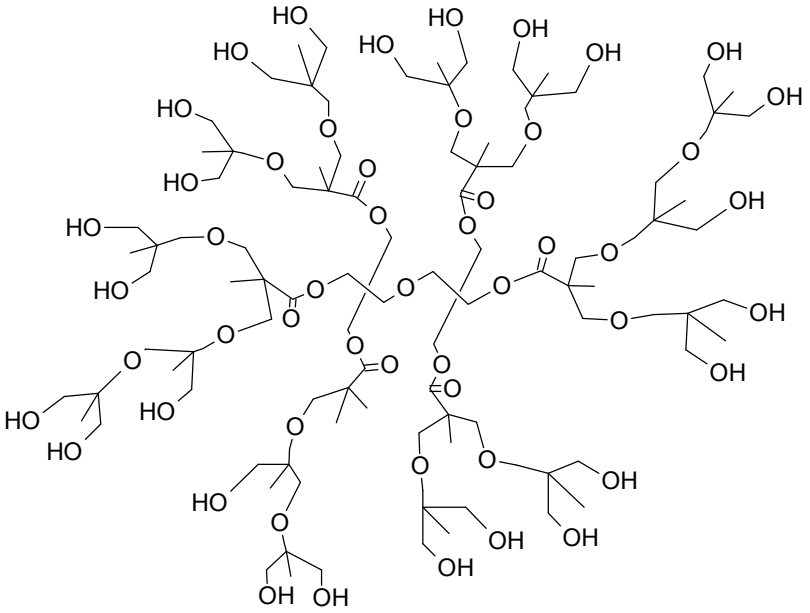

Figure 2.5 Synthesis and theoretical representation of second generation hyperbranched polyesters (HBP-G_2) by esterification of first generation polyesters (HBP-G_1) and DMPA.

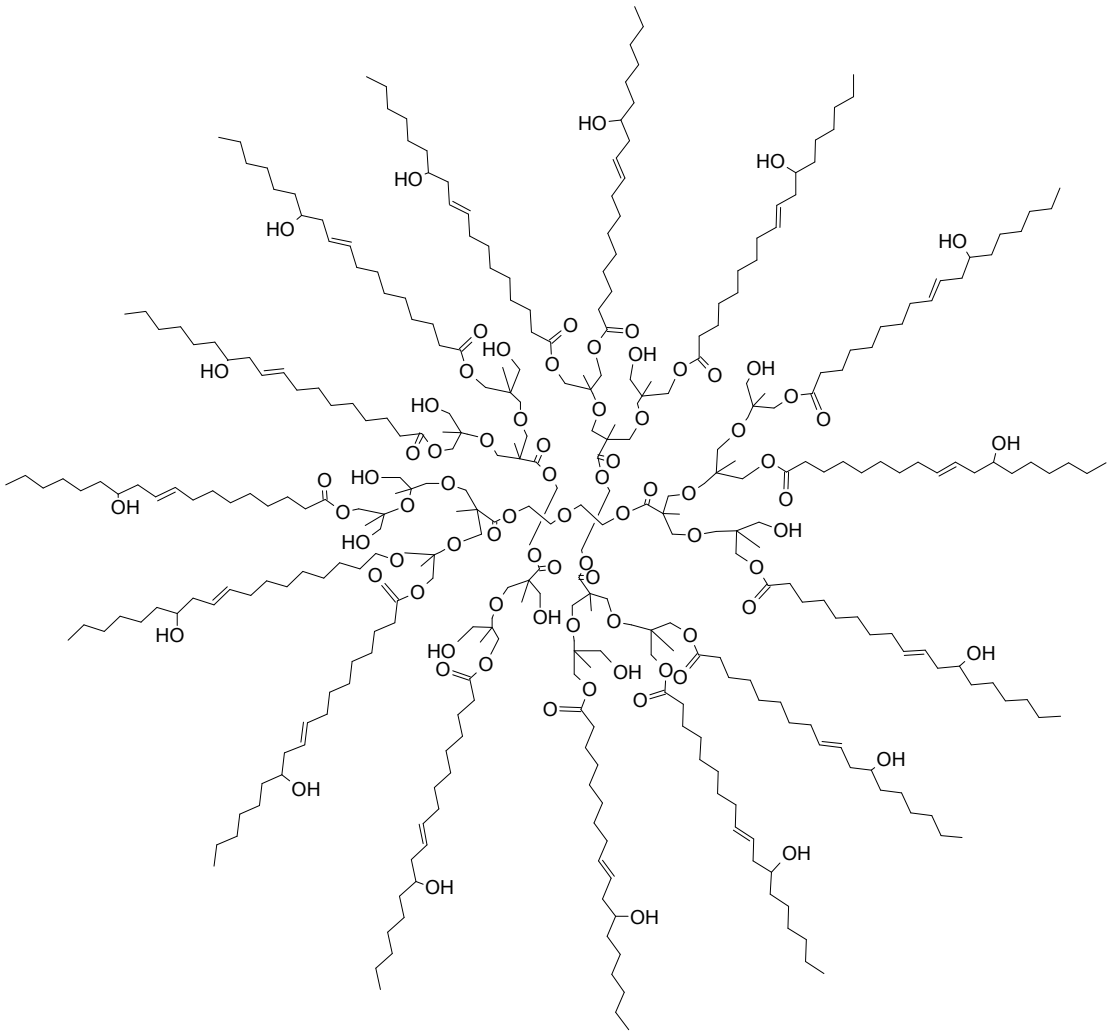

Figure 2.6 Theoretical representation of synthesized hyperbranched resin (HBR).

2.5 Purification of HBR

In order to obtain pure HBR, synthesized polymers were washed with pure methanol to get rid of unreacted ricinoleic acids, DMPA or dipentaerythritol. Impure HBR was first dissolved in methanol but then precipitated by centrifugation at 15,000rpm for 30 min (Thermo IEC, Micromax RF, US). Supernatant was discarded and preciptated HBR was dried near the flame. For the loading studies, purification was applied after drug was loaded to HBR. Detailed explanation is given in *2.6.*

2.6 Loading of Tamoxifen and Idarubicin into HBR

Loading principle of tamoxifen and idarubicin is mainly based on hydrophobic interaction of drugs with HBR. First of all for both tamoxifen and idarubicin were dissolved in N,N Dimethylformamide (DMF). Then predetermined amount of dissolved drug was directly added to certain amount of HBR. Mixture was shaken at 300 rpm overnight. Then mixture was dissolved in methanol until a homogenous solution was obtained. Unloaded drugs and unreacted molecules (dipentaerythritol, DMPA, ricinoleic acid) were dissolved in methanol while drug loaded HBR system was precipitated. In order to obtain pure HBR, mixture was centrifuged at 15,000 rpm for 30 min at room temperature (RT) (Thermo IEC, Micromax RF, US). Dried idarubicin and tamoxifen loaded HBR pellets were then dissolved in DMF in order to determine loading efficiency.

Loading efficiency of idarubicin was analyzed by using UV-vis spectrophotometer (Schimadzu UV-1208, Japan) at 540 nm (λ_{max} of pure idarubicin was shifted from 486 nm to 540 nm after loaded into HBR). For determining the loading efficiency of idarubicin, standard calibration curve was obtained by using UV-vis spectrophotometry at 540 nm. Figure 2.7 shows standard curve of idarubicin in a various concentration from 0.05 mg/ml to 1.7 mg/ml. Loading efficiency for idarubicin were determined by using Equation 1.

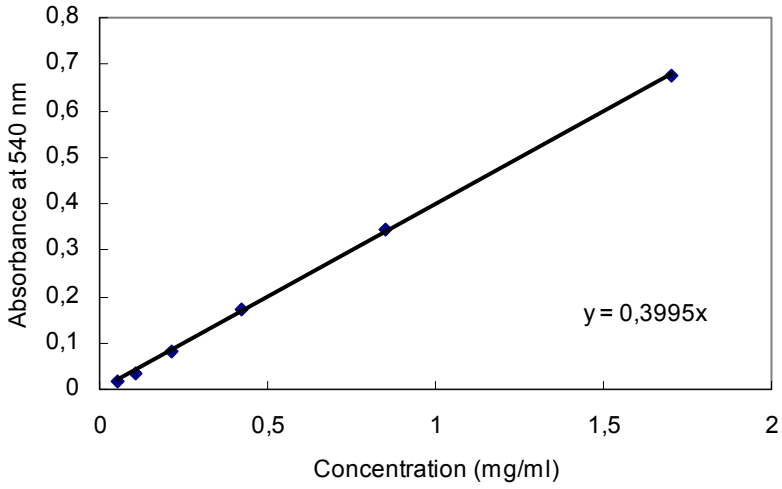

Figure 2.7 Calibration curve of idarubicin which was determined by UV-vis spectrophotometry at λ_{max}=540nm.

Tamoxifen loading efficiency was detected by using high performance liquid chromatography (HPLC) method. HPLC standards are given in *2.9.4 High Performance Liquid Chromatography.* In order to calculate the loading efficiency of tamoxifen standard calibration curve was also determined with HPLC by using free tamoxifen. The standard calibration curve of the tamoxifen is shown in Figure 2.8. In this curve minimum 0.0001mg/ml tamoxifen could be determined. HPLC results showed the mg tamoxifen/ml solvent so loading efficiencies were determined by same formula that was used for idarubicin (Equation 2.1).

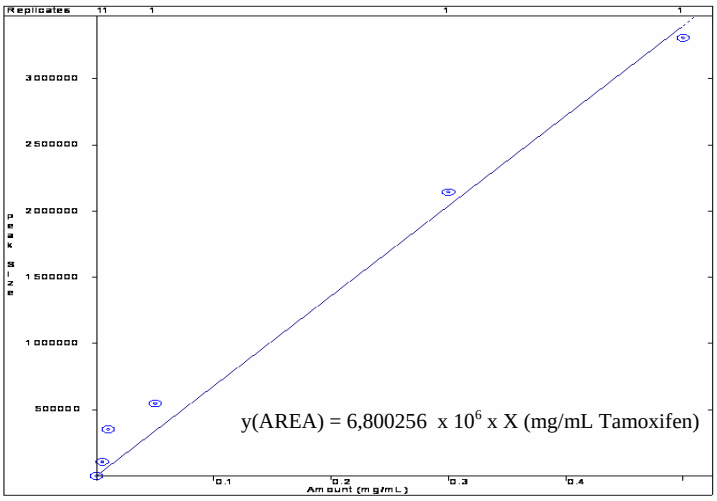

Figure 2.8 Calibration Curve of tamoxifen by using HPLC method.

Loading efficiency of tamoxifen and idarubicin were determined by using the formula (Equation 1). All experiments was carried on in duplicates. Experiments were performed in dark due to light sensitivity of tamoxifen.

$$\text{Loading efficiency (\%)} = \frac{\text{Weight of drug loaded (mg)}}{\text{Initial drug weight (mg)}} \text{ X } 100 \qquad (2.1)$$

2.7 Degradation of HBR

For *in vitro* degradation studies, first HBR samples were immersed into 4 well plates, and then 3 ml phosphate buffered saline (PBS) solution (0.01M, pH 7.4) was added to each HBR sample. For enzymatic degradation study, 50 µl of 4mg/ml lipase (0.9 % NaCl (w/v)) from *Pseudomonas sp.* species was applied to half of the samples. Samples were shaked at 50 rpm at 37°C. At predetermined time intervals, medium and lipase were replenished and a sample of HBR was removed from the system. After washing and drying steps of HBR, molecular weight of the samples was

analyzed by gel permeation chromatography. The detail of the molecular weight determination was explained in *2.9.2 Gel Permeation Chromatography (GPC).*

2.8 Drug Release Studies

Drug release profiles from HBR were studied by using dialysis method. Two sets of experiments were carried on; in the first set only tamoxifen release was determined. To prevent precipitation in aqueous medium, samples were dissolved in 400 µl of DMF and then transferred into dialysis bags. 3 ml of release medium was composed of PBS (0.01M, pH 7.4) and 5 % (v/v) DMF. Dialysis was performed in screw capped falcon tubes at 37°C with 150 rpm shaking (Heidolph Unimax 1010 shaker/1000 incubator, Germany). At certain time points outer medium was replenished with fresh medium.

The second set of experimental conditions was used for both tamoxifen and idarubicin. Drug -HBR complex was dissolved in 100 µL of DMF and then mixture was transferred into dialysis bags. Later, 3 ml of 0.01 M PBS (pH 7.4) was added as outer medium. 0.5 % w/v of sodium dodecyl sulfate (SDS) was used to prevent adsorption of the hydrophobic drugs to the walls of falcon tubes or walls of dialysis bags. In order to accelerate drug release in appropriate time ranges, 50 µl of 4 mg/ml lipase form *Pseudomonas sp.* was added to the samples. Dialysis was begun in screw capped falcon tubes at 37°C with 150 rpm shaking. In certain time periods, outer medium was removed and fresh medium with lipase was added to the system.

In all set of release conditions samples were analyzed by HPLC method. For tamoxifen determination same standard curve used as shown in Figure 2.8. Release profiles of idarubicin were not detected by using UV-vis spectrophotometry since low amount of the drug was released from the system. HPLC detection was applied to determine the release of idarubicin. Standard curve of idarubicin is shown in the Figure 2.9. In all sets of experiments retention time and intensity peak of drugs were determined with control groups of empty HBR and solvent. All experiments were carried on in duplicates and tamoxifen samples were analyzed in dark due to light sensitivity.

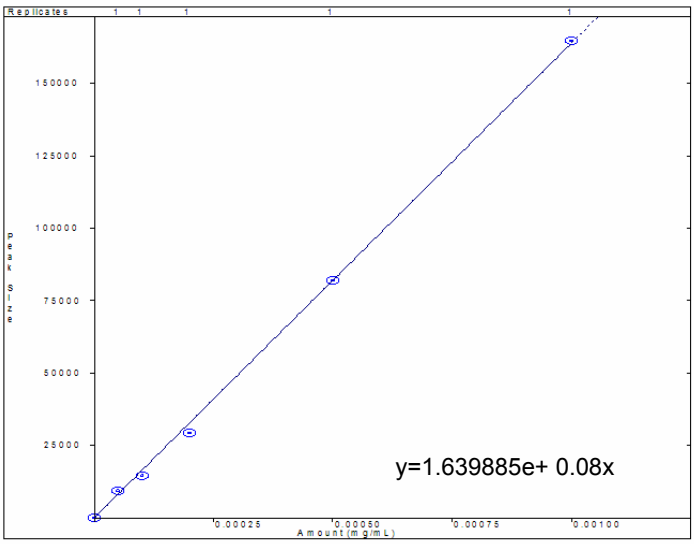

Figure 2.9 Calibration curve of idarubicin determined by HPLC method.

2.9 Chemical Characterization

Experiments that were done by using Fourier Transform Infrared Spectroscopy, Gel Permeation Chromatography, Nuclear Magnetic Resonance were carried on in METU Central Laboratory R&D Training Center, Ankara. For the analysis that were done by using High Performance Liquid Chromatography and ELISA reader were carried on in METU Central Laboratory, Molecular Biology and Biotechnology Research Center, Ankara.

2.9.1 Fourier Transform Infrared (FTIR) Spectroscopy

FTIR spectra were used to understand the chemical composition of the ricinoleic acid, hyperbranched polyesters, HBR, idarubicin and tamoxifen loaded HBR samples. Bruker IFS 66/S,FRA 106/S, RAMANSCOPE was used to generate FTIR spectra of samples. Solid samples were pelleted with KBr (300 mg KBR for 1 mg sample). Cells and cuvettes were used for liquid samples.

2.9.2 Gel Permeation Chromatography (GPC)

Molecular weight and molecular weight distribution of the HBR samples was detected before and after purification of HBR and under the condition of enzymatic and hydrolytic degradation of samples. PL-GPC 220 instrument was used for analysis. 0.050g samples were dissolved in tetrahydrofuran (THF) and polymer was run at room temperature by using polystyrene universal calibration method.

2.9.3 Nuclear Magnetic Resonance (NMR)

Nuclear Magnetic Resonance (NMR) spectroscopy was used to detect the polymeric arrangement and composition of HBR. Due to semi-liquid physical state of HBR, analysis were carried on by liquid ^{13}C NMR. Bruker AVANCE 300 MHz (~7 Tesla) spectrometer was used and deuterated DMSO was used as solvent. 30-40 mg of purified HBR samples was used for the analysis.

2.9.4 Particle Size Analysis and Zeta Potential Measurements

Zeta potential and particle size distribution of samples were measured in order to determine the charge and stability variations of drug loaded and unloaded HBR samples in aqueous conditions. Water was used as dispersant and potential of the samples were measured at 24°C. Malvern Nano Zeta Size Nanoseries Nano-ZS (UK) zeta potential and particle size analyzer was used for zeta potential measurements and for the particle size distribution determination.

2.9.5 High Performance Liquid Chromatography (HPLC)

Varian Prostar HPLC was used to detect the amount of tamoxifen that was entrapped and to determine the release rate of tamoxifen and idarubicin from the HBR composition.

For tamoxifen concentration detection, Microsorb MV C18 (4,6 x 250 mm, 5 mm) column was used. Methanol, distilled water, triethylene amine (93:7:0.01) was used

as mobile phase with a flow rate 1 ml/min, at RT. Fluorescent detector was used and sample concentration was detected with $\lambda_{emssion}$= 375 nm and $\lambda_{excitation}$ = 260 nm (Long *et al.* 2004).

For HPLC detection of released idarubicin, same type of column used and acetonitrile, methanol, phosphoric acid and water (3:2:1:4) was used as mobile phase. The sample was injected with flow rate of 0.8 ml/min at RT and sample concentration was detected at $\lambda_{emssion}$= 470 nm $\lambda_{excitation}$ = 580 nm (Fukushima *et al*. 1998).

Aqueous solutions and mobile phase were filtered with 0.45 μM cellulose filter. Results were given as mg of tamoxifen and idarubicin that were detected in 1 ml of the sample.

2.10 Cell Culture

2.10.1 Cell Culture Medium Preparation and Passaging Cell Cultures

Cell cultures were maintained in RPMI 1640 medium with 10% fetal bovine serum (FBS) and 1% gentamycin supplementation. MCF-7 human breast adenocarcinoma cell lines are epithelial and monoclonal continuous cultures grown as monolayer. As most animal cell cultures MCF-7 cells grow as single thickness cell layer or attach to glass or plastic substrates. When substrate is covered with cells growth slows and ceases. To keep cells healthy they should be subcultured periodically for every 80-90% of viability. Subculturing involves breaking down the cellular bonds between cells and their attachment to the substrate (Ryan 2008). For MCF-7 cell line, trypsinization was applied by using Trypsin-EDTA solution. After a homogenized suspension was obtained, certain amount was discarded and remained cells were diluted with fresh medium. 25cm^2 flasks with filtered caps were used to suspend cells with medium. For the studies which high amounts of cells were needed, 75cm^2 flasks were used with higher amount of medium supplementation. Cell cultures were incubated in humidified 5% CO_2 incubator at 37°C (Heraeus, Germany) and cell culture experiments were studied in sterile laminar flow (BioAir, Italy).

2.10.2 Cell Proliferation Assay with XTT Reagent

Cell proliferation assay by using formazan compound is based on the activity of mitochondria enzymes which are inactivated shortly after death. The use of the XTT reagent based on the fact that live cells reduce tetrazolium salts into orange colored of formazan salts. The dye formed is water soluble and dye intensity is read at a given wavelength with a spectrophotometer. The intensity of the dye is proportional to the number of metabolically active cells. The greater the number of the cells, the greater the activity of mitochondria enzymes and the higher the concentration of dye formed, which can be measured and quantified (Biological Industries 2002).

For the assay 96 well plates were used. First, 100 µl RPMI 1640 medium was added to all wells. Then, highest dose of polymeric concentration was added to the first column and serial dilutions were applied horizontally. Polymeric concentration was prepared by dissolving pre-determined amount of HBR in DMSO and then 100 fold dilution was made by RPMI 1640 medium. Finally 5000 cells/well were seeded. The number of cells was determined by viable cell counting assay which was explained in *2.10.3 Viable Cell Count*. Cells were incubated in humidified CO_2 incubator at 37°C for 48 h, 72 h and 96 h. By the end of the incubation, XTT and activator reagents were applied to each plate and plates were incubated in dark for 2-5 h. The intensity of the color change was measured by using ELISA reader (SPECTRAmax 340PC) at 500 nm.

Viability curves of cells in each plate were determined by considering the intensities of each well subtracting from the intensity of control groups (medium control, cell control and polymer control. In order to determine the toxicity effect, IC_{50} values need to be determined. The IC_{50} is a measure of drug effectiveness. It indicates how much of a particular drug or other substance (inhibitor) is needed to inhibit a given biological process (or component of a process) by half. In other words, it is the half maximal (50 %) inhibitory concentration (IC) of a substance (50 % IC, or IC_{50}) (Wikipedia, 2008). IC_{50} value of the samples was calculated by using the logarithmic equation of the viability curves. All the experiments were applied in duplicates or triplicates.

2.10.3 Viable Cell Count

In order to determine the approximate number of cells that was used in XTT assay, cell count has to be done. For MCF-7 cells before counting, cells were trypsinized and homogenized with fresh medium. Tryphan blue solution was 10-fold diluted with cell suspension to make the total volume 1ml.

Cells were counted using hemocytometer (HHH, Germany) under light microscope. The smallest center square on hemacytometer has 0.00025 mm^3 volume. To calculate the number of cells in 1 cm^3, $4x10^6$ coefficient number was used in calculation. The number of the cell/ml was calculated by the formula given below (Equation 2.2):

Cell number/ml= Average count per square x Dilution factor x 4.10^6 (2.2)

2.10.4 Statistical Analysis

Minitab Statistical Software (Minitab Inc, USA) was used to determine the significant differences between mean of the groups (α= 0.05). 2-sample t-test was used for statistical analysis.

CHAPTER 3

RESULTS AND DISCUSSION

3.1 Synthesis and Purification of Hyperbranched Resin

In this part of the study first fatty acids were extracted from castor oil. Then hyperbranched polyester formation was studied by dipentaerythritol and dimethylol propionic acid components. Fatty acid esterification with hyperbranched polyester was completed and to remove unreacted molecules from the system, ideal conditions were determined. The success of the synthesis was confirmed by characterization with FTIR, GPC and NMR analysis.

3.1.1 Synthesis of Hyperbranched Resin

Fatty acid extraction and hyperbranched resin synthesis were done according to Bat (2005). There are several critical points that should be noticed. During the synthesis of hyperbranched resin, sustaining temperature at 220°C was important because if reaction would begin at lower temperatures, duration of the reaction would be increased. The presence of the catalyst was another critical point for the success of the synthesis. Without using catalyst, a solid deposit formation occurred in the system, on the other hand excess catalyst were resulted cross-linked ethers. Therefore optimum amount of catalyst was determined as 0.4 % for hyperbranched resin formation.

Determining acid number is important for termination of the synthesis. Increasing duration of the process, augmented moles of fatty acids that was esterified with 1 mole of hyperbranched polyesters, however physical structure was converted from

semi-liquid to gel structure because of the overesterification. Therefore it is important not to lower acid number below 15 mg/KOH to prevent gelation. In order to sustain a mild level of hydrophobicity, the reaction was terminated when the acid number was detected as 38.8 ± 2.7 (Mean ± SD, n=3).

3.1.2 Purification of Hyperbranched Resins

For the purpose of removing unreacted molecules from hyperbranched resin (HBR), some preliminary experiments were carried out. Since dipentaerythritol and DMPA were soluble in water, impure HBR was dissolved in N,N Dimethylformamide (DMF) then the solvent was transferred into dialysis bags. Dialysis was started against distilled water and at the end HBR was lyophilized. However by this method gel structured HBR was obtained which was not desired.

It was established that dipentaerythritol, DMPA and ricinoleic acids were dissolved in methanol; however HBR polymers were precipitated and did not dissolve. That property made methanol a purification agent. In the literature there are various studies that used methanol for purification of polymers. In the study of Hoogenboom *et al.* (2005) for purification of synthesized 3,6-di(2-pyridyl)pyridazine-poly lactide polymers methanol was also used and polymers removed from the system by precipitation.

FTIR results of purified HBR showed that methanol did not cause any modification on chemical groups of HBR and FTIR spectral ranges were determined to be same with impure HBR (Data not shown). Changes in molecular weight distribution are explained in *3.3.2.*

3.2 Chemical Characterization

3.2.1 Fourier Transform Infrared (FTIR) Spectroscopy

Ricinoleic acid, hyperbranched polyesters (HBP-G_2) and hyperbranched resins (HBR) were characterized by FTIR spectroscopy. Figure 3.1 displays FTIR spectra of ricinoleic acid. Broad peak at 3400 cm^{-1} was assigned to O-H stretch of ricinoleic acid. At 3016 cm^{-1} the peak of olefinic C-H stretching and unsaturated fatty acids were observed. Peak at 2928 cm^{-1} was corresponded to the methylene asymmetrical C-H stretching and methyne C-H stretching of aliphatic groups. 2856 cm^{-1} was suggested as methyl and methylene symmetrical C-H stretch. Carboxylic acid end groups of castor oil fatty acids vibrated at 1713 cm^{-1} and methylene and methyne C-H bends was vibrated at 1459 cm^{-1} and 1380 cm^{-1} respectively. O-H in-plane bend wave number was determined as 1281 cm^{-1}. Finally peak at 724 cm^{-1} was assigned for methylene rocking (n≥3) of fatty acids.

Figure 3.2 shows the comparison of the chemical groups of HBP-G_2 and HBR. O-H stretching of HBP-G_2 was clearly observed at 3480 cm^{-1}. Peaks at 2952 cm^{-1} was assigned for asymmetrical methyl and methlyene stretching. Symmetrical C-H stretching of the aliphatic groups was assigned for the wavenumber of 2893 cm^{-1}. The frequencies at 1478 cm^{-1} and 1380 cm^{-1} corresponded to the methylene and methyne C-H bends. Absorbtion spectra at 1735cm^{-1} corresponded to the ester functional group and peak of alkyl substituted ether was shown at 1131 cm^{-1}. O-H in plane bend was assigned for the peak at 1304 cm^{-1} and finally skeletal C-C vibrations were observed between 1300 cm^{-1} and 700 cm^{-1} frequency areas.

IR spectrum of HBR is also indicated in Figure 3.2. Since HBR formation was obtained by ricinoleic acid esterification, the main difference was detected by noticing the functional groups of ricinoleic acids in HBR. The IR spectra at 3483 cm^{-1} showed O-H stretching of HBR. This corresponded to both hydroxyl groups of ricinoleic acid and hydroxyl end groups of hyperbranched polyester (HBP-G_2). Peak of 3015 cm^{-1} corresponded to olefinic C-H stretch of fatty acids which was not observed in IR spectra of HBP-G_2. Asymmetrical and symmetrical C-H stretching

peaks of HBR were more similar to the C-H stretching of ricinoleic acids, hence it was suggested that these peaks were mainly corresponded to the aliphatic C-H stretching of ricinoleic acids. The frequency at 1735 cm^{-1} was assigned for ester functional groups, 1464 cm^{-1} corresponded to methylene C-H bend and peak at 1245 cm^{-1} is suggested to O=C-O-C stretching of aliphatic polyesters which were also determined in IR spectra of HBP-G_2. Peak at 725 cm^{-1} was assigned for rocks of methylene groups of (n ≥3) of fatty acids in HBR (Bruker Optics 2006, Coates 2000.)

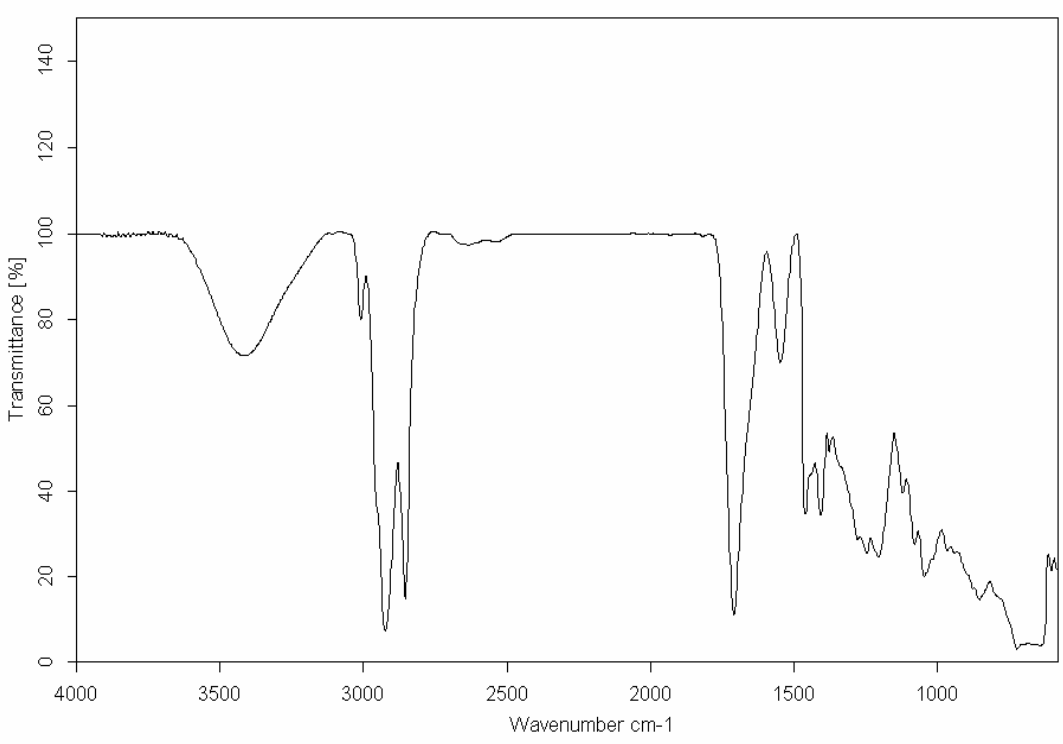

Figure 3.1 FTIR spectra of castor oil fatty acids (mainly ricinoleic acid).

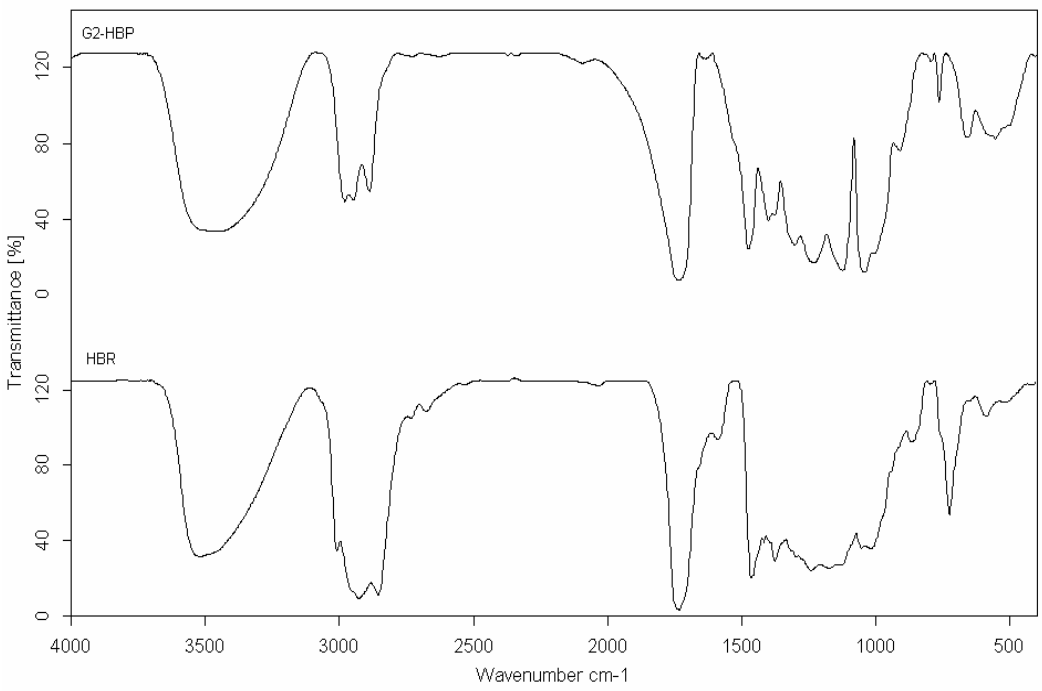

Figure 3.2 FTIR spectra of hyperbranched polyester (HBP-G_2) and HBR.

3.2.2 Molecular Weight Determination

As previously described in Chapter 1, all polymers are composed of mixtures of small and large molecules, so weight of polymer could not have a unique value. Therefore to define molecular weight there are commonly used terms, average molecular weight (Mw) and number average molecular weight (Mn). Mn value is the molecular weight of the polymer divided by number of molecules and Mw is the average molecular weight by considering size and weight of each polymer. Ratio of Mw/Mn gives polydispersity index (PDI) of polymers. For special polymers PDI values approaches to 1 but generally condensation polymers or other types that are commercially available have a PDI value 2 or greater (Polymer 2003, Robello 2002).

In the study molecular weight distribution of HBR before and after methanol purification was determined. As mentioned previously methanol is one of the organic solvents that are used for purifications of polymers. The importance of purification

during molecular weight determinations was also explained in literature. The study of Allen *et al.* (1973) mentioned the methanol purification after synthesis of intermolecular cross-linked polystyrene molecules. In order to maintain narrow polydispersity, purification is one of the important points for polymer characterization.

Determination of molecular weight was accomplished by gel permeation chromatography (GPC) which universal calibration method was used in tetrahydrofuran (THF) solvent. Results are shown in Table 3.1. Since HBR polymers were condensation type of polymers, polydispersity was expected as closer to 2. After purification of HBR polymers with methanol average molecular weights were determined to be increased. Removing small molecules from the system increased average molecular weight. Moreover due to the principle of molecular weight distribution, it was expected to narrow down the polydispersity index after methanol washing. Results showed the decrease of dispersity from 2.58 to 2.11 which approached to 2. By these results purification process was confirmed since distribution profiles narrowed by removing of unreacted molecules.

Table 3.1 Molecular weight and polydispersity of HBR before and after purification with methanol (Mean±SEM, n=2)

	Mn (g/mol)	**Mw (g/mol)**	**Mn/Mw (Polydispersity)**
HBR	8546 ±2400	21989 ± 3901	2.58 ± 0.056
HBR (purified by methanol)	10913 ± 90	23099 ± 3142.5	2.11 ± 0.27

3.2.3 Liquid ^{13}C NMR Analysis of HBR

FTIR results showed the chemical groups of synthesized components however the sign of hyperbranched resin synthesis could not clarified. ^{13}C NMR analysis was performed to determine the carbon groups of HBR structure in particular. Due to

semi-liquid structure of HBR polymer, liquid ^{13}C NMR analysis was done by using deuterated DMSO solvent. Figure 3.3 shows main carbon atoms that bonded with substituents that were found in HBR structure. ^{13}C NMR results in Figure 3.4 was correlated with these carbon atoms.

Carboxylic esters that were formed by interaction of dipentaerythritol and dimethylolpropionic acid was determined at 174.56 ppm resonance range. Quaternary carbon atom of dipentaerythritol was determined at 48.55 ppm and quaternary carbon atom of DMPA was determined at 26.68 ppm ranges. Carbon atoms that linked to carboxylic esters substituents were give a peak at 77.5 ppm.

"Cis" –CH=CH- carbon atoms of ricinoleic acids gave peak at 130.44 ppm and 130.34 ppm. α carbon atoms at 12^{th} position was linked to hydroxyl substituents and these atoms were read at 38.61 while β and γ carbons gave peak at 25.16 and 31.50 ppm. Since it was expected that some of the end groups of DMPA could not make reaction with ricinoleic acid, hydroxyl bonded carbons was read at 75.00 ppm value. Methyl groups of DMPA structure was also corresponded to the peak at 24.73 ppm.

By the results of ^{13}C NMR, the structure of HBR was shown. The major esterification peaks of dipentaerythritol-DMPA and carboxylic esters of ricinoleic acid- DMPA were detected in the resonance results, therefore it could be concluded that HBR formation was established. However to determine the branching degree or to calculate the number of moles of active end groups, further and detailed ^{13}C NMR analysis are required.

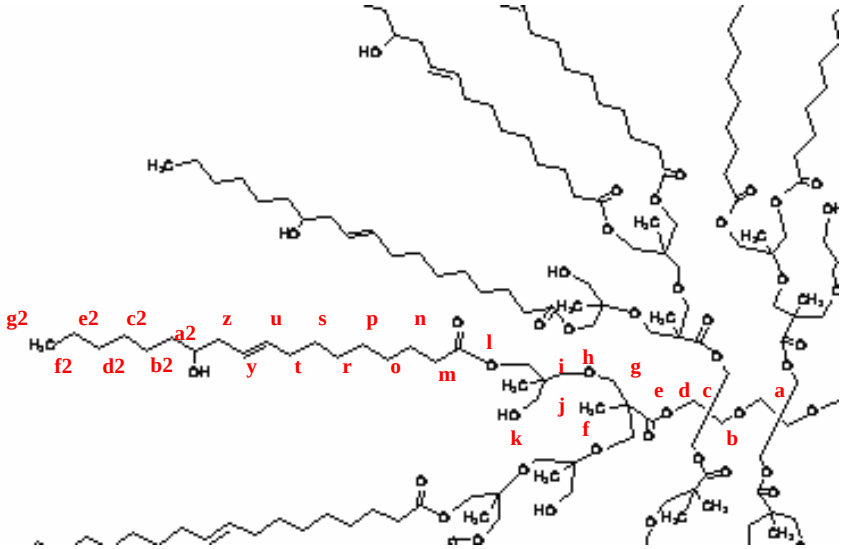

Figure 3.3 Functional carbon atoms that are found in HBR structure.

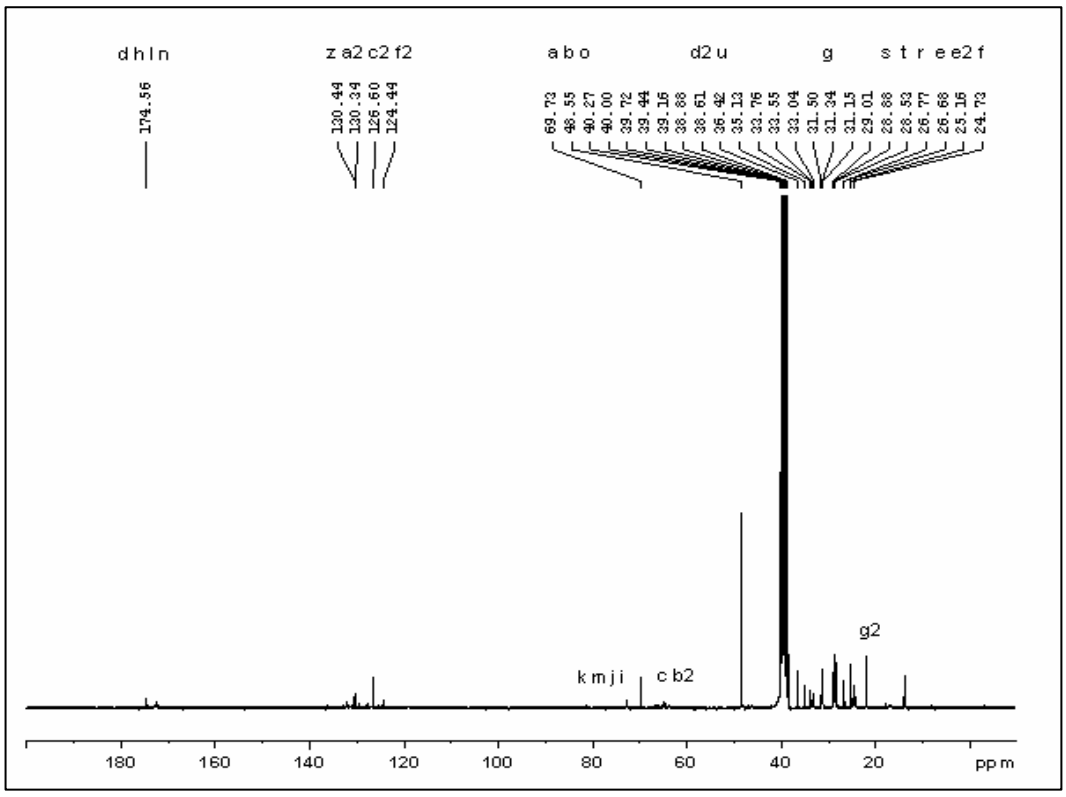

Figure 3.4 ^{13}C NMR results of HBR structure. Letters on the top of the peaks are correlated with the letters that shows carbon atoms of HBR in Figure 3.3.

3.3 Use of HBR in Drug Delivery

After synthesis and characterization of HBR the behavior of HBR in drug delivery studies were investigated. In order to suggest a system as a drug delivery vehicle, drug loading ability, release behavior, biodegradation and biocompatibility properties are some of the important factors that should be determined. Therefore properties were investigated in the next part of the study.

3.3.1 In Vitro Degradation of HBR

For the success of drug delivery studies, biodegradation of the polymer is an important parameter. As explained in detail in section *1.6,* molar mass, chemical structure, hydrophobicity or hydrophilicity are the important factors that should be considered related to biodegradation.

Both hydrolytic and enzymatic degradation of HBR were studied by shaking at 50 rpm in 0.01M PBS at 37°C. To sustain enzymatic degradation, 2 % of Lipase from *Pseudomonas sp.* was added (4 mg/ml). At certain time intervals samples were removed and molecular weight analysis was carried on by GPC. According to the results (Figure 3.5), in initial 10 days molecular weight was increased in both conditions. HBR was almost completely dissolved in 70 days with lipase, however by hydrolytic degradation, molecular weight was not changed significantly.

Initial increase in molecular weight could be interpreted by various ways. First possibility is swelling of HBR in PBS solution. When HBR is placed into the PBS buffer aqueous solution might create surface and bulk erosion to the HBR nanoparticles. This change might led to water penetration by swelling molecular weight increase might be detected. This type of swelling is also studied in Unger *et al.* (2008) which they used different type of polymers but swelling could be explained in same manner. After initial increase of molecular weight, polymers started to molecularly degrade. Water penetration to polymers might led to enter lipase through out the branches of HBR , therefore breaking ester bonds might led to decrease molecular weight. At the same time surface erosion might fasten this process. To

confirm swelling and erosion of nanoparticles, their mass change in aqueous media should also be analyzed.

Another proposal for initial molecular weight increase could be formation of intermolecular hydrogen bonds between functional groups. In the present study incubation of HBR in aqueous solution caused more intense physical structure was viscosity was seem to be increased. According to Hecker et al. (1998), viscosity increasing as a result of intermolecular hydrogen bonding might result to deform the segments, therefore lipase and water could attack to the polymer. Therefore initial condensed structure of HBR with higher viscosity replaced with degrading polymer at the end.

Agglomeration is another suggestion that might be occurred to HBR. According to Hecker and co-workers physical and thermal changing might result to agglomeration of polymers. In the study temperature was set to 37°C therefore at this temperature HBR nanoparticles might agglomerate and molecular weight might be increased.

As a result, initial molecular weight increase might be explained by swelling, erosion, intermolecular hydrogen bonding or agglomeration. To confirm all these suggestions it is clear that further analysis should be done. If mass, size viscosity changes analyzed during the experiment then these proposals could be verified.

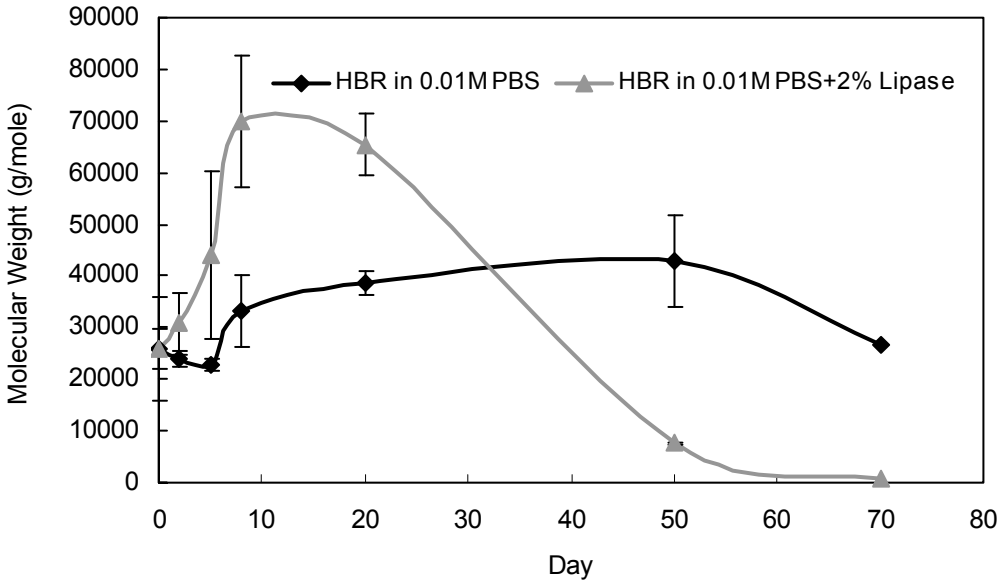

Figure 3.5 Hydrolytic degradation of HBR in 0.01 M PBS and enzymatic degradation in 0.01M PBS and 2% lipase from *Pseudomonas sp.* (4mg/ml) at 37°C with 50 rpm shaking.

After an increase in molecular weight a sharp decrease and degradation was begun by lipase adding. The efficiency of lipases on the degradation of aliphatic polymers was explained in the previous chapter. It was expected that lipase from *Pseudomonas sp.* species break the ester bond of the HBR structure and increase the degradation rate. HBR was degraded almost completely which indicated the efficiency of the lipase. The effect of lipase was increased by increasing the incubation time of HBR in PBS. Graph shpws that degradation became faster a certain time period. Since lipase concentration was kept constant during degradation more efficient decompositions was determined by the end of the experiment. Similar proposals was given in the study of Jugminder *et al.* (2002). The yals ostudied the degradation of polymers with same lipase and which they suggested that lipase degrades nanoparticles one by one so degradation rate become faster at the end of the process. In addition *Pseudomonas sp.* lipase was lipophilic therefore in first days lipase concentration was not sufficient to compensate the molecular weight increase, so the effect of lipase was not observed. However after water entering to the HBR

cores lipase might show its efficiency and show which contribute to the decompositions of HBR.

As a result of this study the effect of the lipase was observed by analyzing the molecular weight decrease of the HBR but in order to explain the changes in molecular weight or to prove the suggestions, particle size analysis, viscosity measurements, FTIR analysis or mass change determinations should be one for the future analysis.

3.3.2 Tamoxifen and Idarubicin Loading Studies

3.3.2.1 Preliminary Experiments

Several attempts were made to optimize the loading effectivness of the drugs. In the first case, since both of the drugs and HBR were highly hydrophobic, all components were dissolved in organic solvent and then they transferred into inorganic solution to supply the interaction of the drug with HBR. Then the samples were lyophilized. However with this procedure, it was not possible to remove unentrapped drugs from the system since unentrapped drugs were not dissolved in inorganic solvents.

The next attempt was made by adding drug powder to the HBR without using any organic or inorganic solvent. Then unloaded drugs were removed by methanol. Low amount of drug has to be loaded, therefore the exact loading percentage was undetectable, as a result loading efficiency of the samples were not coherent.

Finally, the most efficient loading was obtained firstly by dissolving the drug with DMF, then applying them into the HBR. By using the solubility difference unloaded drug was removed by methanol. Drug loaded HBR was precipitated and could be analyzed for the drug loading efficiency. Detailed explanation of the procedure was given in section *2.6.*

3.3.2.2 Loading Efficiency

Due to highly hydrophobic nature of tamoxifen, lipid based carriers are preferred for controlled delivery studies. In this study high loading efficiency was expected due to highly hydrophobic interactions of tamoxifen and ricinoleic acid. The results confirmed the expectations and a desirable loading efficiency were obtained.

Drug loading studies was performed by increasing concentration of the drug while HBR amount was remained constant. The Figure 3.6 shows the loading efficiency of the tamoxifen (µg) per 1 mg of HBR. Maximum loading efficiency was determined as 73.28 % for 0.66 µg/mg. When the amount of loaded drug was increased to 1.33 µg/mg and to 2.66 µg/mg, efficiencies were declined to 59.31 % and to 43.5 %, respectively. Decrease in the entrapment efficiency became stationary at higher ratios. For instance by increasing the ratio from 4 µg/mg to 8 µg/mg the efficiency was only changed from 40.16 % to 37.47 %.

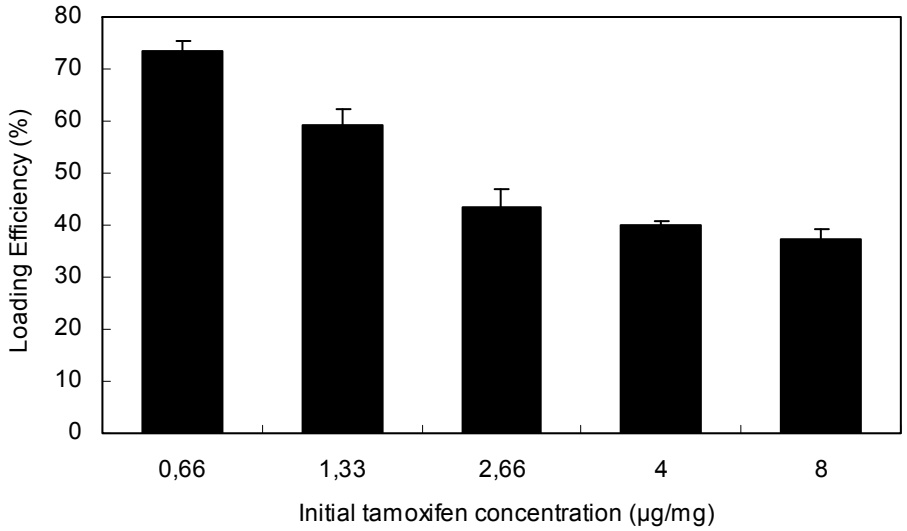

Figure 3.6 Loading efficiency of µg of tamoxifen/mg of HBR (Mean ± Standard error of the mean (SEM), n=2)

During loading process, hyperbranched resin-tamoxifen (HBR-TAM) formulations were washed with methanol to remove unloaded tamoxifen. Increasing the concentration of drug may lead the saturation of the system. During methanol wash some of the weakly interacted tamoxifen molecules might be removed. Therefore increasing the drug concentration might result in a decrease of the loading efficiency.

Hydrophobic nature of idarubicin was also sustained higher loading efficiency to the fatty acid based HBR systems. Idarubicin entrapment efficiency results are shown in Figure 3.7. The maximum loading efficiency was determined as 80 % for the ratio of 0.66 µg/mg. As shown in the figure, there is significant difference between highest and lowest HBR-TAM concentrations. For the amount of 0.66 µg/mg, 1.33 µg/mg and 2.66 µg/mg the loading percentages were stated as 73.9 %, 61.8 %, and 59.63 % respectively. For 1µg/mg, 2 µg/mg, 4µg/mg efficiency was determined as 68.48 %, 61.24 %, 53.41 % and for 3 µg/mg and 6µg/mg the efficiencies were 54.71 %, 45.65 % respectively. Finally for 8 µg/mg, the percentage was examined as 45.26 % which was the lowest among the samples.

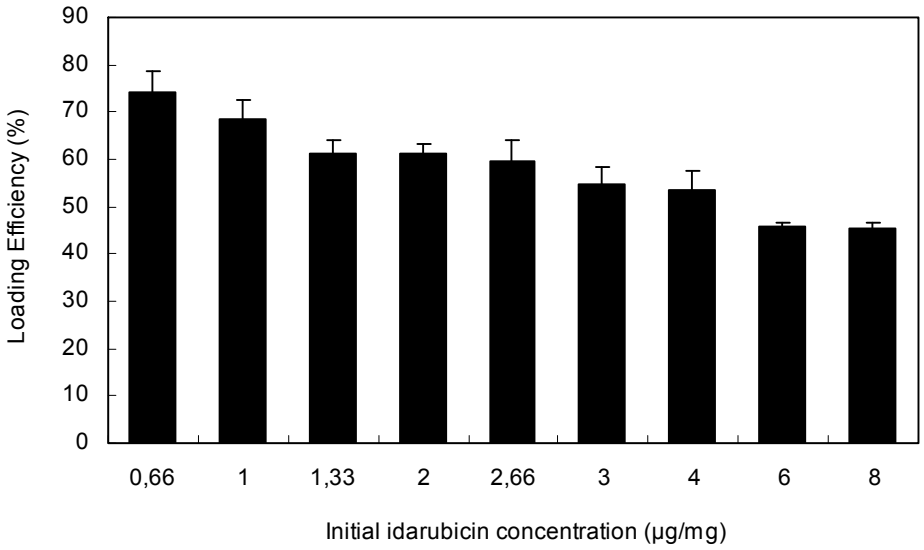

Figure 3.7 Loading efficiency of µg idarubicin per mg of HBR (Mean ± SEM, n=2)

Although the entrapment efficiency of idarubicin and tamoxifen are different, idarubicin entrapment behavior was similar to tamoxifen. Increasing the concentration of the drug led to decrease the efficiency. The reason could also be explained with the methanol washing step which excess idarubicin molecules removed from HBR and might be dissolved in methanol like tamoxifen.

Loading efficiency of both drugs were almost same at initial loading concentrations of 0.66 µg/mg and 1.33 µg/mg, however the efficiency of tamoxifen entrapment was significantly lower for the diminishing concentrations. As it is seen from Figure 3.8, logarithmic scale both drugs gave a straight line. Therefore the relation between initial concentration and entrapment efficiency can be shown by power law equation. For idarubicin the equation is Efficiency= $67.922C_{initial}^{-\ 01836}$ and for tamoxifen the equation is Efficiency= $62.815C_{initial}^{-\ 0.2861}$. Power equation of tamoxifen is lower, in other words detachment of drug from HBR is higher with respect to idarubicin. Equation difference between two drugs was probably because of the structural differences and interaction differences with HBR. Molecular weight of drugs may affect loading efficiency. Since tamoxifen (Mw= 371.51g/mole) has lower molecular weight than idarubicin (Mw= 533.95 g/mole), it is more likely that tamoxifen may be detached during methanol treatment. In addition, by considering FTIR results which were explained in section *3.4.3.1,* it was estimated that tamoxifen was physically entrapped into the inner part of HBR, while idarubicin was chemically interacted. Adsorbed tamoxifen into the HBR chain could be more easily desorbed, therefore these results confirms the physical interaction behavior of tamoxifen with HBR nanoparticles. Consequently, higher idarubicin loading efficiency relative to tamoxifen could be explained by higher molecular weight of idarubicin and chemical interaction of the molecule with nanoparticles.

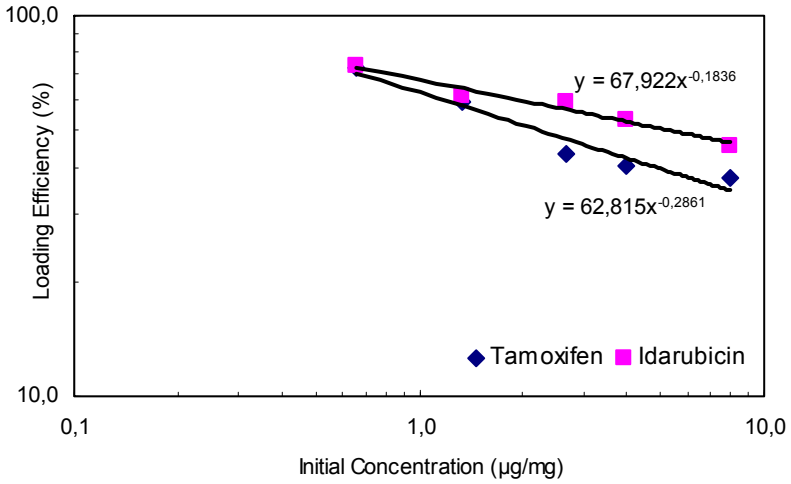

Figure 3.8 Loading efficiencies of µg tamoxifen and µg idarubicin per mg HBR in logarithmic scale. Power equations are shown in the graph.

3.3.3 Chemical Characterization of Drug Loaded HBR

3.3.3.1 FTIR Results

In drug delivery studies to determine the drug-polymer interactions the most commonly used characterization method is the FTIR analysis. In this study, HBR and drug loaded HBR were analyzed by FTIR and the interactions were determined. Changes in the transmittance peaks were compared by the FTIR results of free drug (Data not shown).

3.3.3.1.1 Tamoxifen Loaded HBR

FTIR results of tamoxifen loaded HBR (HBR-TAM) and empty HBR are shown in Figure 3.9. When all peaks were identified no difference was observed between tamoxifen loaded and empty HBR. This might be due to the fact that tamoxifen could not be entrapped into HBR. However after tamoxifen loading, HPLC analysis proved the presence of tamoxifen. In addition changes that occur after tamoxifen loading

was determined with various analysis that was discussed in this chapter. Therefore the presence of tamoxifen in HBR was shown with different methods. In the second assumption tamoxifen could present in the sample but it might not be entrapped into HBR. If tamoxifen was not entrapped into HBR polymers then transmittance peaks of free drug should be detected with the same wavelength ranges; however peak of tamoxifen was not found. All these have suggested that tamoxifen was physically entrapped into HBR polymers and the chemical groups of tamoxifen were masked by HBR.

In the literature similar results were obtained. In the study of Vishnu *et al.* (2007) carvedilol and muchoadhesive type polymers were investigated. The IR spectra showed that there were no differences between hydoxypropyl methyl cellulose (HPMC) polymers and carvedilol, which proposed a physical interaction and drug molecules was present in an unchanged state in the HPMC polymer. The study of Tayade *et al.* (2003) also showed the physical interaction with FTIR results. The mixtures of iburprofen-gelatin micropellets indicated no difference compared with the free components and they suggested a physical interaction.

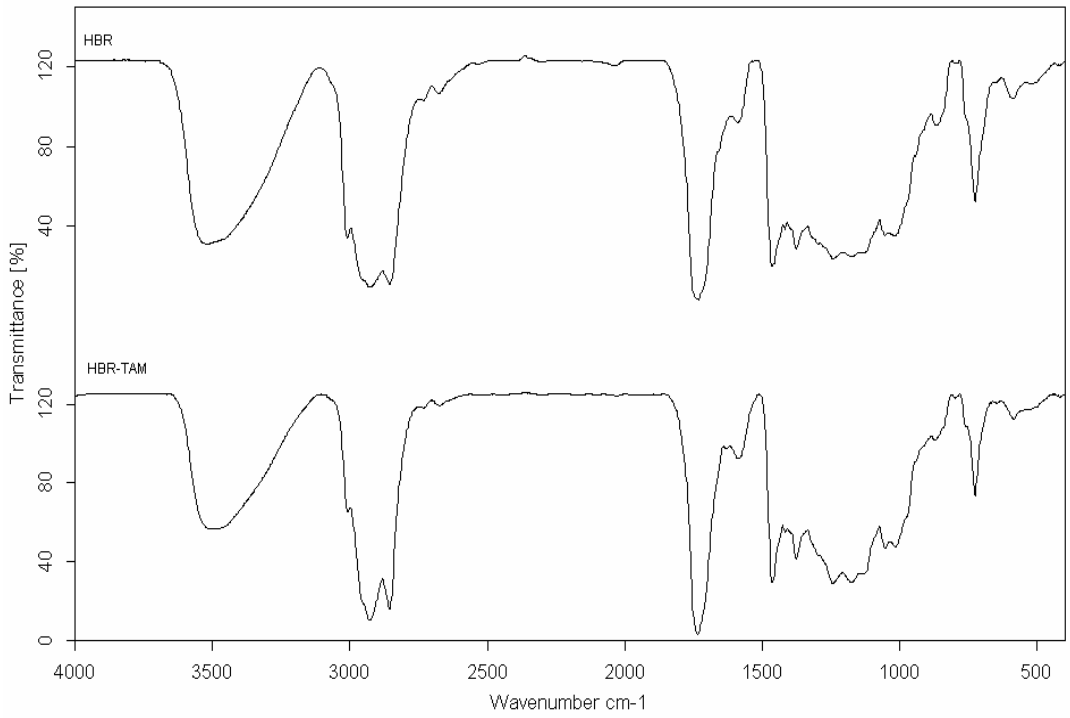

Figure 3.9 IR spectra of HBR and HBR-tamoxifen (HBR-TAM).

3.3.3.1.2 Idarubicin Loaded HBR

Figure 3.9 shows the FTIR results of HBR and hyperbranched resin-idarubicin (HBR-IDA) formulations. According to the absorbtion spectra it was noticed that the intensity of O-H stretching frequency at 3483 cm^{-1} did not changed, which means there were no hydrogen bonding with O-H groups of idarubicin. By idarubicin entrapment new peak was formed at 1675 cm^{-1} which might be suggested as –C-N- , –C=N- or C=O bonding. Since the frequencies of these chemical groups overlapped with each other the exact chemical interaction could not be identified. Primary amine N-H bend of pure idarubicin gave peak at 1636 cm^{-1} (Data is not shown). Amine group of idarubicin might be covalently interacted with carbon atoms of HBR and new peak was formed at 1675 cm^{-1}. Because of the intensity of ester peak (1735 cm^{-1}) did not change, an amide bond formation probably did not occur but -C-N- covalent bond might be formed by methyl or methylene carbons of HBR. The

chemical interaction of idarubicin with HBR was shown by IR spectra but in order to identify exact interaction, further analysis may be needed (Bruker Optics 2006, Coates 2000).

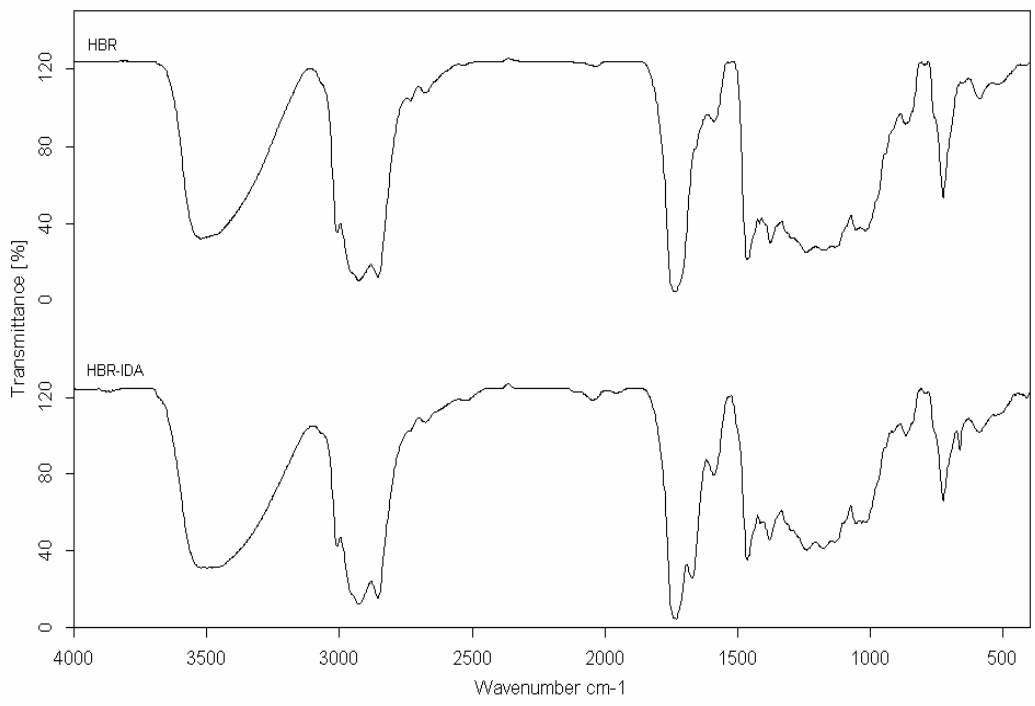

Figure 3.10 The comparison of FTIR spectra of HBR and HBR-Idarubicin (HBR-IDA).

3.3.3.2 Particle Size Distribution and Zeta Potential

Particle size and distribution plays an important role in drug release. Reports indicate that small particles (<500 nm) could pass through epithelial barriers by endocytosis which suggests an advantage for nanoparticles in order to permeate across physiological drug barriers (Zhang *et al*. 2006, Dong *et al*. 2004).

Particle size and distribution profile of the samples are shown in Table 3.2 and Figure 3.11. Tamoxifen and idarubicin (2.66 µg/mg and 8 µg/mg) were loaded to HBR and particle sizes were compared. Size of HBR formulations varied from

approximately from 206 nm to 276 nm with low polydispersity. The results indicated that after loading tamoxifen and idarubicin, size of the nanoparticles get smaller. Since HBR could entrap idarubicin and tamoxifen either physically or chemically, in both conditions fatty acid tails may surround the drug molecules which may cause decrease in particle size. By increasing the concentrations of these drugs, a significant decrease was detected for HBR-TAM. For HBR-IDA, increasing drug concentrations did not affect the size significantly. This difference might be related to greater molecular weight and chemical interaction of idarubicin. Particle size distribution of samples was in Appendix B.

There are examples in the literature relating with the particle size decrease after loading with drug. In the study of Ameller and co workers (2003) pure anti estrogen RU 58668 was loaded into nanospheres and nanocapsules prepared from different polyester copolymers. Similarly in the study of Maillar *et al.* (2005) RU 58668 incorporated into nanocapsules coupling with polyethylene glycol chains. In both study particle size of the nanoparticles decreased after drug loading study. The reason of this decrease was explained by the property of RU 58668 drug. Low solubility and high hydrophobicity might lead to more compact structure with nanoparticle. In our study since two highly hydrophobic drugs were used, it might also increase the compaction and adsorption into the HBR thus particle size might be decreased.

A particle in an aqueous medium constitutes always a fixed charge and surrounds by a counter ion that is present in the solution. (Bhattacharya *et al*. 2006). Zeta potential is the magnitude of the electrostatic potential at the plane of shear and is an important index to evaluate the stability of the particles (Huang *et al*. 2006). It gives an idea about overall surface charges of the particle and how it is affected by the environment. The potential also suggests the route of the particles *in vivo* conditions against physiological barriers (Barrat 1999). It plays an important factor to determine their interaction with the cell membrane, which is usually negatively charged (Dong *et al*. 2003)

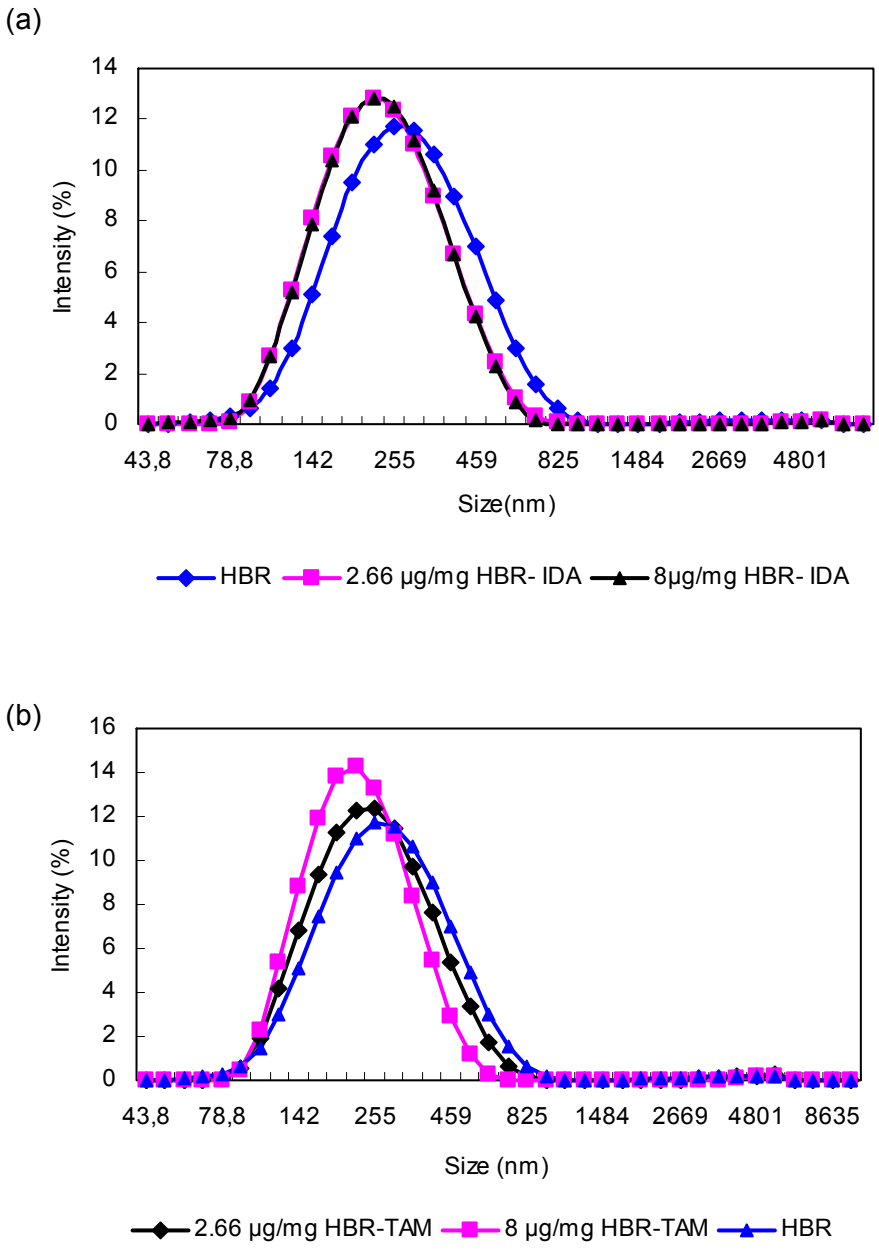

Figure 3.11 Size distribution graph of the HBR-IDA (a) and HBR-TAM (b) based on particle size analyzer samples, measured in aqueous dispersant at 24°C. (Mean±SEM, n=2)

Table 3.2 Particle Size (nm), Polydispersity Index (PDI) and Zeta Potential (mV) results of HBR, HBR-IDA and HBR-TMX samples. Drug/HBR (μg/mg) ratio that is used for the analysis and their loading efficiencies are also given. (Mean ± SEM, n=2).

	μgdrug/ mgHBR	***Loading Efficiency (%)***	***Particle Size (nm)***	***Poly dispersity Index (PDI)***	***Zeta Potential (mV)***
HBR	-	-	276.46 ± 8.63	0.187 ± 0.005	-41.2 ± 0.7
	2.66	59.6 ± 4.32	217.1 ± 5.56	0156 ± 0.014	-41.35 ± 1.55
HBR-IDA	8	45.26 ± 1.18	215.16 ± 4.16	0.163 ± 0.003	-40.55 ± 0.95
	2.66	40 ± 1.38	232.2 ± 2.73	0.172 ± 0.002	-43.65 ± 2.15
HBR-TAM	8	37.47 ± 1.67	206.93 ± 0.01	0.142 ± 0.012	-40.15 ± 1.15

Table 3.2 shows zeta potential results of the samples. The potential value of drug unloaded HBR particles were detected as -41.2 mV. After loading drugs in different concentrations, potential of HBR did not significantly changed. According to the results, it was suggested that potential of the drugs might be masked by entrapping into fatty acid tails of HBR (Ameller *et al*. 2003, Cavallaro *et al*. 2004).

When the potential ranges of all HBR formulations were investigated it was detected that all samples had a potential smaller than -30 mV. The particles that have zeta potential charge in between -30 mV and +30 mV have physical instability (Zeta Sizer Nanoseries 2008) and have potential of aggregation in aqueous solutions. HBR formulations were in the range of full electrostatic stabilization and negative charge prevents aggregation in buffer solutions (Lee *et al*. 2007, Zhang *et al*. 2006).

3.3.4 Drug Release Study

Drug release conditions of HBR polymers were studied by considering the chemical characterization results. The nature of HBR was hydrophobic and zeta potential results showed the stability of the particles in aqueous environment. Moreover, biodegradation results of HBR in the absence of lipase proposed the stability of these particles. As a result of this analysis lipase from *Pseudomonas sp*. was added to the system to increase the degradation of HBR structure so the rate of drug delivery would be increased (Jugminder *et al.* 2002, Yu *et al.* 2005). The effect of the lipase on HBR degradation was discussed in *3.4.1.*

All release studies were performed by using dialysis methods in phosphate buffered saline (pH 7.4) at 37°C. In one set of tamoxifen release experiments, 5% (v/v) of DMF was applied to the PBS solution. Yang *et al.* (2005) used DMF for facilitating the solubilization due to poor water solubility of polymers. The second experiment was maintained for idarubicin and tamoxifen by adding 0.5 % (w/v) sodium dodecyl sulfate (SDS) and 50 µl of *Pseudomonas sp*. lipase (4 mg/ml) to the 3 ml of PBS solution. In order to prevent the adsorbtion of the drugs into the dialysis bags or walls of the falcon tubes, SDS was used (Hu *et al.* 2006).

3.3.4.1 Tamoxifen Release

HPLC results of released tamoxifen in PBS (5 % DMF) at 37°C are illustrated in Figure 3.12 below. For the release study 2.66 µg tamoxifen was loaded per mg of HBR with a 43.5 % loading efficiency. HPLC results indicated that the presence of DMF was insufficient for the release of tamoxifen. At 100 days approximately 4.53 % of tamoxifen was released from HBR polymers. A non-significant release was detected up to 17 days while release was increased linearly up to 69 days and 4.53 % of tamoxifen was delivered. Release became a steady state form 69 days to 100 days. Poor solubility of tamoxifen could be also the reason which released tamoxifen might not be detected by HPLC due to adsorbtion to the walls of the tubes or dialysis bags.

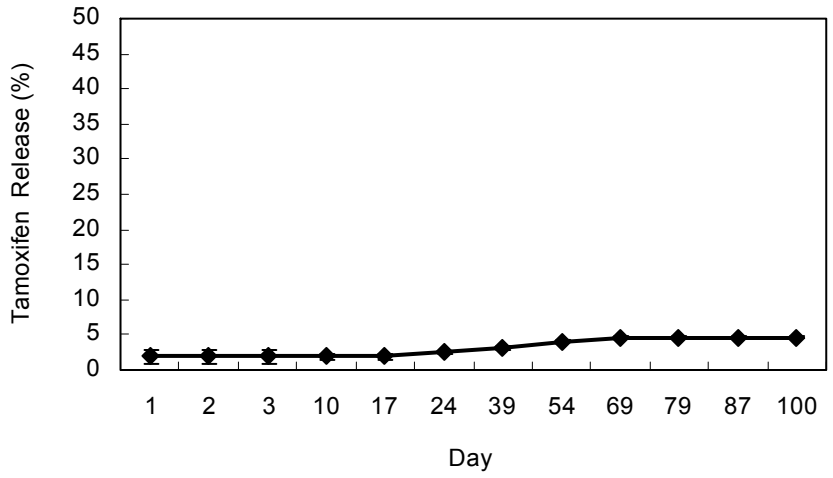

Figure 3.12 Cumulative release of tamoxifen from HBR in 5% (v/v) DMF containing 0.01 M PBS (pH 7.4) at 37°C (Mean ± SEM, n=2).

In the second set, tamoxifen release was investigated in 0.5 %(w/v) SDS and *Pseudomonas sp*. lipase containing PBS at 37°C and efficient delivery results were detected in these conditions. The concentration of 2.66 μg/mg and 8μg/mg of tamoxifen were used for release with 43.5 % and 37.48 % entrapment efficiency. For the concentration of 2.66 μg/mg, release began at day of 5 and 87 % of the loaded drug was released in 55 days (Figure 3.13). Release of 8 μg/mg tamoxifen was increased linearly up to 20 days and totally 61.34 % of tamoxifen was released in 55 days. It was noticed that during release process burst effect of the polymer did not observed which might be beneficial for the bioavailability. Another point that was noticed is the efficiency of the tamoxifen release which varied according to the concentration of the loaded tamoxifen. By considering the experiments it was proposed that increasing the amount of drug lowered the rate of release.

In the literature there are studies that discussed the concentration effect on the release rate of the drug. Skolosky-Popkov *et al*. (2008) studied paclitaxel release from ricinoleic acid based polyanhydrides and copolyesters. In this study increasing the concentration of the drug caused to increase the hydrophobicity of the system. By this effect, water penetration into the polymer matrix and degradation of the polymer was decreased, hence increasing the concentration of the drug, slowed

down the release rate. The results of Skolosky-Popkov *et al*. (2008) could also be acceptable for the tamoxifen release from HBR. Considering the results of FTIR and particle size distribution, a proposal was made by concerning with the physical interaction of tamoxifen with HBR and decreasing the particle size by entrapment of the drug. Increasing the amount of drug might lead to increasing the hydrophobicity of the system and drug molecules might be adsorbed into the HBR more efficiently. As a result, tamoxifen was released more slowly in higher concentrations.

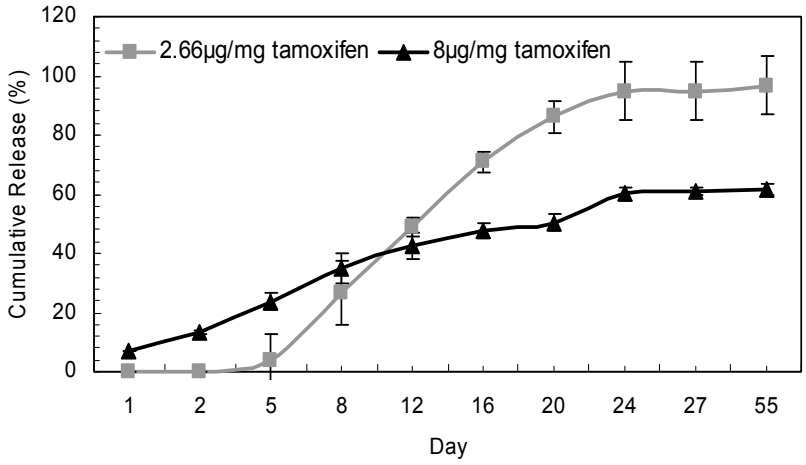

Figure 3.13 Cumulative release of tamoxifen from HBR in PBS (pH 7.4) which contains 0.5%(w/v) SDS and *Pseudomonas sp.* lipase at 37°C (Mean ± SEM, n=2).

3.3.4.2 Idarubicin Release

As discussed previously, idarubicin was chemically interacted with HBR polymers thus release were expected to be slower than tamoxifen. Results of idarubicin release confirmed the expectations, however the rate of release was determined to slower than the estimation (Figure 3.14). For 2.66µg/mg and 8µg/mg concentration of idarubicin, cumulative release was obtained less than 1% in 75 days in PBS buffer (pH 7.4, 0.5% SDS, *Pseudomonas sp.* lipase at 37°C) which indicated a dramatically slower release than expected.

Idarubicin release rate was also changed by increasing drug concentration. When the amount was increased from 2.66µg/mg to 8µg/mg cumulative release was declined significantly. Since idarubicin had a hydrophobic nature, results could be explained by the same reasons that was explained for the concentration dependent tamoxifen release.

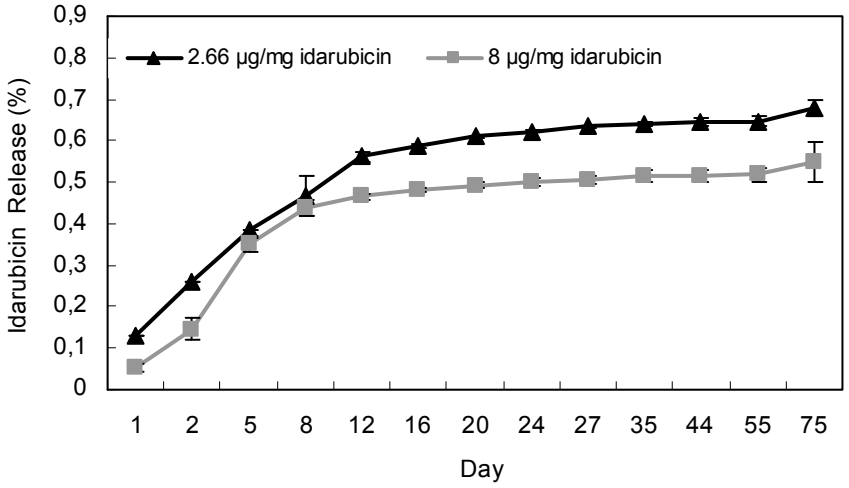

Figure 3.14 Cumulative release of idarubicin from HBR in PBS (pH 7.4) which contains 0.5%(w/v) SDS and *Pseudomonas sp.* lipase at 37°C (Mean ± SEM, n=2).

To investigate the reason of slow idarubicin release, various parameters should be considered. First of all due to chemical interaction of idarubicin, water penetration might not be as fast as in tamoxifen release, therefore only small amount of drug might be released. Moreover the amount of enzyme application might not be enough for degradation of the complex or released idarubicin might be adsorbed into the walls of dialysis bags or tubes even in the presence of SDS.

Although slow release rate results were determined, cytotoxicity of the HBR-IDA showed (the results will be discussed in the next chapter) the efficiency of the drug on MCF-7 cell lines in 96h at 37°C. All these results and suggestions should be considered for the future studies.

3.3.5 Cytotoxicity

Testing for cytotoxicity is a good first step toward ensuring the biocompatibility of biomaterials for drug delivery systems. To reduce the extent of safety issues in laboratory animals, *in vitro* cell cultures have gained importance. A negative result indicates that a material is free of harmful products or has an insufficient quantity of them to cause acute effects to isolated cells. On the other hand, a positive cytotoxicity test result can be taken as an early warning sign that a material contains one or more extractable substances that could be of clinical importance. In such cases, further investigation is required to determine the utility of the material. (Ameller *et al*. 2004, Wallin *et al*. 1998).

Cytotoxiciy of empty HBR and drug loaded HBR was determined by using XTT assay kit. 5000 MCF-7 cells/well were seeded to 96 well plates at 37°C. Cells that are exposed to empty HBR were incubated for 96h and cells that are exposed to drug loaded HBR samples were incubated for 48h, 72h and 96h at 37°C. In the study of Kars *et al.* (2007) doubling time of MCF-7 cells was determined as 28.55h ± 1.57 therefore 96h of incubation is determined to be the highest value for MCF-7 to tolerate. Cell proliferation profiles were determined by considering control groups. The procedure was explained in detail in *2.10.2.*

Ideal HBR concentration was determined by preliminary experiments. Since the solubility of the HBR in aqueous medium is quite low, dimethyl sulfoxide (DMSO) was used as solvent. By considering the toxicity of DMSO, predetermined amount of solvent was used (10 % v/v) and maximum amount of HBR was dissolved.

An important point was to determine the maximum amount of drug that was toxic to sensitive MCF-7. The optimum concentration of the drug was determined as 2.66 µg per mg of HBR. Drug loading efficiency of HBR was calculated and the amount of drug that could be exposed to the cells was determined. Cell viability profiles and IC_{50} values were determined after each sample exposure. Logarithmic equations of these viability graphs are given in detail in Appendix C.

3.3.5.1 Cytotoxicity of Empty and Drug Loaded HBR

Empty HBR were applied to the cells in order to see the toxicity profile of HBR. Figure 3.15 shows MCF-7 cell viability after 96h of incubation with HBR formulations between 1.59 µg/ml to 812 µg/ml. Toxicity profile of empty HBR suggested that concentration amounts of 812 µg/ml and 406 µg/ml caused a mild level toxicity, while other concentrations caused a slight decrease in the viability of MCF-7 cells. Concentration ranges between 1.59 µg/ml and 101.5 µg/ml did not cause a significant decrease in cell viability. However after exposure to 203 µg/ml of HBR, cell proliferation decreased significantly. The lowest cell viability was determined after 812 µg/ml HBR treatment which was 52.58 %. These results indicated that exposure to empty HBR even after 96 h of incubation was well tolerated by the cells.

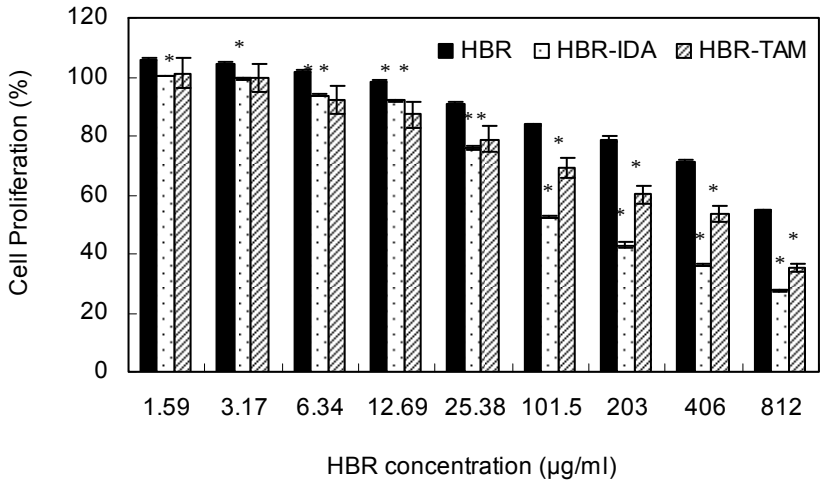

Figure 3.15 Cell proliferation profiles of MCF-7 cell line after 96h incubation with HBR, HBR-IDA, HBR-TAM at 37°C. Cell proliferation was determined by XTT assay. Cell proliferation percentage of samples was determined by considering the 100% proliferation of control groups. Results in the figure represent Mean± SEM. All experiments were carried out in duplicates and HBR-TAM experiment were carried on triplicates, *p<0.05 relative to empty HBR treated cells.

Figure 3.15 also shows cytotoxicity profiles after HBR-IDA and HBR-TAM treatment. HBR-TAM and HBR-IDA concentrations between 25.38 µg/ml to 812 µg/ml displayed a significant toxicity relative to empty HBR. 812 µg/ml of HBR-IDA had the greatest toxicity which was determined as 27.47 %. Results indicated the efficiency of drug loaded HBR. It was suggested that drug was released in the cell and showed its toxic effect.

IC_{50} values of the empty and drug loaded HBR is given in Table 3.3. After 96 h of incubation with empty HBR, IC_{50} was determined as 11.12 mg/mL which was quite different from the IC_{50} values of the drug loaded HBR. IC_{50} of HBR-IDA was 72.8-fold smaller than the empty HBR and determined as the most potent formulation. IC_{50} values of HBR-TAM was also examined as 25-fold more potent in comparison with empty HBR. When time dependent IC_{50} values were compared, after 96h of incubation, HBR-IDA was found to be 6.90-fold more toxic than 48h of incubation. For HBR-TAM, 96h of treatment showed 4 times and 1.96 times more potency relative to 48 h and 72 h of incubation respectively. These results indicated time dependent toxicity of HBR-IDA and HBR-TAM as expected.

Table 3.3 IC_{50} profiles of empty and drug loaded HBR at different incubation periods. (Mean ± SEM, n=2, [a] n=3)

IC_{50} of HBR (µg/ml)	**48 h**	**72 h**	**96 h**
HBR	-	-	11.12 ± 0.039
HBR-IDA	1.055 ± 0.084	0.460 ± 0.001	0.153 ± 0.001
HBR-TAM	1.801 ± 0.017	0.918 ± 0.019	0.445 ± 0.003[a]

3.3.5.2 Cytotoxicity of Free Drugs and Drug Loaded HBR

In order to investigate the efficiency of HBR-IDA and HBR-TAM on MCF-7 cells, cytotoxicity of free drugs were determined. The concentration of free drug was determined by considering the concentration of entrapped drug in HBR.

The illustration in Figure 3.16 shows the toxic effects of HBR-IDA and free idarubicin on cells with respect to exposure time. In all 48 h, 72 h, 96 h of incubation periods, more toxicity was observed by idarubicin loaded nanoparticles and the most significant difference of HBR-IDA relative to free idarubicin was determined at 48 h [Figure 3.16 (a)]. After application of 4000 nM of entrapped idarubicin for 48h, 72 h, and 96 h, the viability was examined as 47 %, 40 % and 27.5 % respectively.

When time dependent toxicity of HBR-IDA were analyzed, it was shown that increasing the incubation time, leads to decrease the differences between dose dependent viability percentages [Figure 3.16 (b) and (c)]. In addition, the significant difference between HBR-IDA and free idarubicin decreased to non-significant ranges when the incubation exposure was increased from 48 h to 96 h for the concentration of 250 nM and 62.5 nM. IC_{50} values confirmed these results. Table 3.3 below shows the IC_{50} values after 48 h, 72 h and 96 h incubations. 48 h incubation of HBR-IDA seemed 4.8 fold more potent than the free drug. However, when incubation was increased to 72 h and 96 h, difference was decreased to 3.4 fold and to 1.9 fold.

Figure 3.17 shows the cytotoxicity effects of tamoxifen and HBR-TAM. The highest three doses of HBR-TAM showed the most significant toxicity relative to free tamoxifen. By increasing the incubation time to 96h, HBR-TAM showed more potency relative to free tamoxifen. For the highest dose of entrapped tamoxifen, the cell viability was determined as 52 % for 48 h, 45 % for 72 h and 35.4 % for 96 h of incubation.

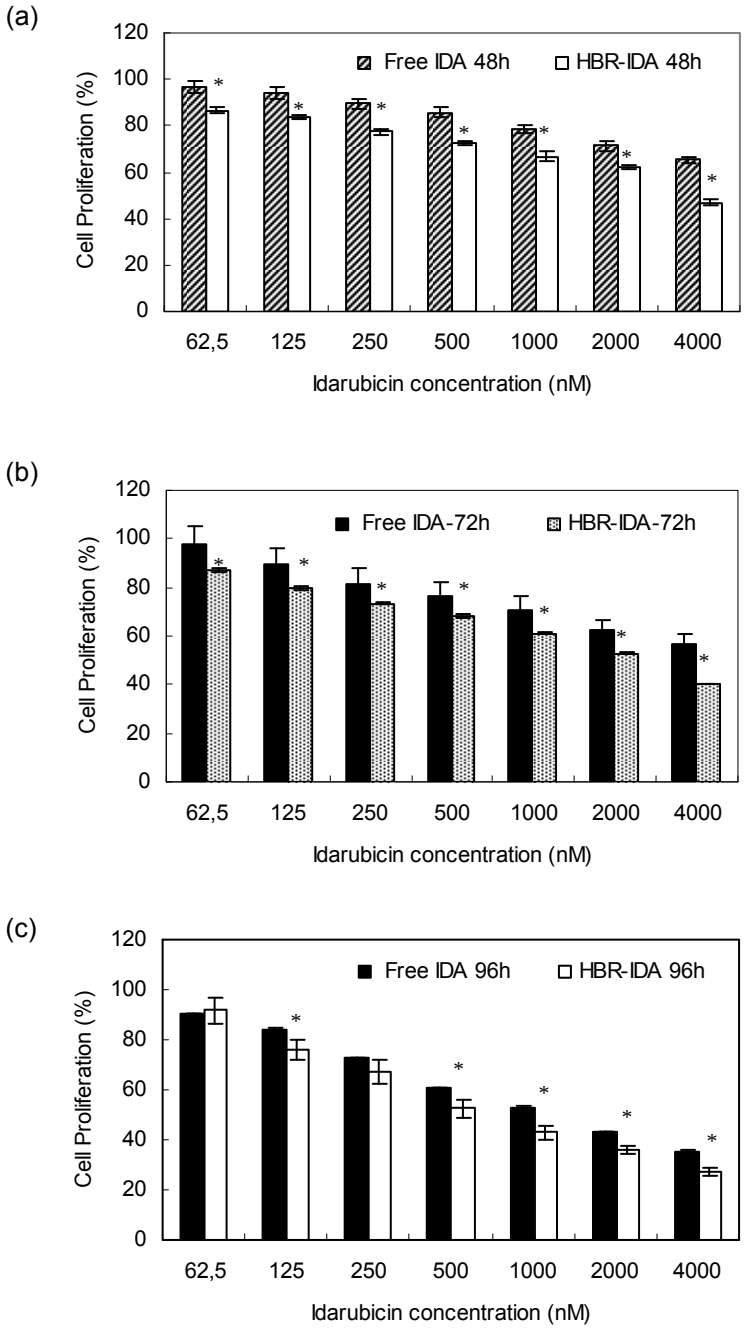

Figure 3.16 Cell proliferation profiles of MCF-7 cells after exposure to idarubicin and HBR-IDA at 37°C for 48h (a), 72h (b) and 96h (c). Cell proliferation was determined by XTT assay. Cell proliferation percentage of samples was determined by considering the 100% proliferation of control groups. Results in the figure represent Mean± SEM, experiments were carried out in duplicates and triplicates (Idarubicin application for 48h and 72h), *$p<0.05$ relative to free idarubicin treated cells.

IC_{50} values of the HBR-TAM and tamoxifen formulation is given in the Table 3.4. Results indicated that at 48 h HBR-TAM was 109 times more potent that free tamoxifen exposure. Furthermore the toxicity of HBR-TAM was determined as 100.5 and 29 times more toxic at the incubation time of 72 h and 96 h respectively.

According to the release studies, 12.5 % of tamoxifen and 0.38 % of idarubicin was released in 4 days. However cyototoxicity profiles of both formulations suggested that both drugs showed their effect on breast cancer cells which might be explained by release of the drugs. Since diameter of HBR-IDA and HBR-TAM were suitable for endosomal uptake, idarubicin and tamoxifen might be released from the HBR and might be activated by a less specific process, pH controlled hydrolysis or by very specific enzymolysis (Ulbrich *et al*. 2003). The results might be explained by very significantly different conditions of drug release in dialysis bags and in cell cultures. During release experiments, concentrated HBR-Drug formulations in the dialysis bags might inhibit diffusion of drugs from the nanoparticles. However for cytotoxicity analysis more dilute HBR-Drug formulation was applied onto the cells so release rate might be increased.

Table 3.4 IC_{50} concentrations of Drug-HBR formulations and free drugs after 48 h, 72 h, 96 h of treatment to MCF-7 cells. (Mean ± SEM, n=2, [a] n=3)

IC_{50} of drugs (μM)	**48 h**	**72 h**	**96 h**
HBR-IDA	5.19 ± 0.42	2.26 ± 0.036	0.752 ± 0.003
IDA	24.95 ± 10.9 [a]	7.6 ± 0.2[a]	1.415 ± 0.031
HBR-TAM	8.52 ± 0.078	3.58 ± 0.75	2.1 ± 0.016[a]
TAM	921 ± 281	360 ± 2.5	60.9 ± 3.7[a]

Lee *et al*. (2007) studied release and cytotoxicity effects of paclitaxel loaded solid lipid nanoparticles. According to this study 10% of loaded paclitaxel released in 24 h, however these formulations displayed efficient effects on ovarian cancer cells. Lee

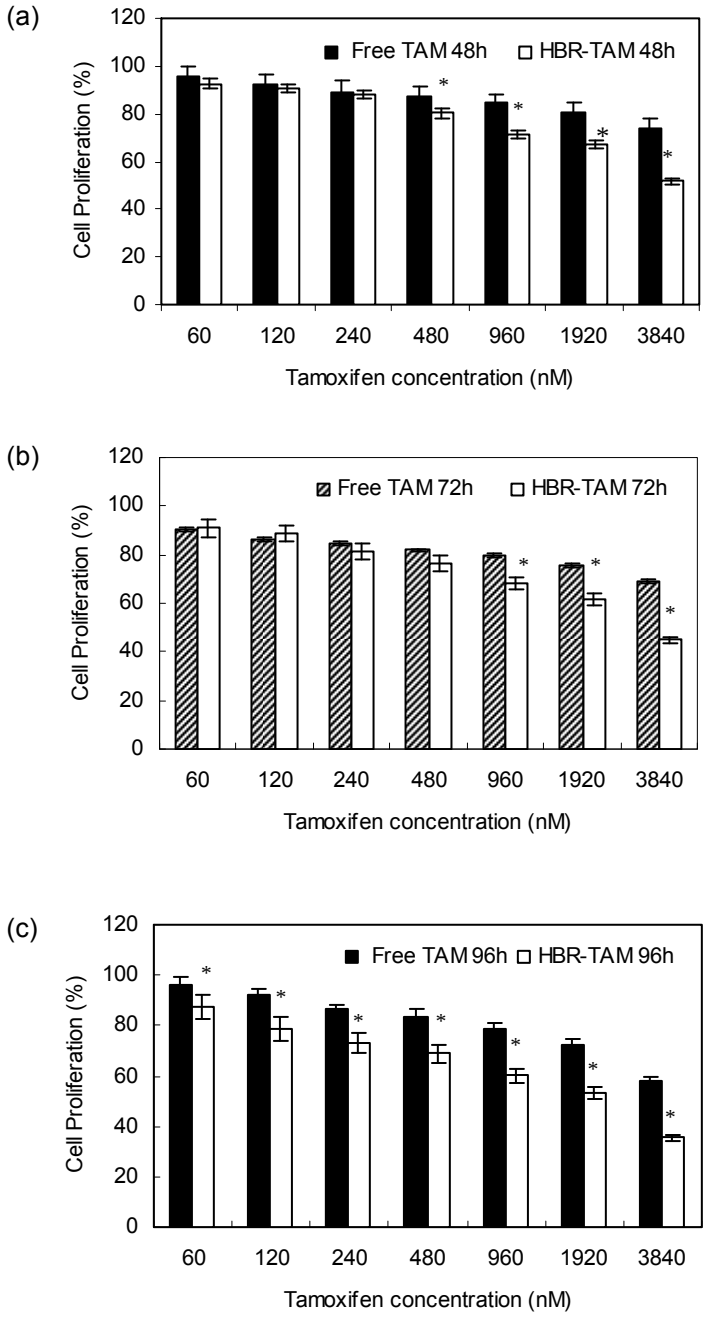

Figure 3.17 Cell Proliferation profiles of MCF-7 cell line after exposure to tamoxifen and HBR-TAM at 37°C for 48h (a), 72h (b) and 96h (c). Cell proliferation was determined by XTT assay. Cell proliferation percentage of samples was determined by considering the 100% proliferation of control groups. Results in the figure represents Mean± SEM, experiment were carried out in duplicates and triplicates (Tamoxifen and HBR-TAM application for 96h), *$p<0.05$ relative to free tamoxifen treated cells.

and co-workers suggested an additional work by addition of serum or lipase could cause enhanced release. In addition, tumor cells showed higher endocytotic activity leading to increase in the internalization of the particles into the cells.

It has been known that MCF-7 cells develop resistance after drug applications. These cellular resistance mechanisms trigger the effectiveness of efflux pumps which resulting pumping out drugs from the cell. P-gp pumps are the transmembrane proteins that are responsible for the efflux mechanism of the resistant cancer cells. In this study, sensitive cell lines are used which had not overexpressed P-gp pumps, but efflux mechanism was exist. Therefore after application of free idarubicin and free tamoxifen to the cells, partial amount of drug probably removed out from the cell. The effectiveness of the HBR-drug nanoparticles over sensitive MCF-7 cells suggested that by HBR nanoparticles, efflux of the drugs might be partially slowed down. Similar results were obtained in other studies. In the study of Vaulthier *et al.* (2003) the effect of nanoparticles over resistant tumor cells were investigated. According to this study certain mechanisms were suggested in order to explain the inhibition of P-gp efflux. These nanoparticles might attach to the cell surface and might release drug through the membrane, by this way drug might not be recognized by the P-gp pumps as free drugs. In addition, nanoparticles might enter to the cells by endocytosis and drug release starts by degradation of the polymer. Thus the time of interaction of drug with the cell will be longer, causing a higher affectivity on cancer cells. As a result of these mechanisms the function of P-gp pumps might be slowed down. Since multidrug resistance mechanisms are one of the major problems in cancer chemotherapy, these types of drug delivery systems could be a candidate to inhibit chemotherapy resistance in cancer patients.

When these mechanisms are adapted to the study, similar suggestions might be proposed. *In vitro* release results and degradation profiles showed that HBR nanoparticles could not release drugs significantly in 96h, therefore an effective degradation of these particles without entering the cell might not be possible. However the suggestion of attaching to the cell membrane and releasing drug into the cell might be investigated. In addition, as discussed previously nanoparticles might enter through the cell by endocytosis and after lysosomal degradation

sustained drug release might lead to the more toxic effect relative to free drug. In order to confirm these suggestions, cytotoxicity analysis might be applied to the drug resistant cells and the behavior might be investigated. Furthermore the route of the nanoparticles in the cells should be searched.

CHAPTER 4

CONCLUSION

Hyperbranched polymers are used in drug delivery studies due to their wide range of chemical and physical properties. In this study, fatty acid based hyperbranched polymers were synthesized, and characterization results showed the potential of the polymer in drug delivery researches. By the end of the study biodegradation property, hydrophobic drug entrapment efficiency was shown. In addition, drug loaded HBR polymer were more effectively killed breast cancer cells with respect to the free drug application. As a result, the potential of the HBR polymers in drug delivery studies was shown.

- To prevent complete esterification of ricinoleic acid with hyperbranched polyesters, reaction was stopped at acid value of 38.8 ± 2.7.

- The chemical groups of ricinoleic acid in hyperbranched resins were shown by FTIR analysis and the presence of expected carbon atoms and HBR synthesis was shown by ^{13}C NMR.

- Molecular weight distribution of HBR was lowered after washing with methanol. Molecular weight determied as Mn: 10913 ± 90, Mw: 23099 ± 3142.5 and polydispersity as 2.11 ± 0.27.

- Degradation was determined in the presence and absence of lipase. With lipase, HBR polymer was degraded almost completely while without lipase the degradation was not significant in PBS buffer.

- Tamoxifen was loaded into HBR with maximum 73% and idarubicin was loaded with 74 % of efficiency.The most efficient loading was obtained for initial drug concentration of 0.66µg/mg.

- By considering FTIR results, it was suggested that tamoxifen was physically entrapped while idarubicin entrapment was chemical.

- Zeta potential results of drug loaded and empty HBR were around -40 mV and -44 mV indicating the stability of HBR in aqueous solutions.

- Particle size of empty HBR was determined as 276.46 ± 8.63. When drugs were loaded, particle size was decreased depending on initial drug/polymer ratio.

- In the test tube tamoxifen was released approximately 4.5 % in PBS. By the adding lipase and SDS release was increased 19-fold for tamoxifen concentration of 2.66 µg/mg and 13.4-fold increased for the tamoxifen concentration of 8 µg/mg. The release of idarubicin in the test tube was not increased significantly by lipase and SDS addition.

- IC_{50} value of empty HBR nanoparticles was determined as 11 mg/ml at 96 h of incubation. It was concluded that empty polymer did not cause a significant toxicity to breast cancer cells.

- HBR-IDA was determined to be maximum 4.8-fold more potent relative to free idarubicin at 48h and the potency of HBR-TAM was maximum 108-fold more potent at 48h when compared with free tamoxifen.

4.1 Recommendations

There are few recommendations that should be noticed for the further studies:

- In order to increase the solubility of HBR in aqueous medium and to increase the degradation rate, hydroxyl based molecules like poly(ethylene glycol) might be esterified with the hydroxyl groups of ricinoleic acids. By this way hydrophobic drug could be entrapped into the core of HBR while outer part of the polymer could be more hydrophilic.

- To determine the branching units and number of functional end groups of the system, ^{1}H NMR and ^{13}C NMR analysis could be analyzed in detail.

- To increase the release rate of idarubicin, different release conditions might be tested.

- The route of HBR-Drug formulation in the cells could be analyzed more detailed and enzymatic degradation of HBR in the cells could be investigated.

- Cytotoxicity analysis could be done onto resistant MCF-7 cells. Deveopment of resistance could also be tested by using drug loaded HBR nanoparticles.

REFERENCES

Alberts B, Johnson A, Lewis J, Raff M, Roberts K, Walter P. 2001. Molecular Biology of the Cell. 4th Ed. NY: Garland Science. http://www.ncbi.nlm.nih.gov/sites/entrez?db=books&doptcmdl=DocSum&term=cancer+AND+mboc4%5Bbook%5D>. Accessed 2008 Mar 25.

Allen G, Burgess J, Edwards SF, Walsh DJ. 1973. On the dimensions of intramolecularly crosslinked polymer molecules. I. The synthesis and chemical characterization of intramolecularly crosslinked polystyrene molecules having a narrow distribution of molecular weight. Proceedings of the Royal Society of London. Series A, Mathematical and Physical Sciences 334 (1599) : 453-463.

Allen TM, Cullis PR. 2004. Drug delivery systems: Entering the mainstream. Science 303 : 1818-1822.

Ameller T, Marsaud V, Legrand P, Gref R, Barratt G, Renoir JM. 2003. Polyester–Poly(Ethylene Glycol) nanoparticles loaded with the pure antiestrogen RU 58668: physicochemical and opsonization properties. Pharmaceutical Research 20 : 1063-1070.

Ameller T, Marsaud V, Legrand P, Gref R, Renoir JM. 2004. Pure antiestrogen RU 58668—loaded nanospheres: morphology, cell activity and toxicity studies. European Journal of Pharmaceutical Sciences 21 : 361–370.

Barrat G. 1999. Characterization of colloidal drug carrier systems with zeta potential measurements. Pharmaceutical Technology Europe. <http://www.malvern.co.uk/LabEng/industry/colloids/colloid_application_notes.htm>. Last accessed date: 2008, Mar 12.

Bat E. 2005. Synthesis and characterization of hyperbranched and air drying fatty acid based resins. [Msc Thesis] Ankara : METU.

Bharathi P, Moore JS. 2000. Controlled synthesis of hyperbranched polymers by slow monomer addition to core. Macromolecules 33 : 3212-3218.

Bhattacharya J, Choudhuri U, Siwach O, Sen P, Dasgupta AK. 2006. Interaction of hemoglobin and copper nanoparticles: implications in hemoglobinopathy. Nanomedicine: Nanotechnology, Biology, and Medicine 2 : 191– 199.

Billmeyer Jr FW. 1984. Textbook of polymer science. 3rd Ed. Canada : John Wiley & Sons, Inc. p 3-11.

Biological Industries. 2002. Cell Proliferation Assay with XTT Reagent Protocol. <http://nd.com/Htmls/article.aspx?C2004=12557&BSP=12410&BSS51=1201>. Last accessed date: 2008, Jan 28.

Brannon-Peppas L, Blanchette JO. 2004. Nanoparticle and targeted systems for cancer therapy. Advanced Drug Delivery Systems 56 : 1649-1659.

Brannon-Peppas L. 1997. Polymers in controlled drug delivery. Medical Plastica and Biomaterials. <http://www.devicelink.com/mpb/archive/97/11/003.html>. Last accessed date: 2008, Apr 13.

Bruker Optics. 2006. Guide for infrared spectroscopy.<http://www.brukeroptics.com/downloads/index.html>. Last accessed date: 2008, Jan 21.

Cavallaro G, Maniscalco L, Licciardi M, Giammona G. 2004. Tamoxifen-loaded polymeric micelles: Preparation, physico-chemical characterization and *in Vitro* evaluation studies. Macromolecular Bioscience 4 :1028–1038.

Chawla JS, Amiji MM. 2002. Biodegradable poly(ε-caprolactone) nanoparticles for tumor targeted delivery of tamoxifen. International Journal of Pharmaceutics 249 : 127-138.

Cheng K-C. 2003. Effect on feed rate on structure of hyperbranched polymers formed by stepwise addition of AB_2 monomers into functional cores. Polymer 44 : 1259:1266.

Chin SF, Makha M, Raston CL. 2006. Encapsulation of magnetic nanoparticles with biopolymer for biomedical application. ICONN. p 374-376.

Coates J. 2000. Interpretation of infrared spectra, a practical approach. In: Meyers RA, editor. Encyclopedia of Analytical Chemistry. Chichester : John Wiley & Sons Ltd. p 10815-10837.

Cooper, GM. 2000. The Cell A Molecular Approach. 2nd Ed. Washington DC: Sinauer Associates, Inc. <http://www.ncbi.nlm.nih.gov/books/bv.fcgi?highlight=cancer&rid=cooper.section.2603#2604> Last accessed date: 2008, Apr 25.

Demetçi D. 2007. Preparation and evaluation of polymer based micro-carriers for hydrophobic anti-cancer Drugs. [MSc Thesis] Ankara : METU p 6-7, 23.

Denny B, Wansbrough H. 2005. Design and development of anti-cancer drugs. XII Biotech Journal of Cancer Drugs. New Zeland Institute of Chemistry. <http://www.nzic.org.nz/ChemProcesses/biotech/12J.pdf>. Last accessed date: 2008, Jan 28.

Dong Y, Feng SS. 2004. Methoxy poly(ethylene glycol) poly(lactide) (MPEG-PLA) nanoparticles for controlled delivery of anticancer drugs. Biomaterials 25 : 2843–2849.

Duncan R, Izzo L. 2005. Dendrimer biocompatibility and toxicity. Advanced Drug Delivery Reviews 57 : 2215– 2237.

The Cosmetic Ingredient. 2007 Final report on the safety assessment of ricinus communis (Castor) seed oil, hydrgenated castor oil, glyceryl ricinoleate, glyceryl ricinoleate SE, ricinoleic acid, potassium ricinoleate, sodium ricinoleate, zinc ricinoleate, cetyl ricinoleate, ethyl ricinoleate, glycol ricinoleate, isopropyl ricinoleate, methyl ricinoleate, and octyldodecyl ricinoleate. International Journal of Toxicology. 26(3) : 31–77.

Fontana G, Maniscalco L, Schillaci D, Cavallaro G, Giammona G. 2005. Solid lipid nanoparticles containing tamoxifen characterization and *in vitro* antitumoral activity. Drug Delivery 12 :385–392.

Fréchet JMJ. 2003. Dendrimers and other dendritic macromolecules: From building blocks to functional assemblies in nanoscience and nanotechnology. Journal of Polymer Science : Part A : Polymer Chemistry 41 : 3713–3725.

Fukushima T, Inoue H, Takemura H, Kishi S, Yamauchi T, Inai K, Nakayama T, Imamura S, Urasaki Y, Nakamura T, Ueda T. 1998. Idarubicin and idarubicinol are less affected by topoisomerase II-related multidrug resistance than is daunorubicin. Leukemia Research 22(7) : 625-9.

Gillies ER, Fréchet JMJ. 2005. Dendrimers and dendritic polymers in drug delivery. Drug Discovery Today 10 : 35-43.

Gupta U, Agashe HB, Asthana A, Jain NK. 2006. Dendrimers: Novel polymeric nanoarchitectures for solubility enhancement. Biomacromolecules 7(3) : 649-658.

Hecker R, Fawell PD, Jefferson A. 1998. The agglomeration of high molecular mass polyacrylamide in aqueous solutions. Journal of Applied Polymer Science 70 : 2241-2250.

Herzog K, Müller RJ, Deckwer WD. 2006. Mechanism and kinetics of the enzymatic hydrolysis of polyester nanoparticles by lipases. Polymer Degradation and Stability 91 : 2486-2498.

Hoogenboom R, Moore BC, Schubert US. 2005. Supramolecular star-shaped polymers based on the 3,6-Di(2-pyridyl) pyridazine ligand. Polymeric Materials : Science & Engineering 93 : 873.

Hu FX, Neoh KG, Kang ET. 2006. Synthesis and *in vitro* anti-cancer evaluation of tamoxifen-loaded magnetite/PLLA composite nanoparticles. Biomaterials 27 : 5725–5733.

Huang CY, Lee YD. 2006. Core-shell type of nanoparticles composed of poly [(n-butyl cyanoacrylate)-co-(2-octyl cyanoacrylate)] copolymers for drug delivery application : Synthesis, characterization and in vitro degradation. International Journal of Pharmaceutics 325(1-2) : 132-139.

Hule RA, Pochan DJ. 2007. Polymer nanocomposites for biomedical applications.. MRS Bulletin 32 : 354-358.

Ihre HR, Padilla de Jesus OL, Szoka Jr FC, Frechet JMJ. 2002. Polyester dendritic systems for drug delivery applications: Design synthesis and characterization. Bioconjugate Chem 13 : 443-452.

Jain JP, Modi S, Kumar N. 2008. Hydroxy fatty acid based polyanhydride as drug delivery system: Synthesis, characterization, *in vitro* degradation, drug release, and biocompatibility. Journal of Biomedical Materials Research 84(3) : 740-52.

Jelic S. 2005. How Chemotherapy is administered. 4 Routes of administration of chemotherapy. About.com:Lung diseases.<http://lungdiseases.about.com/od/lungcancer/a/chemoroutes.htm>. Last accessed date: 2008, Apr 7.

Jessani N, Humphrey M, McDonald WH, Niessen S, Masuda K, Gangadharan B, Yates JR, Mueller BM, Cravatt BF. 2004. Carcinomaa and stromal enzyme activity profiles associated with breast tumor growth in vivo. PNAS101(38) : 13756-13761.

Karp G. Cell and Molecular Biology Concepts and Experiments. 2002. 3rd Ed. NY : JohnWiley &Sons, Inc. p 672-680.

Kars DM, İşeri DÖ. Ural AU, Gündüz U. 2007. *In vitro* evaluation of zoledronic acid resistance developed in MCF-7 Cells. Anticancer Research 27 : 4031-4038.

Klajnert B, Bryszewska M. 2001. Dendrimers: properties and applications. Acta Biochimica Polonica 8 : 199-208.

Kohane DS. 2007. Microparticles and nanoparticles for drug delivery. Biotechnology and Bioengineering 96(2) : 203-209.

Kufe D, Pollock R, Wiechselbaum R, Bast R, Gansler Holland J, Frei E. 2003. Cancer Medicine. 6th edition. London: BC Decker Inc. <http://www.ncbi.nlm.nih.gov/sites/entrez?db=books&doptcmdl=DocSum&term=cancer+AND+cmed6%5Bbook%5D> Last accessed date: 2008, Jan 8.

Lodish H, Berk A, Zipursky LS, Matsudaria P, Baltimore D, Darnell J. 2000 Molecular Cell Biology. 4th Ed. NY :W. H. Freeman and Company. <http://www.ncbi.nlm.nih.gov/sites/entrez?db=books&doptcmdl=DocSum&term=cancer+AND+mcb%5Bbook%5D>. Last accessed date: 2008, Apr 25.

Long BJ, Jelovac D, Handratta V, Thiantanawat A, MacPherson N, Ragaz J, Goloubeva OG, Brodie AM. 2004. Therapeutic strategies using the aromatase inhibitor letrozole and tamoxifen in a breast cancer model. Journal of the National Cancer Institute 96 : 456-65.

Maillard S, Ameller T, Gauduchon J, Gougelet A, Gouilleux F, Legrand P, Marsaud V, Fattal E, Sola B, Renoir J-M. 2005. Innovative drug delivery nanosystems improve the anti-tumor activity *in vitro* and *in vivo* of anti-estrogens in human breast cancer and multiple myeloma. Journal of Steroid Biochemistry & Molecular Biology 94 : 111–121.

Malmström E, Johansson M, Hult A. 1995. Hyperbranched aliphatic polyesters. Macromolecules 28 : 1698-1703.

Marcucci F, Lefoulon F. 2004. Active targeting with particulate drug carriers in tumor therapy: fundimentals and recent progress. Drug Discovery Today 9(5) : 219-228.

Marten E, Müller RJ, Deckwer WD. 2005. Studies on the enzymatic hydrolysis of polyesters. II. Aliphatic aromatic copolyesters. Polymer Degradation and Stability 88 : 371-381.

Medline Plus Tamoxifen American Society of Health-System Pharmacist. Inc. 2007. <http://www.nlm.nih.gov/medlineplus/druginfo/medmaster/a682414.html> Last accessed date: 2008, Mar 21.

Mesothelomia. Categories of Chemotherapeutic Agents. 2008. <http://www.mesotheliomaweb.org/categories.htm>. Last accessed date: 2008, Feb 24.

Miao ZM, Cheng SX, Zhang XZ, Zhuo RX. 2005. Synthesis, characterization, and degradation behavior of amphiphilic poly-α,β-[N-(2-hydroxyethyl)-L-aspartamide]-g-poly(ε-caprolactone). Biomacromolecules 6 : 3449-3457.

Mueller RJ. 2006. Biological degradation of synthetic polyesters—enzymes as potential catalysts for polyester recycling. Process Biochemistry 41 : 2124–2128.

Muvaffak A. 2003. Controlled release systems for anticancer drugs and drug targeting in cancer therapy [PhD Thesis] Ankara : METU. p.8-12.

Najlah M, D'Emanuele A. 2006. Crossing cellular barriers using dendrimer nanotechnologies. Current Opinion in Pharmacology. 6 : 522–527.

Nothern Lipids Inc. 2008. Lipid Based Drug Formulation. <http://www.northernlipids.com/ourfacilities.htm>. Last accessed date: 2008, May 14.

Noble ML. 2004. Drug Delivery Systems. Biomaterials Tutorial. University of Washington Engineered Biomaterials. <http://www.uweb.engr.washington.edu/research/tutorials/drugdelivery.html>. Last accessed date: 2008, Apr 13

Nori A, Kopecek J. 2005. Intracellular targeting of polymer- bound drugs for cancer chemotherapy. Advanced Drug Delivery Systems 57 : 609-636.

Oncolink. 2001. Introduction to Chemotherapy. <http://www.oncolink.upenn.edu/treatment/article.cfm?c=2&s=9&id=55>. Last accessed date: 2005, Dec 21.

Orive G, Hernandez RM, Gascon AR, Pedraz JL. 2005. Micro and nano drug delivery systems in cancer therapy. Cancer Therapy 3 : 131-138.

Paleos CM, Tsiourvas D, Sideratou Z. 2007. Molecular engineering of dendritic polymers and heir application as drug and gene delivery systems. Molecular Pharmaceutics 4(2) : 169-188.

Papagiannaros A, Dimas K, Papaioannou GT, Demetzos C. 2005. Doxorubicin - PAMAM dendrimer complex attached to liposomes: Cytotoxic studies against human cancer cell lines. International Journal of Pharmaceutics 302 : 29-38.

Pfizer. 2008. Idamycin PFS product monograph, Canada Inc. <http://www.ncbi.nlm.nih.gov/books/bv.fcgi?rid=medmaster.chapter.a682414>. Last accessed date: 2008, Mar 2.

Polymeric Drug Delivery: A Brief Review. 2005. Drugdel.Com. < http://www.drugdel.com/polymer.htm>. Last accessed date: 2008, Apr 28.

Polymer molecular weight Chapter3. 2003. Indian Academy of Science. <http://www.ias.ac.in/initiat/sci_ed/resources/chemistry/MolWeight.pdf>. Last accessed date: 2008, May 21.

Purves KP, Sadava D, Gordon HO, Heler HC. 2001. Life, The Science of Biology. 6th Ed. Massachusetts: W.H. Freeman and Company. p 343.

Razzacki SZ, Thawar PK, Yang M, Ugaz MV, Burns MA. 2004. Integrated microsystems for controlled drug delivery. Advanced Drug Delivery Reviews 56 : 185-198.

Reusch W. 1999. Lipids <http://www.cem.msu.edu/~reusch/VirtualText/lipids.htm >. Last accessed date: 2008, May 7.

Reusch W. 1999. Polymers. <http://www.cem.msu.edu/~reusch/VirtualText/polymers.htm#polmr1>. Last accessed date: 2007, May 23.

Ring A, Dowsett M. 2004. Mechanisms of tamoxifen resistance. Endocrine-Related Cancer 11 : 643–658.

Rizzarelli P, Impallomeni G. 2004. Evidence for selective hydrolysis of aliphatic copolyesters induced by lipase catalysis. Biomacromolecules 5(2) : 433-444.

Robello DR. 2002. Chem 421: Introduction to polymer chemistry. <http://chem.chem.rochester.edu/~chem421/propsmw.htm>. Accessed 2008 May 21.

Ryan JA. Subculturing Monolayer Cell Cultures Protocol. <http://catalog2.corning.com/Lifesciences/enCN/TDL/techInfo_abstract.aspx?productid=3125>. Accessed 2008 July 09.

Santos ND, Waterhouse D, Masin D, Tardi PG, Karlsson G, Edwards Ker, Ball MB. 2005. Substantial increases in idarubicin plasma concentration by liposome encapsulation mediate improved antitumor activity. Journal of Controlled Release 105 : 89–105.

Shikanov A, Vaisman B, Krasko MY, Nyska A, Domb AJ. 2004 Poly(sebacic acid-co-ricinoleic acid) biodegradable carrier for paclitaxel: *In vitro* release and *in vivo* toxicity. Journal of Biomedical Materials Research. 69(1) : 47-54.

Sigma-Aldrich Co. 2008. Tutorial-biocompatible/biodegradable materials. <http://www.sigmaaldrich.com/Area_of_Interest/Chemistry/Materials_Science/BiocompatibleBiodegradable/Tutorial.html>. Last accessed date: 2008, May 7.

Singh G. 2006. New chemotherapy delivery methods. International Biopharmaceutical Association Publication. <http://www.ibpassociation.org/IBPAarticles/feb2006issue/New_Chemo_by_Gurdeep.doc> Last accessed date: 2008, May 10.

Slivniak R, Ezra A, Domb AJ. 2006. Hydrolytic degredation and drug release of ricinoleic acid-lactic acid copolyesters. Pharmaceutical Research 23(6) : 1306-1312.

Svenson S, Tomalia DA. 2005. Dendrimers in biomedical applications—reflections on the field. Advanced Drug Delivery Reviews 57 : 2106– 2129.

Sokolsky-Papkov M, Shikanov A, Kumar N, Vaisman B, Domb AJ. 2008. Fatty acid based biodegradable polymers-synthesis and applications. Bulletin of the Israel Chemical Society 23 :12-17.

Tayade PL, Kale RD. 2004. Encapsulation of water insoluble drug by a cross- linking technique: Effect of process and formulation variables on encapsulation efficiency, particle size, and *in vitro* dissolution rate. AAPS PharmSci 6(1) : 1-8.

Teomim D, Nyska A, Domb AJ. 1999. Ricinoleic acid-based biopolymers. Journal of Biomedical Materials Research 45(3) : 258-67.

Tomalia DA. 2003. Supramolecular chemistry: Fluorine makes a difference. Nature Materials 2 : 711–712.

Tomalia DA, Fréchet JMJ. 2002 Discovery of dendrimers and dendritic Polymers: A brief historical perspective. Journal of Polymer Science: Part A: Polymer Chemistry 40 : 2719–2728.

Wallin RF, Arscotta EF. 1998. Practical Guide to ISO 10993-5: Cytotoxicity. Medical Device & Diagnostic Industry Magazine. <http://www.devicelink.com/mddi/archive/98/04/013.html>. Last accessed date: 2008, Feb 15.

Wikipedia Encyclopedia. 2008 Chemotherapy. <http://en.wikipedia.org/wiki/Chemotherapy#Plantalkaloidsandterpenoids.28L01C.29>. Last accessed date: 2008, Jan 15.

Ulbrich K, Subr V. 2004. Polymeric anti-cancer drugs with pH-controlled activation. Advanced Drug Delivery Reviews 56 : 1023-1050.

Unger F, Wittmar M, Morell F, Kissel T. 2008. Branched polyesters based on poly[vinyl-3-(dialkylamino) alkylcarbamate-co-vinyl acetate-co-vinyl alcohol]-graftpoly(D,L-lactide-co-glycolide): Effects of polymer structure on *in vitro* degradation behavior. Biomaterials 29 : 2007-2014.

Vauthier C, Dubernet C, Chauvierre C, Brigger I, Couvreur P. 2003. Drug delivery to resistant tumors: The potential of poly(alkyl cyonoacrylate) nanoparticles. Journal of Controlled Release 93 : 151-160.

Verma RK, Garg S. 2001. Current status of drug delivery technologies and future directions. Pharmaceutical Technology On-Line 25(2) : 1-14.

Vert M. 2005. Aliphatic polyesters: Great degradable polymers that cannot do everything. Biomacromolecules 6 : 538-546.

Vishnu YV, Chandrasekhar K, Ramesh G, Rao YM. 2007. Development of mucoadhesive patches for buccal administration of carvedilol current drug delivery 4 : 27-39.

Vogelson CT. 2001 Advances in drug delivery systems. American Chemical Society <http://pubs.acs.org/subscribe/journals/mdd/v04/i04/html/MDD04FeatureVogelson.html >. Last accessed date: 2008, Apr 14.

Yang H, Lopina ST. 2006. *In vitro* enzymatic stability of dendritic peptides. Journals of Biomedical Materials Research Part A 76(2) : 398-407.

Yates CR, Hayes W. 2004. Synthesis and applications of hyperbranched polymers. European Polymer Journal 40 : 1257–1281.

Yu L, Zhang H, Cheng SX, Zhuo RX, Li H. 2006. Study on the drug release property of cholesteryl end-functionalized poly(epsilon-caprolactone) microspheres. Journal of Biomedical Materials Research. Part B Applied Biomaterials 77(1) : 39-46.

Zagar E, Zigon M. 2002. Characterization of a commercial hyperbranched aliphatic polyester based on 2,2-Bis(methylol)propionic acid. Macromolecules 35 : 9913-9925.

Zara GP, Bargoni A, Cavalli R, Fundaro A, Vighetto D, Gasco MR. 2002. Pharmacokinetics and tissue distribution of idarubicin-loaded solid lipid nanoparticles after duodenal administration to rats. Journal of Pharmaceutical Sciences 91(5) : 1324-1333.

Zeta Sizer NanoSeries. 2008. Zeta potential theory. Nanobiotechnology Center. <http://www.nbtc.cornell.edu/facilities/downloads/Zetasizer%20chapter%2016.pdf>. Last accessed date: 2008, Dec 18.

Zhang Z, Feng SS. 2006. The drug encapsulation efficiency, *in vitro* drug release, cellular uptake and cytotoxicity of paclitaxel-loaded poly(lactide)–tocopheryl polyethylene glycol succinate nanoparticles. Biomaterials 27 : 4025–4033.

Zou J, Shi W, Wang J, Bo J. 2005. Encapsulation and controlled release of a hydrophobic drug using novel nanoparticle forming hyperbranched polyester. Macomolecular Bioscience 5 : 662-668.

APPENDIX A

ACID NUMBER DETERMINATION

Acid value (or Acid number) is the mass of potassium hydroxide (KOH) that is required to neutralize fatty acids that is found in 1 gram of chemical substance. In other words acid number is a measure of carboxylic acid groups in chemical substance.

In acid number determination procedure, standaridized 0.1M KOH is used for titration. Standard potassium hydroxide solution is prepared by titration with standardized 0.1M HCl solution.

Dry resin sample (0.005g) is dissolved in isopropyl alcohol:toluene (1:1) mixture. Phenolphthalein is used as a indicator for both titration steps. Then solution is titrated with 0.1M KOH solution. Acid value is determined by the equation as follows (Equation A.1):

$$\text{Acid Number} = \frac{V_{KOH} x\ N_{KOH} x\ Mw_{KOH}}{W_s} \qquad (A.1)$$

V_{KOH} is volume of KOH used to titrate sample,
N_{KOH} is normality of KOH,
W_s is weight of sample in grams.

APPENDIX B

PARTICLE SIZE DISTRIBUTION

Table B1. Experimental conditions that had been used for particle size measurements.

Material RI: 1.59	**Temperature:** 24°C
Material Absorbtion: 0.01	**Cell Description:** Disposable Sizing Cuvette
Dispersant Name : Water	**Measurement Position(nm):** 5.50
Dispersant RI: 1.33	**Duration Used:** 60
Viscosity: 0.9086	**Temperature:** 24°C
Cell Description: Disposable Sizing Cuvette	

Table B2. Average particle size distribution data and average particle size values of HBR sample.

Sample Name: HBR	**Z-Average (nm)**	**PDI**
Sample 1:	267.83	0.193
Sample 2:	285.1	0.181

Size	**Mean % Intensity**	**Size**	**Mean % Intensity**	**Size**	**Mean % Intensity**
0.4	0	13.54	0	458.7	6.966667
0.4632	0	15.69	0	531.2	4.883333
0.5365	0	18.17	0	615.1	3.016667
0.6213	0	21.04	0	712.4	1.583333
0.7195	0	24.36	0	825	0.633333
0.8332	0	28.21	0	955.4	0.15
0.9649	0	32.67	0	1106	0.016667
1.117	0	37.84	0	1281	0
1.294	0	43.82	0	1484	0.016667
1.499	0	50.75	0	1718	0.033333
1.736	0	58.77	0.05	1990	0.066667
2.01	0	68.06	0.15	2305	0.1
2.328	0	78.82	0.283333	2669	0.133333
2.696	0	91.28	0.6	3091	0.166667
3.122	0	105.7	1.45	3580	0.166667
3.615	0	122.4	3	4145	0.166667
4.187	0	141.8	5.116667	4801	0.166667
4.489	0	164.2	7.416667	5560	0.15
5.615	0	190.1	9.5	6439	0
6.503	0	220.2	11.03333	7456	0
7.531	0	255	11.75	8635	0
8.721	0	295.3	11.58333	1000	0
10.1	0	342	10.61667		
11.7	0	396.1	8.966667		

Table B3. Average particle size distribution data and average particle size values of HBR-TAM (2.66µg/mg).

Sample Name: HBR-TAM (2.66µg/mg)	**Z-Average (nm)**	**PDI**
Sample 1:	234.93	0.174
Sample 2:	229.46	0.170

Size	**Mean % Intensity**	**Size**	**Mean % Intensity**	**Size**	**Mean % Intensity**
0.4	0	13.54	0	458.7	5.4
0.4632	0	15.69	0	531.2	3.35
0.5365	0	18.17	0	615.1	1.716667
0.6213	0	21.04	0	712.4	0.633333
0.7195	0	24.36	0	825	0.15
0.8332	0	28.21	0	955.4	0
0.9649	0	32.67	0	1106	0
1.117	0	37.84	0	1281	0
1.294	0	43.82	0	1484	0
1.499	0	50.75	0	1718	0
1.736	0	58.77	0	1990	0.016667
2.01	0	68.06	0.016667	2305	0.016667
2.328	0	78.82	0.116667	2669	0.033333
2.696	0	91.28	0.566667	3091	0.066667
3.122	0	105.7	1.9	3580	0.116667
3.615	0	122.4	4.183333	4145	0.183333
4.187	0	141.8	6.85	4801	0.216667
4.489	0	164.2	9.4	5560	0.233333
5.615	0	190.1	11.31667	6439	0
6.503	0	220.2	12.31667	7456	0
7.531	0	255	12.33333	8635	0
8.721	0	295.3	11.41667	1000	0
10.1	0	342	9.766667		
11.7	0	396.1	7.65		

Table B4. Average particle size distribution data and average particle size values of HBR-TAM (8µg/mg).

Sample Name: HBR-TAM (8µg/mg)	**Z-Average (nm)**	**PDI**
Sample 1:	206.93	0.154
Sample 2:	206.93	0.130

Size	**Mean % Intensity**	**Size**	**Mean % Intensity**	**Size**	**Mean % Intensity**
0.4	0	13.54	0	458.7	2.9
0.4632	0	15.69	0	531.2	1.166667
0.5365	0	18.17	0	615.1	0.3
0.6213	0	21.04	0	712.4	0
0.7195	0	24.36	0	825	0
0.8332	0	28.21	0	955.4	0
0.9649	0	32.67	0	1106	0
1.117	0	37.84	0	1281	0
1.294	0	43.82	0	1484	0
1.499	0	50.75	0	1718	0
1.736	0	58.77	0	1990	0
2.01	0	68.06	0	2305	0
2.328	0	78.82	0	2669	0
2.696	0	91.28	0.45	3091	0
3.122	0	105.7	2.283333	3580	0.033333
3.615	0	122.4	5.333333	4145	0.083333
4.187	0	141.8	8.816667	4801	0.15
4.489	0	164.2	11.9	5560	0.2
5.615	0	190.1	13.83333	6439	0
6.503	0	220.2	14.3	7456	0
7.531	0	255	13.31667	8635	0
8.721	0	295.3	11.15	1000	0
10.1	0	342	8.333333		
11.7	0	396.1	5.416667		

Table B5. Average particle size distribution data and average particle size values of HBR-IDA (2.66µg/mg).

Sample Name: HBR-IDA (2.66µg/mg)	**Z-Average (nm)**	**PDI**
Sample 1:	222.66	0.166
Sample 2:	211.53	0.146

Size	**Mean % Intensity**	**Size**	**Mean % Intensity**	**Size**	**Mean % Intensity**
0.4	0	13.54	0	458.7	4.35
0.4632	0	15.69	0	531.2	2.41666667
0.5365	0	18.17	0	615.1	1.05
0.6213	0	21.04	0	712.4	0.31666667
0.7195	0	24.36	0	825	0.06666667
0.8332	0	28.21	0	955.4	0
0.9649	0	32.67	0	1106	0
1.117	0	37.84	0	1281	0
1.294	0	43.82	0	1484	0
1.499	0	50.75	0	1718	0
1.736	0	58.77	0	1990	0
2.01	0	68.06	0.01666667	2305	0
2.328	0	78.82	0.1	2669	0
2.696	0	91.28	0.83333333	3091	0.01666667
3.122	0	105.7	2.66666667	3580	0.03333333
3.615	0	122.4	5.3	4145	0.06666667
4.187	0	141.8	8.08333333	4801	0.1
4.489	0	164.2	10.5333333	5560	0.13333333
5.615	0	190.1	12.1333333	6439	0
6.503	0	220.2	12.7833333	7456	0
7.531	0	255	12.35	8635	0
8.721	0	295.3	11.0166667	1000	0
10.1	0	342	9		
11.7	0	396.1	6.65		

Table B6. Average particle size distribution data and average particle size values of HBR-IDA (8 µg/mg).

Sample Name: HBR-IDA (8 µg/mg)	**Z-Average (nm)**	**PDI**
Sample 1:	211	0.165
Sample 2:	219.33	0.159

Size	**Mean % Intensity**	**Size**	**Mean % Intensity**	**Size**	**Mean % Intensity**
0.4	0	13.54	0	458.7	4.283333
0.4632	0	15.69	0	531.2	2.266667
0.5365	0	18.17	0	615.1	0.85
0.6213	0	21.04	0	712.4	0.166667
0.7195	0	24.36	0	825	0.033333
0.8332	0	28.21	0	955.4	0
0.9649	0	32.67	0	1106	0
1.117	0	37.84	0	1281	0
1.294	0	43.82	0	1484	0
1.499	0	50.75	0.05	1718	0
1.736	0	58.77	0.1	1990	0
2.01	0	68.06	0.133333	2305	0
2.328	0	78.82	0.2	2669	0
2.696	0	91.28	0.966667	3091	0
3.122	0	105.7	2.7	3580	0.016667
3.615	0	122.4	5.2	4145	0.05
4.187	0	141.8	7.9	4801	0.1
4.489	0	164.2	10.36667	5560	0.133333
5.615	0	190.1	12.08333	6439	0
6.503	0	220.2	12.81667	7456	0
7.531	0	255	12.5	8635	0
8.721	0	295.3	11.2	1000	0
10.1	0	342	9.166667		
11.7	0	396.1	6.716667		

APPENDIX C

CELL PROLIFERATION GRAPHS AND LOGARITHMIC EQUATIONS

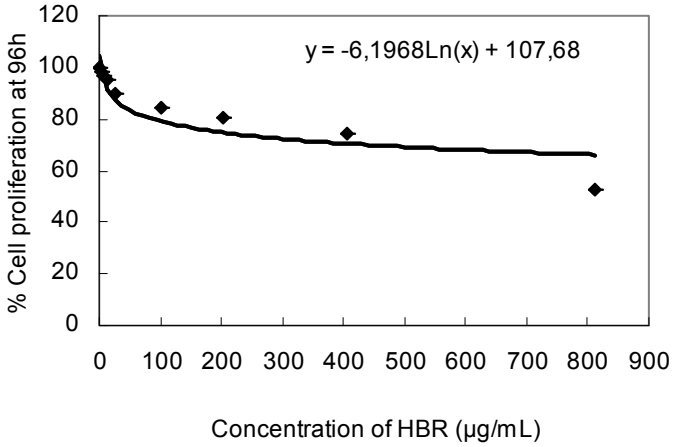

Figure C.1 Cell Proliferation of MCF-7 after incubation with 96 h of empty HBR.

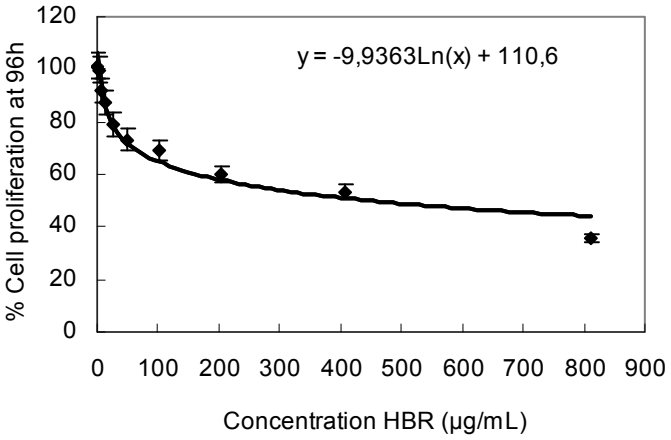

Figure C.2 Cell Proliferation of MCF-7 after incubation with 96 h of HBR-TAM. Logarithmic equation determined according to the HBR concentration.

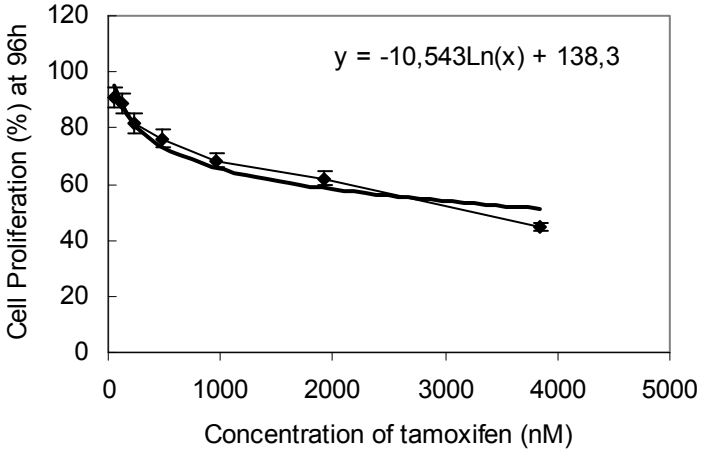

Figure C.3 Cell Proliferation of MCF-7 after incubation with 96 h of HBR-TAM. Logarithmic equation determined according to the tamoxifen concentration.

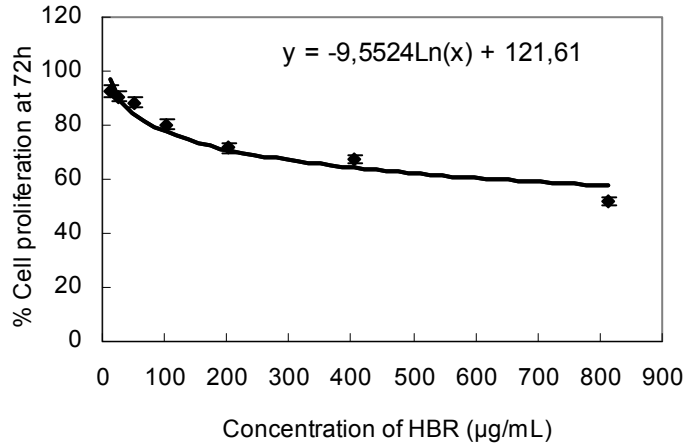

Figure C.4 Cell Proliferation of MCF-7 after incubation with 72 h of HBR-TAM. Logarithmic equation determined according to the HBR concentration.

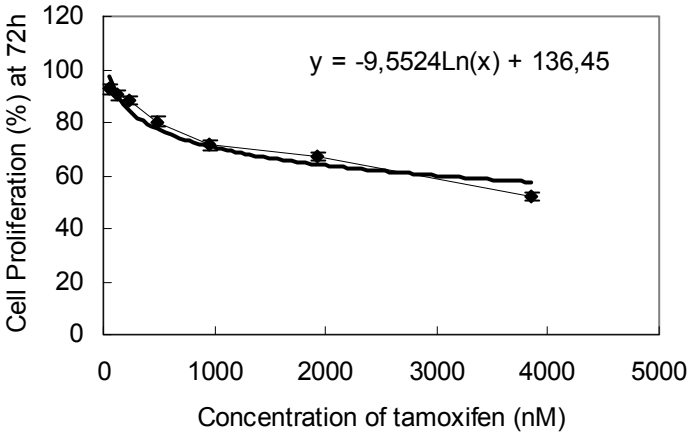

Figure C.5 Cell Proliferation of MCF-7 after incubation with 72 h of HBR-TAM. Logarithmic equation determined according to the tamoxifen concentration.

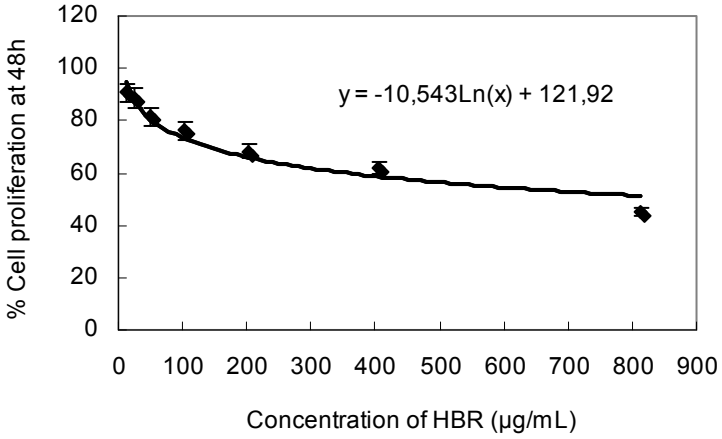

Figure C.6 Cell Proliferation of MCF-7 after incubation with 48 h of HBR-TAM. Logarithmic equation determined according to the HBR concentration.

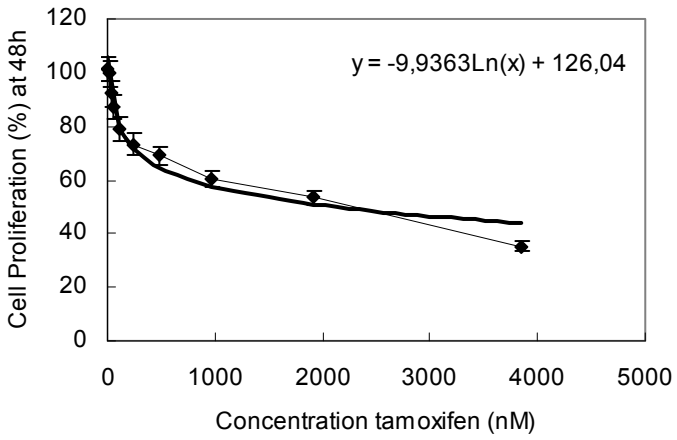

Figure C.7 Cell Proliferation of MCF-7 after incubation with 48 h of HBR-TAM. Logarithmic equation determined according to the tamoxifen concentration.

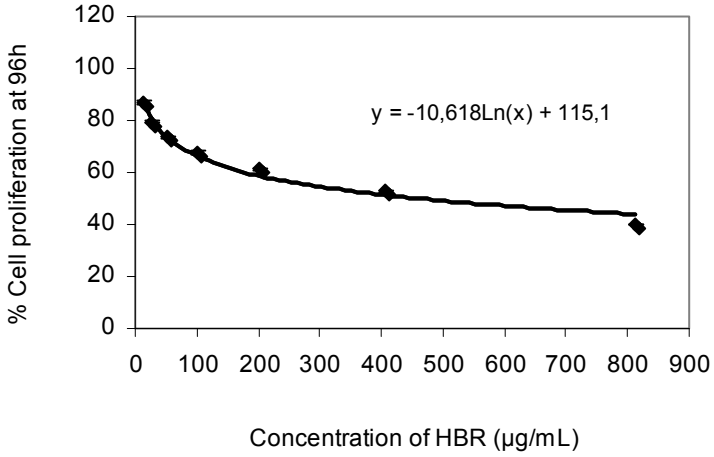

Figure C.8 Cell Proliferation of MCF-7 after incubation with 96 h of HBR-IDA. Logarithmic equation determined according to the HBR concentrationn.

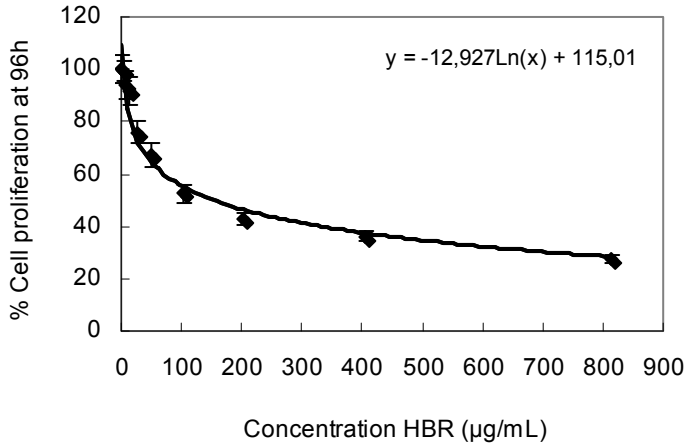

Figure C.9 Cell Proliferation of MCF-7 after incubation with 96 h of HBR-IDA. Logarithmic equation determined according to the idarubicin concentration.

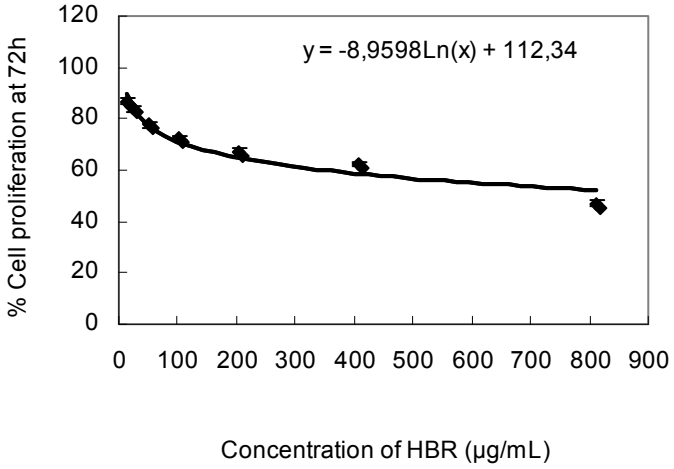

Figure C.10 Cell Proliferation of MCF-7 after incubation with 72 h of HBR-IDA. Logarithmic equation determined according to the HBR concentration.

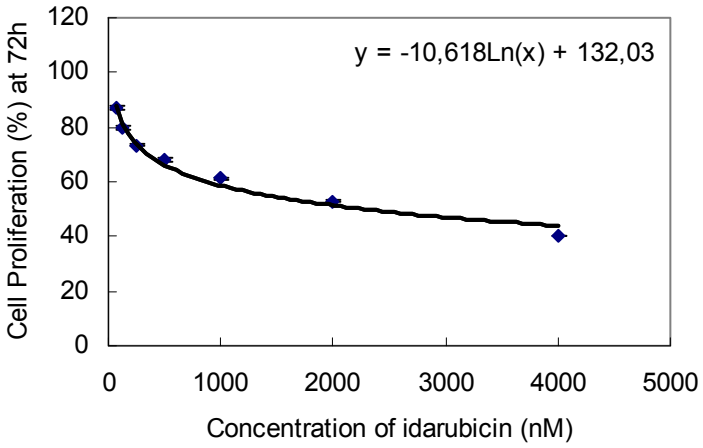

Figure C.11 Cell Proliferation of MCF-7 after incubation with 72 h of HBR-IDA. Logarithmic equation determined according to the idarubicin concentration.

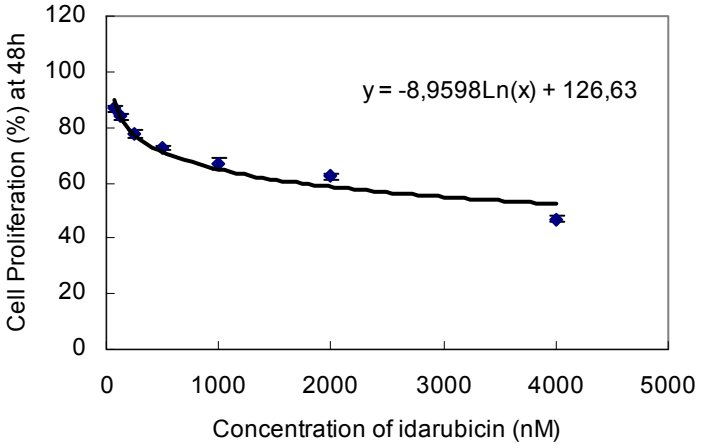

Figure C.12 Cell Proliferation of MCF-7 after incubation with 48 h of HBR-IDA. Logarithmic equation determined according to the HBR concentration.

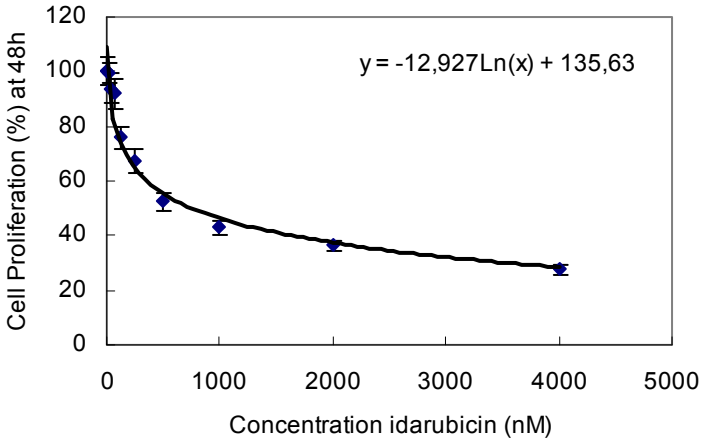

Figure C.13 Cell Proliferation of MCF-7 after incubation with 48 h of HBR-IDA. Logarithmic equation determined according to the idarubicin concentration.

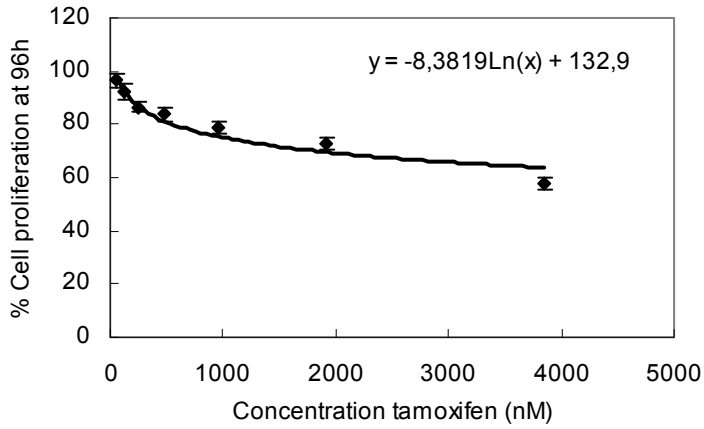

Figure C.14 Cell Proliferation of MCF-7 after incubation with 96 h of tamoxifen

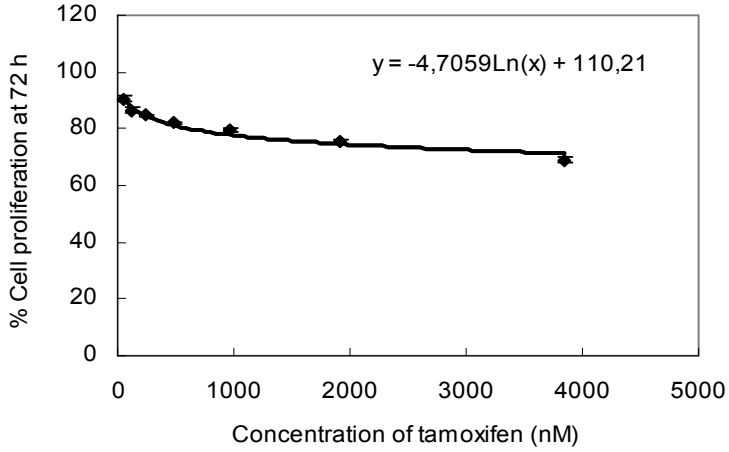

Figure C.15 Cell Proliferation of MCF-7 after incubation with 72 h of tamoxifen

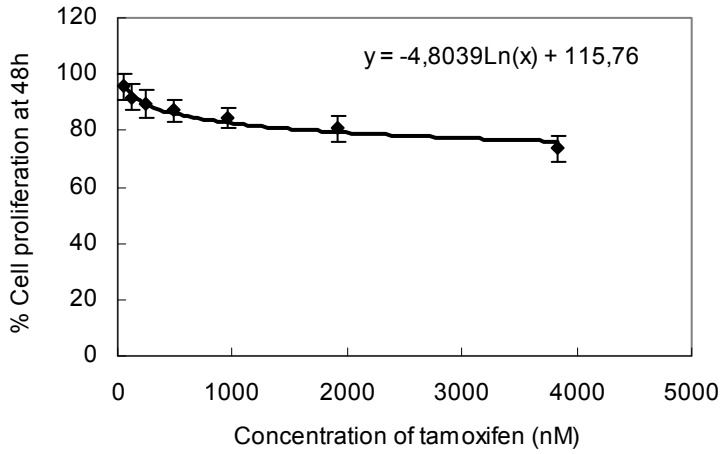

Figure C.16 Cell Proliferation of MCF-7 after incubation with 48 h of tamoxifen

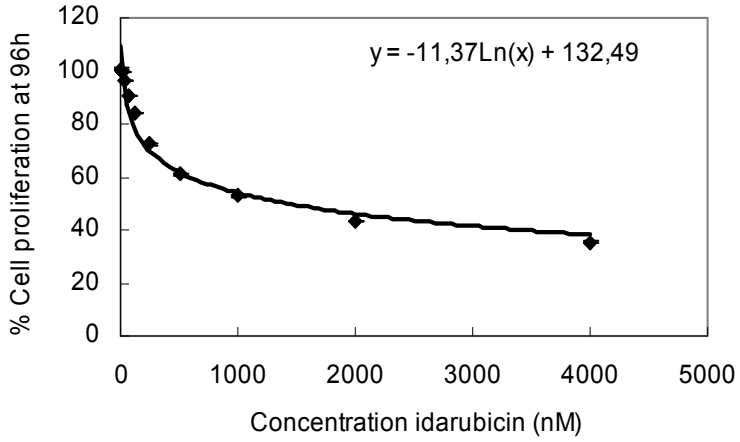

Figure C.17 Cell Proliferation of MCF-7 after incubation with 96 h of idarubicin

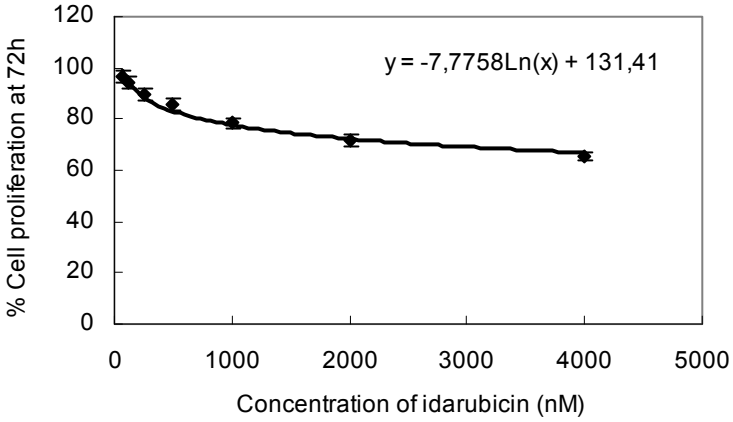

Figure C.18 Cell Proliferation of MCF-7 after incubation with 72 h of idarubicin

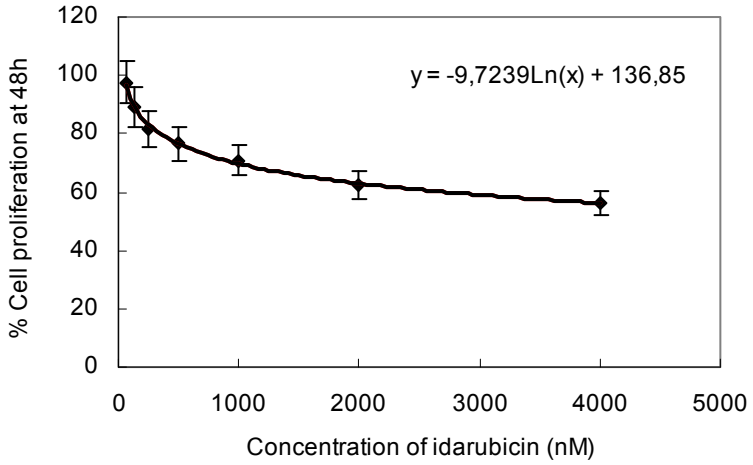

Figure C.19 Cell Proliferation of MCF-7 after incubation with 48 h of idarubicin.